



Università degli Studi di Padova

FACOLTÀ DI INGEGNERIA
Corso di Laurea Magistrale in Ingegneria Aerospaziale

TESI DI LAUREA MAGISTRALE

**Performance of modern unmixed turbofan engines:
model simulation, analysis and optimization using
GasTurb software**

Relatore:
Ernesto Benini

Laureando:
Bruno Fanzago
Matricola 1180012

Anno Accademico 2018–2019

ABSTRACT

Nowadays unmixed turbofan engines characterized by high bypass ratios are commonly used for propulsion of modern airliners. The major driving factor is fuel consumption efficiency thus achieving the lowest possible thrust specific fuel consumption. This is obtained with turbofan engines capable of higher propulsive efficiency compared to normal turbojet engines which however produce a lower specific thrust.

The common trend is achieving the highest possible bypass ratio: in fact General Electric and Pratt & Whitney most advanced turbofan engines are characterized by bypass ratios higher than 12.

In this thesis two modern turbofan engines, both with unmixed flows but implementing different mechanical solutions, are analysed using the gas turbine software GasTurb 13. It is possible to determine both the thermodynamic cycle of the engine and the performance for in design and off-design points. Once the simulated engine model is defined, flight performance of the two engines are compared in a hypothetical test flight.

Furthermore the geometrical configuration of the fan, reproduced using performance information of the engine obtained in GasTurb simulations, is compared to the geometry of the real fan made by the manufacturer.

CONTENTS

1. <i>Introduction</i>	1
2. <i>The turbofan engine</i>	3
2.0.1 Bypass ratio	4
2.0.2 Thermodynamic cycle	6
2.0.3 Thrust	13
2.0.4 Thrust Specific Fuel Consumption	14
2.0.5 Propulsive efficiency	15
2.0.6 Unmixed flow turbofan	16
2.0.7 Nozzles	17
2.0.8 Geared turbofan	18
3. <i>Simulated engine models</i>	21
3.1 General Electric GE9X	21
3.1.1 Geometrical information	25
3.2 Pratt & Whitney PW1100G	26
3.2.1 Geometrical information	28
4. <i>Engine ratings and technical data</i>	31
4.1 Engine Ratings	31
4.2 Type Certificate Data Sheet	34
4.2.1 Example of TCDS: PW1124G-JM	34
4.2.2 No TCDS: GE9X	37
4.3 ICAO Aircraft Engine Emissions Databank	38
4.4 Engine components efficiency and losses	40
4.5 Engine components pressure ratios	43
4.5.1 GE9X	43
4.5.2 PW1124G-JM	51
5. <i>GasTurb software</i>	57
5.1 Introduction and basic functions	57
5.1.1 Program scope	57
5.1.2 Engine models	58

5.1.3	Setting up the calculation	58
5.1.4	Additional functions: Formulas and Iterations	60
5.1.5	Parametric analysis	61
5.1.6	Cycle Optimization	63
5.1.7	Sensitivity analysis	65
5.2	The cycle design point	66
5.2.1	Input data	66
5.3	Off-Design Calculations	71
5.3.1	Input Data	71
5.3.2	Operating Line	74
5.3.3	Operating Line errors	76
5.3.4	Automatic Bleed schedule	77
5.3.5	Off-Design Parametric analysis	78
5.3.6	Mission analysis (flight)	79
5.3.7	Flight Envelope	79
5.4	Off-Design component modeling	81
5.4.1	Gas Properties	81
5.4.2	Standard Atmosphere	81
5.4.3	Component modeling	83
5.4.4	Component Maps	86
5.5	Engine model and stations	93
6.	<i>Design cycle</i>	95
6.1	GE9X	96
6.1.1	Design Point: Take-Off	96
6.1.2	Ambient Conditions	96
6.1.3	Component's efficiency and pressure ratio	97
6.1.4	TCDS Data	98
6.1.5	Thrust	99
6.1.6	Cycle optimization	99
6.1.7	Results	101
6.2	PW1124G-JM	102
6.2.1	Design Point: Cruise	102
6.2.2	Ambient Conditions	102
6.2.3	Component's efficiency and pressure ratios	103
6.2.4	Cycle optimization	104
6.2.5	Results	104

7. <i>Off-design cycle and component maps</i>	107
7.1 GE9X	107
7.1.1 Off-Design Point: Cruise	107
7.2 PW1124G-JM	119
7.2.1 Off-design point: Take-Off	119
8. <i>Simulated mission</i>	131
8.1 GasTurb mission setup	133
8.2 Engine comparison and results	134
9. <i>Fan design</i>	137
9.1 The fan	137
9.2 Real data	140
9.3 GasTurb simulated data	142
9.4 Preliminary fan design	143
9.4.1 Fan inner part (subsonic)	147
9.4.2 Fan outer part (transonic)	154
10. <i>Conclusions and further improvements</i>	167
<i>References</i>	169

LIST OF FIGURES

2.1 Turbojet engine: The Rolls-Royce Olympus 593 cross-section and scheme (Cumptsy, see [5])	3
2.2 Turbofan engine: The Rolls-Royce Trent 884 cross-section (Cumptsy, see [5])	4
2.3 Low BPR vs high BPR (Kurzke Halliwell, see [2])	5
2.4 Turbofan cycle (El-Sayed, see [10])	6
2.5 Propulsive efficiency of different types of engine (Rolls-Royce, see [12])	16
2.6 Contour lines for constant TSFC (Kurzke Halliwell, see [2]) . .	17
2.7 Turbofan without and with gearbox, common core, BPR=12 (Kurzke Halliwell, see [2])	18
2.8 Pratt & Whitney gearbox system (Pratt & Whitney, see [25])	19
2.9 Pratt & Whitney Geared Turbofan evolution (NASA, see [25])	20
3.1 GE9X cutaway (General Electric, see [18])	21
3.2 Aerodynamics advantages (Credit: General Electric)	23
3.3 Materials innovation (Credit: General Electric)	24
3.4 Additive manufacturing (Credit: General Electric)	24
3.5 PW1000G engine (MTU, see [24])	26
3.6 PW1000G cutaway (Credit: P&W)	28
3.7 Pratt & Whitney PW1000G cutaway (Kurzke Halliwell, see [2])	29
4.1 TCDS thrust ratings (EASA, see [16])	35
4.2 TCDS air bleed limits (EASA, see [16])	36
4.3 TCDS temperature limits (EASA, see [16])	36
4.4 TCDS speed limits (EASA, see [16])	37
4.5 PW1124G-JM datasheet (ICAO, see [17])	39
4.6 Component polytropic efficiencies and total pressure losses (Mattingly Heiser Pratt, see [3])	41
4.7 Loss assumptions for the turbofan at cruise conditions 35000ft and M=0.8 (Kurzke Halliwell, see [2])	42
4.8 Kacker & Okapuu diagram (Benini, see [1])	48
5.1 Engine models	58

5.2	Design Point input menu	59
5.3	Summary cycle page	60
5.4	Parametric selection window	62
5.5	Parametric example with contour lines and a boundary	62
5.6	Optimization input menu	64
5.7	Optimization window	65
5.8	Secondary Air System window	67
5.9	Conical convergent nozzle (Kurzke Halliwell, see [2])	70
5.10	Off-Design input window	72
5.11	Max Limiters window	73
5.12	HPC Operating line window	75
5.13	Multiple Operating line Output window	75
5.14	Relabel Speed Lines (GasTurb, see [4])	77
5.15	Automatic Bleed schedule	78
5.16	Temperature profile in ISA atmosphere and MIL210 conditions (Gasturb GmbH, see [4])	82
5.17	Beta,ds definition in a compressor map (Kurzke Halliwell, see [2])	88
5.18	Efficiency scaling parameters (Gasturb GmbH, see [4])	90
5.19	Efficiency and flow factors based on efficiency	91
5.20	Efficiency and flow factors based on losses	92
5.21	GasTurb "Geared Turbofan A" model	93
6.1	GE9X design ambient conditions	97
6.2	GE9X design component efficiencies	98
6.3	GE9X design optimization variables	100
6.4	GE9X design optimization constraints	100
6.5	GE9X Design Cycle: SL, static	101
6.6	PW1124G-JM design ambient conditions	102
6.7	PW1124G-JM design component pressure losses and efficiencies	103
6.8	PW1124G-JM Design Cycle: h=36000 [ft], M=0.85	105
7.1	GE9X Off-Design ambient conditions	108
7.2	GE9X LPC map settings	109
7.3	GE9X IPC map settings	110
7.4	GE9X HPC map settings	110
7.5	GE9X HPT map settings	111
7.6	GE9X LPT map settings	111
7.7	GE9X LPC operating line at Cycle Design Point (Take-Off)	112
7.8	GE9X IPC operating line at Cycle Design Point (Take-Off)	113
7.9	GE9X HPC operating line at Cycle Design Point (Take-Off)	113

7.10	GE9X HPT operating line at Cycle Design Point (Take-Off)	114
7.11	GE9X LPT operating line at Cycle Design Point (Take-Off)	114
7.12	GE9X LPC operating line at Off-Design Point (Cruise)	115
7.13	GE9X IPC operating line at Off-Design Point (Cruise)	115
7.14	GE9X HPC operating line at Off-Design Point (Cruise)	116
7.15	GE9X HPT operating line at Off-Design Point (Cruise)	116
7.16	GE9X LPT operating line at Off-Design Point (Cruise)	117
7.17	GE9X Off-Design Cycle: Cruise $h=36000$ [ft], $M=0.8$	118
7.18	PW1124G-JM Off-Design ambient conditions	120
7.19	PW1124G-JM LPC map settings	121
7.20	PW1124G-JM IPC map settings	121
7.21	PW1124G-JM HPC map settings	122
7.22	PW1124G-JM HPT map settings	122
7.23	PW1124G-JM LPT map settings	123
7.24	PW1124G-JM LPC operating line at Cycle Design Point (Cruise)	124
7.25	PW1124G-JM IPC operating line at Cycle Design Point (Cruise)	124
7.26	PW1124G-JM HPC operating line at Cycle Design Point (Cruise)	125
7.27	PW1124G-JM HPT operating line at Cycle Design Point (Cruise)	125
7.28	PW1124G-JM LPT operating line at Cycle Design Point (Cruise)	126
7.29	PW1124G-JM LPC operating line at Off-Design Point (Take-Off)	126
7.30	PW1124G-JM IPC operating line at Off-Design Point (Take-Off)	127
7.31	PW1124G-JM HPC operating line at Off-Design Point (Take-Off)	127
7.32	PW1124G-JM HPT operating line at Off-Design Point (Take-Off)	128
7.33	PW1124G-JM LPT operating line at Off-Design Point (Take-Off)	128
7.34	PW1124G-JM Off-Design Cycle: Take-Off SL, $M=0$	129
8.1	Aircraft missions (Gudmundsson, see [13])	131
8.2	Formula editor and mission composed values	134
8.3	GE9X mission results window	136
8.4	PW1124G-JM mission results window	136
9.1	Isometric view of a turbofan (US7374403B2 patent, see [26])	138
9.2	Axial sectional view through the turbofan portion of the engine (US7374403B2 patent, see [26])	138
9.3	Top planiform view of two adjacent fan blades (US7374403B2 patent, see [26])	139

9.4	Forward-facing-aft elevational view of the turbofan (US7374403B2 patent, see [26])	140
9.5	Typical single-stage fan configuration (Walsh Fletcher, see [15])	143
9.6	NACA 65-series Mellor data (Farokhi, see [9])	150
9.7	LPC rotor and stator configuration for the inner subsonic part	153
9.8	DCA rotor blade design angles (Farokhi, see [9])	157
9.9	LPC rotor and stator configuration for the outer transonic part	160
9.10	LPC rotor profile configuration at tip radius for the outer transonic part	164
9.11	LPC rotor profiles of both the inner and the outer part of the fan	165

LIST OF TABLES

3.1	GE9X technical data	25
3.2	PW1124G-JM technical data	28
5.1	Station numbering	94
6.1	PW1124G-JM avg. cruise known data	104
7.1	GE9X selected GasTurb maps	109
7.2	PW1124G-JM TCDS information	119
7.3	PW1124G-JM selected GasTurb maps	120
8.1	Mission: holding phase required thrust	133
8.2	GE9X Mission summary	134
8.3	PW1124G-JM Mission summary	135
9.1	PW1124G-JM avg. cruise and max take-off measured data . .	141
9.2	PW1124G-JM flight condition assumptions	141
9.3	Cruise and Maximum Take-Off fan results	142

LIST OF SYMBOLS AND ABBREVIATIONS

A	Area
c	Blade absolute velocity
c_a	Flight speed
C_d	Nozzle discharge coefficient
c_e	Exhaust velocity
C_{fg}	Nozzle thrust coefficient
c_p	Specific heat capacity at constant pressure
D	Diameter
D_r	Rotor diffusion factor
D_s	Stator diffusion factor
f	Fuel-to-air ratio
F	Thrust
F_s	Specific thrust
h	Altitude
Hu	Fuel heating value
i	Blade angle of incidence
k	Heat capacity ratio
l	Blade chord length
L	Specific work
M	Mach number
M_a	Flight Mach number
p	Pressure
p^0	Total pressure

\dot{m} Mass flow rate
 r Radius
 R Ideal gas constant
 $^{\circ}R$ Degree of reaction
 Re Reynolds number
 s Blade spacing
 T Temperature
 T^0 Total temperature
 u Blade linear velocity
 V Velocity
 w Blade relative velocity
 W Mass flow rate
 α Blade absolute velocity angle
 β Blade relative velocity angle
 η Isentropic efficiency
 η_p Polytropic efficiency
 ρ Density
 ρ^0 Total density
 ν Hub-to-tip diameter ratio
 π Pressure ratio
 σ Blade row solidity
 ϕ Flow coefficient
 ψ Work coefficient
 ω Angular velocity

BPR Bypass ratio

CR Cruise

CRP Cycle Reference Point (Cycle Design Point)

EAS Equivalent Air Speed

EGT Exhaust Gas Temperature

EPR Engine Pressure Ratio

FHV Fuel Heating Value

FOM Figure of Merit

GTF Geared Turbofan

HPC High-Pressure Compressor

HPT High-Pressure Turbine

IGV Inlet Guide Vanes

IPC Intermediate-Pressure Compressor (Booster)

ISA International Standard Atmosphere

ITT Indicated Turbine Temperature

LPC Low-Pressure Compressor (Fan)

LPT Low-Pressure Turbine

MCL Maximum Climb

MCR Maximum Cruise

MCT Maximum Continuous Thrust

MTO Maximum Take-Off

N1 Low-Pressure spool Speed

N2 High-Pressure spool Speed

OPR Engine Overall Pressure Ratio

RNI Reynolds Number Index

SAS Secondary Air System

SL Sea Level

SM Surge Margin

TAS True Air Speed

TCDS Type Certificate Data Sheet

TET Turbine Entry Temperature

TIT Turbine Inlet Temperature

TO Take-Off

TSFC Thrust specific fuel consumption

1. INTRODUCTION

The objective of this thesis is to analyse the performance of a turbofan engine using a gas turbine 0-D software in order to evaluate the accuracy of this type of calculation on performance prediction and geometry estimate of the real engine.

In particular two modern turbofan engines with unmixed flows are here taken into consideration. The first one is the General Electric GE9X which is a high-bypass turbofan engine characterized by huge fan diameter and is designed to produce 105 [klbf] of thrust. The second one is the Pratt & Whitney PW1000G high-bypass geared turbofan which however employs a smaller fan. A gearbox is in this case implemented in the engine in order to optimize the velocity of both the fan and the Low-Pressure turbine which are connected to the same shaft.

First of all, properties and characteristics of the turbofan engine are analysed. This brings to a better understanding of the turbofan peculiarities and design choices.

Then the two engines analysed in this thesis are introduced. It will be clear how difficult it is to obtain information and technical data required for the simulation of the existing engine, and all the types of technical documentation used for this scope will be presented.

The software employed for the engine simulation is GasTurb 13, which was purchased in a student version from the undersigned for this thesis. Every function, menu and quantity set during the analysis and simulation are described in a sort of how-to manual.

For each engine the simulation begins with the setting of the cycle design point. Then other off-design points corresponding to different operating conditions of the engine are calculated using the component scaled maps, because once that the component map is obtained the behaviour of the engine is known for every operating condition that differs from the design one. It is then possible to diagram the correct operating line in each component map. In GasTurb 13 it is also possible to calculate engine efficiency in terms of fuel flow or by using a wide variety of engine performance parameters calculated by selecting specific program scopes. This permits to compare the two engines also during a hypothetical flight envelope.

Finally a preliminary design of the fan is done for the Pratt & Whitney engine starting by the performance data obtained from the engine simulation carried out in GasTurb. This is done in order to compare a presumed simulation-derived design to the actual real design of the fan.

2. THE TURBOFAN ENGINE

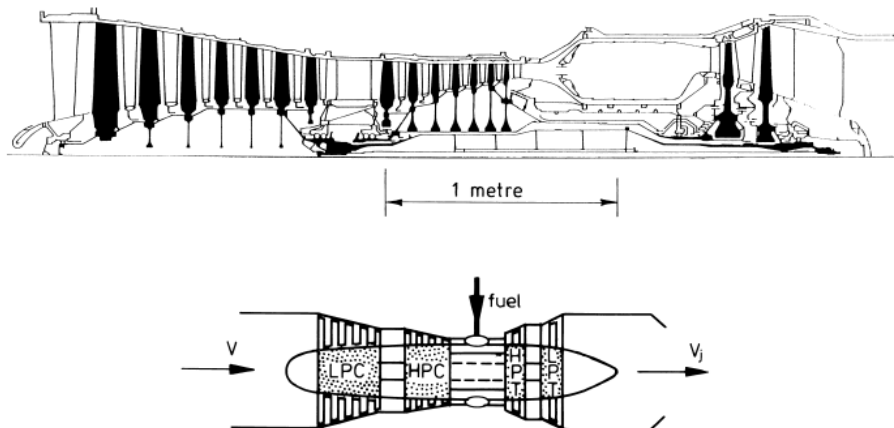
The turbofan engine represents an adaptation of the turbojet engine design to particular requirements and constraints, and therefore shares with it the most of its design.

The turbojet engine essentially consists of a gas turbine followed by an exhaust nozzle. The gas turbine section in its simplest way is composed of an air intake, a compressor, a combustor and a turbine. The compressor is driven by the turbine which is connected to the same shaft. In case of a multiple spool engine it is possible to have more than one compressor driven by more than one turbine.

The engine operating cycle is the Brayton thermodynamic cycle and it is implemented to produce the requested thrust necessary for the airplane to lift.

Below it is reported the Rolls-Royce Olympus 593 example from literature [5].

Fig. 2.1: Turbojet engine: The Rolls-Royce Olympus 593 cross-section and scheme (Cumptsy, see [5])



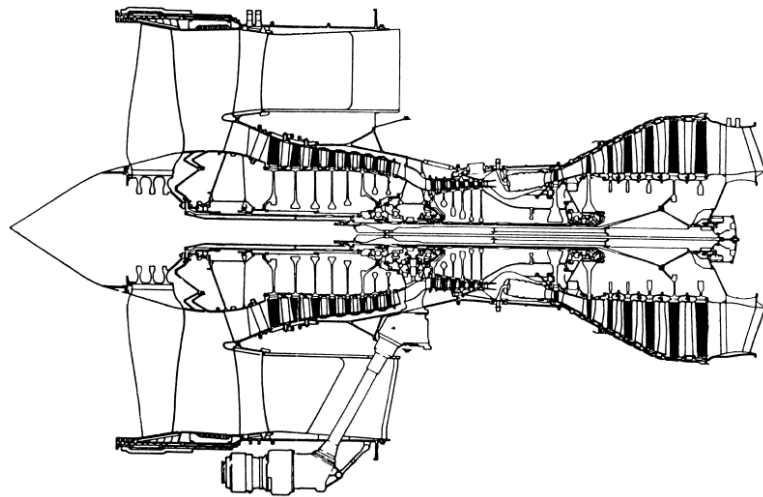
In a turbofan engine, however, a part of the mechanical energy extracted by the turbine is used for moving an additional compressor, the fan, which is

positioned at the engine fore part in front of the main compressor, in order to produce a big amount of air moderately accelerated rearwards which does not flow through the gas turbine section.

This alteration brings to the main difference between turbojet and turbofan engines: while in the former all the air elaborated by the engine passes through the gas turbine section of the engine, which is called the core, in the latter a big amount of that air bypasses the core.

In a turbofan both the airflows contribute to generate thrust, which is however mainly produced by the massive bypass airflow.

Fig. 2.2: Turbofan engine: The Rolls-Royce Trent 884 cross-section (Cumptsy, see [5])



As reported from literature [5] in Figure 2.2 which represents the Rolls Royce Trent 884, modern turbofans usually employ a large single-stage fan. Another possible configuration could implement a smaller fan equipped with several stages.

The reason that led to the development of turbofan engines is that turbojets are characterized by low propulsive efficiencies during subsonic flight while turbofans are able to overcome this turbojet flaw.

2.0.1 Bypass ratio

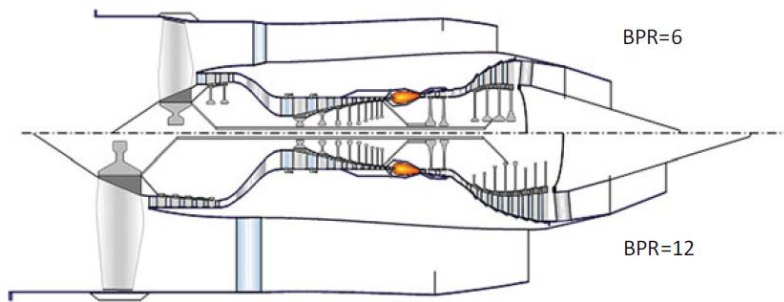
As far as turbofan engines are concerned, the bypass ratio (BPR) is defined as the ratio between the air mass flow rate of the bypass stream and the air mass flow rate flowing into the the core. Nowadays turbofan engines

employed in commercial airliners are characterized by BPRs that are higher than 10. This means that only one eleventh of the total air mass flow rate ingested by the engine actually passes through the core while the majority of the airflow bypasses it.

The turbine extracted power which is used in a turbojet engine to move the compressor, in a turbofan engine is used also to produce an additional high mass flow rate with low jet velocity which is accelerated from the front fan. The bypass stream contributes to generate thrust and allows to obtain a higher propulsive efficiency compared to a pure turbojet engine. Bypass thus consists on generating a bypass airstream that reduces the overall fuel consumption.

Another positive feature of the turbofan engine is that the bypass stream allows also to reduce noise, which is such an important aspect in modern aircraft's propulsion.

Fig. 2.3: Low BPR vs high BPR (Kurzke Halliwell, see [2])



However, the implementation of a bypass flow defines also some trade-offs: in a turbofan engine the Low-Pressure turbine is larger and is characterized by an increased number of stages because it has to drive also the fan. As the BPR increases the number of stages and the dimension of the LP turbine increases as reported in the example illustrated in Figure 2.3 from literature [2].

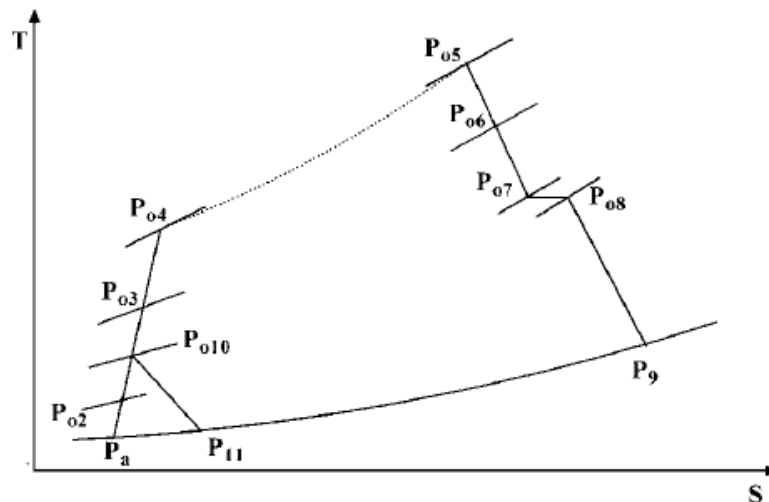
The implementation of a front fan makes the engine frontal area much bigger and this leads to higher aerodynamic drag in addition to increased engine weight derived from additional necessary machinery, components and ducts. Turbofan engines can be divided into low-bypass and high-bypass models according to the entity of the bypass airstream. In commercial aviation, where fuel consumption is an important driving factor, high-bypass turbofans are normally employed, while in military aircrafts usually low-bypass turbofan engines or turbojets are preferred.

The configuration of a high-bypass turbofan engine makes the engine be best suited for subsonic flight speeds, and once the optimal fan compression ratio has been determined in order to minimize the specific fuel consumption, the modest required fan pressure drop makes it possible to use a single-stage fan.

2.0.2 Thermodynamic cycle

Taking into consideration from literature [10] the T-s (temperature-entropy) diagram reported in Figure 2.4 of a turbofan engine cycle, for both the gas turbine section and the bypass stream, together with the thermodynamic station layout reported in the same diagram, it is possible to analyse the variation of thermodynamic quantities such as total temperature and total pressure along the engine in order to study engine's performance.

Fig. 2.4: Turbofan cycle (El-Sayed, see [10])



Below it is analysed how it is possible to calculate engine performance by making simplifying assumptions for each engine component. The same assumptions will be considered later in order to simulate the engine using GasTurb 13 software.

The unmixed double-spool turbofan configuration is now taken into consideration from literature [10].

Diffuser

The surrounding air enters the engine through the air intake diffuser where it is initially decelerated.

The process cannot be considered isentropic because of friction losses that occur along the diffuser. Defining the isentropic efficiency of the diffuser as

$$\eta_d = \frac{T_{2,is}^0 - T_a}{T_2^0 - T_a} \quad (2.1)$$

makes possible to evaluate the total pressure at the end section of the diffuser as

$$p_2^0 = p_a \left[1 + \eta_d \cdot \left(\frac{T_2^0}{T_a} - 1 \right) \right]^{\frac{k}{k-1}} \quad (2.2)$$

The total temperature at the diffuser's outlet can therefore be estimated as

$$T_2^0 = T_a \left(1 + \frac{k-1}{2} \cdot M_a^2 \right) \quad (2.3)$$

where M_a is the flight Mach number.

In this component there is however a loss of total pressure due to friction effects of the flow with the internal walls of the diffuser. The loss can be taken into account by considering the pressure ratio

$$\pi_d = p_2^0 / p_a^0 \quad (2.4)$$

Compressor

The air downstream the diffuser flows into the compressor where both its total pressure and total temperature increase. A compressor usually is made up by several stages, each of them composed by a series of rotor blades followed by a series of stator ones. The mean velocity of the fluid remains almost constant along the compressor stages.

The compression process can be considered adiabatic but not isentropic. In this example two compressors, the Intermediate-Pressure compressor and the High-Pressure compressor, are employed.

Intermediate-Pressure compressor (booster) Thus can be defined the isentropic efficiency of the Intermediate-Pressure compressor as

$$\eta_{ipc} = \frac{T_{3,is}^0 - T_{10}^0}{T_3^0 - T_{10}^0} \quad (2.5)$$

Usually the isentropic efficiency of a compressor ranges from 0.85 to 0.9 .

The required compression ratio is obtained by using a provided input work (shaft power), delivered from the Low-Pressure turbine and shared with the

fan, and is equal to the sum of the partial compression ratios produced by each compressor stage. It results

$$\pi_{ipc} = p_3^0/p_{10}^0 \quad (2.6)$$

and it represents a design parameter for the compressor. Usually IPC compression ratio is at most equal to 2:1.

The compression ratio sets the total pressure at the Intermediate-Pressure compressor's outlet as

$$p_3^0 = \pi_{ipc} \cdot p_2^0 \quad (2.7)$$

The temperature rise depends on the efficiency of the process, and the total temperature at the outlet section of the IP compressor results

$$T_3^0 = T_{10}^0 \cdot \left[1 + \frac{1}{\eta_{ipc}} \cdot \left(\pi_{ipc}^{\frac{k-1}{k}} - 1 \right) \right] \quad (2.8)$$

High-Pressure compressor As done for the Intermediate-Pressure compressor, the isentropic efficiency of the High-Pressure compressor can be defined as

$$\eta_{hpc} = \frac{T_{4,is}^0 - T_3^0}{T_4^0 - T_3^0} \quad (2.9)$$

The HP compressor pressure ratio results

$$\pi_{hpc} = p_4^0/p_3^0 \quad (2.10)$$

Usually HPC compression ratio ranges from 4:1 to 25:1 .

The total pressure at the High-Pressure compressor's outlet is

$$p_4^0 = \pi_{hpc} \cdot p_3^0 \quad (2.11)$$

The total temperature at the outlet section of the High-Pressure compressor results

$$T_4^0 = T_3^0 \cdot \left[1 + \frac{1}{\eta_{hpc}} \cdot \left(\pi_{hpc}^{\frac{k-1}{k}} - 1 \right) \right] \quad (2.12)$$

Combustor

In the combustor the hotter pressurized flow is then mixed with fuel and burnt producing a high temperature raise. Combustor's exit temperature usually ranges from 1100 [K] to 2000 [K] depending on the technological level of the engine. The combustor converts the chemical energy of the fuel into thermal energy, introducing however a loss of total pressure due to friction effects

between the mixture and the combustion chamber walls. The total pressure loss can be taken into account by the term π_{comb} so the total pressure at the end of the combustion chamber finally results

$$p_5^0 = \pi_{comb} \cdot p_4^0 \quad (2.13)$$

which is usually 0.94 to 0.98 times the total pressure at the combustion chamber's inlet.

Applying the first principle of thermodynamics between combustor's inlet and outlet planes the following relation is obtained:

$$(1 + f) \cdot c_{ph} \cdot T_5^0 = c_{pc} \cdot T_4^0 + \eta_b \cdot f \cdot Hu \quad (2.14)$$

This expression allows to calculate the fuel-to-air ratio, which is defined as the ratio between the fuel mass flow rate and the air mass flow rate, as

$$f = \frac{\dot{m}_f}{\dot{m}_a} \quad (2.15)$$

and which results a function of total temperatures at inlet and outlet sections of the combustion chamber, the specific heat at constant pressure c_p of the fluid evaluated at different temperature at the combustion chamber's inlet and outlet sections, the heating value Hu of the injected fuel and the burning efficiency η_b of the combustor.

$$f = \frac{\frac{c_{ph}}{c_{pc}} \cdot \left(\frac{T_5^0}{T_4^0} \right) - 1}{\eta_b \cdot \left(\frac{Hu}{c_{pc} \cdot T_4^0} \right) - \frac{c_{ph}}{c_{pc}} \cdot \left(\frac{T_5^0}{T_4^0} \right)} \quad (2.16)$$

Turbine

The hot gases at high pressure obtained from the combustion are expanded in the turbine thus producing mechanical power. The mechanical power extracted from the turbine is used to drive the compressor which is connected to the turbine by means of a mechanical shaft. Mechanical power in real engines is also used to drive other customer accessories, and to overcome mechanical losses which are taken into consideration by the mechanical efficiency η_m .

The high temperature gases impose that turbine blades especially on the first turbine stage have to be cooled, in order to maintain acceptable temperatures on the blade's surface. This is achieved by using a certain amount of air extracted from the compressor flow which bypasses the combustion chamber and in different ways cools the turbine blades (e.g. the air could flow through cavities made into each blade).

High-Pressure turbine The expansion is an irreversible process so it is possible to define the isentropic efficiency of the High-Pressure turbine as

$$\eta_{hpt} = \frac{T_5^0 - T_6^0}{T_5^0 - T_{6,is}^0} \quad (2.17)$$

Considering that the power extracted from the turbine is ideally equal to the power absorbed from the High-Pressure compressor, it is possible to evaluate the turbine outlet temperature by applying a power balance between the High-Pressure compressor and the High-Pressure turbine as

$$\dot{m}_a \cdot c_{pc} \cdot (T_4^0 - T_3^0) = \eta_{m1} \cdot \lambda_1 \cdot [\dot{m}_a \cdot (1 + f) \cdot c_{ph} \cdot (T_5^0 - T_6^0)] \quad (2.18)$$

In the above equation the mechanical efficiency of the High-Pressure spool η_{m1} and the ratio of energy used from the High-Pressure compressor to the energy produced by the High-Pressure turbine λ_1 are considered.

Total temperature at the outlet plane of the High-Pressure turbine T_6^0 is obtained from the ratio

$$\frac{T_6^0}{T_5^0} = 1 - \frac{(c_{pc}/c_{ph}) \cdot T_3^0}{\lambda_1 \cdot \eta_{m1} \cdot (1 + f) \cdot T_5^0} \cdot \left[\left(\frac{T_4^0}{T_3^0} \right) - 1 \right] \quad (2.19)$$

The total pressure at the High-Pressure turbine outlet section can be evaluated as

$$p_6^0 = p_5^0 \cdot \left(1 - \frac{T_5^0 - T_6^0}{\eta_{hpt} \cdot T_5^0} \right) \quad (2.20)$$

Low-Pressure turbine A power balance between the fan, the Intermediate-Pressure compressor (booster) and the Low-Pressure turbine yields to the following equation

$$\begin{aligned} BPR \cdot c_{pc} \cdot (T_{10}^0 - T_2^0) + \dot{m}_a \cdot c_{pc} \cdot (T_3^0 - T_2^0) = \\ = \eta_{m2} \cdot \lambda_2 \cdot [\dot{m}_a \cdot (1 + f) \cdot c_{ph} \cdot (T_6^0 - T_7^0)] \end{aligned} \quad (2.21)$$

or similarly

$$\begin{aligned} (1 + BPR) \cdot c_{pc} \cdot (T_{10}^0 - T_2^0) + \dot{m}_a \cdot c_{pc} \cdot (T_3^0 - T_{10}^0) = \\ = \eta_{m2} \cdot \lambda_2 \cdot [\dot{m}_a \cdot (1 + f) \cdot c_{ph} \cdot (T_6^0 - T_7^0)] \end{aligned} \quad (2.22)$$

where the mechanical efficiency of the Low-Pressure spool η_{m2} and the ratio of energy used from both the Intermediate-Pressure compressor (booster) and the fan to the energy produced by the Low-Pressure turbine λ_2 are considered.

It is possible to calculate the total temperature at the Low-Pressure turbine outlet as

$$T_7^0 = T_6^0 - \frac{c_{pc}}{\eta_{m2} \cdot \lambda_2 \cdot (1 + f) \cdot c_{ph}} \cdot [(1 + BPR) \cdot (T_{10}^0 - T_2^0) + (T_3^0 - T_{10}^0)] \quad (2.23)$$

The total pressure at the Low-Pressure turbine outlet plane can be evaluated as

$$p_7^0 = p_6^0 \cdot \left(1 - \frac{T_6^0 - T_7^0}{\eta_{hpt} \cdot T_6^0} \right) \quad (2.24)$$

Bleed from High-Pressure compressor

Usually a certain amount of bleed air is extracted from the High-Pressure compressor and the total pressure at the extraction point is denoted as p_{3b}^0 . It is possible to consider a power balance between the High-Pressure compressor and the High-Pressure turbine as

$$\begin{aligned} \dot{m}_a \cdot c_{pc} \cdot (T_{3b}^0 - T_3^0) + \dot{m}_a \cdot (1 - b) \cdot c_{pc} \cdot (T_4^0 - T_{3b}^0) = \\ = \eta_{m1} \cdot \lambda_1 \cdot [\dot{m}_a \cdot (1 + f - b) \cdot c_{ph} \cdot (T_5^0 - T_6^0)] \end{aligned} \quad (2.25)$$

where the ratio between the bleed air mass flow rate and the core mass flow rate is

$$b = \frac{\dot{m}_b}{\dot{m}_a} \quad (2.26)$$

The extraction of a bleed airstream modifies also the power balance of the Low-Pressure spool because the air mass flow rate elaborated from the turbine is changed and now it is lower. Equation (2.22) is therefore

$$\begin{aligned} (1 + BPR) \cdot c_{pc} \cdot (T_{10}^0 - T_2^0) + \dot{m}_a \cdot c_{pc} \cdot (T_3^0 - T_{10}^0) = \\ = \eta_{m2} \cdot \lambda_2 \cdot [\dot{m}_a \cdot (1 + f - b) \cdot c_{ph} \cdot (T_6^0 - T_7^0)] \end{aligned} \quad (2.27)$$

Hot exhaust nozzle

Finally in the propelling nozzle the exhaust gases are highly accelerated and released into the atmosphere thus producing the desired thrust. Usually convergent nozzles are employed in order to accelerate the flow and to obtain an high jet velocity.

It is useful to assume that the nozzle is adapted to the ambient pressure in case of a subsonic exhaust, so the exhaust pressure equals the ambient pressure p_a .

It is possible to define the isentropic efficiency of the nozzle as

$$\eta_n = \frac{T_8^0 - T_9}{T_8^0 - T_{9,is}} \quad (2.28)$$

The isentropic efficiency of the nozzle takes usually a value that ranges from 0.95 to 0.98.

It is possible to evaluate the critical pressure at nozzle exhaust from the equation

$$\frac{p_8^0}{p_c} = \frac{1}{\left[1 - \frac{1}{\eta_n} \cdot \left(\frac{k-1}{k+1}\right)\right]^{\frac{k}{k-1}}} \quad (2.29)$$

If $p_c \geq p_a$ then the nozzle is choked and the exhaust velocity equals the local speed of sound

$$c_e = \sqrt{k \cdot R \cdot T_9} \quad (2.30)$$

Hence $T_9 = T_c$ and $p_9 = p_c$.

When the nozzle is unchoked the exhaust pressure equals the ambient pressure (adapted exhaust) and the hot exhaust jet velocity c_e can be calculated using the relation

$$c_e = \sqrt{2 \cdot \eta_n \cdot \frac{k}{k-1} \cdot R \cdot T_8^0 \left[1 - \left(\frac{p_a}{p_8^0}\right)^{\frac{k-1}{k}}\right]} \quad (2.31)$$

Fan

Considering the fan inlet section (subscript 2) and the fan outlet section (subscript 10), the total temperature and total pressure at fan inlet result

$$T_2^0 = T_a^0 \quad (2.32)$$

$$p_2^0 = p_a^0 \quad (2.33)$$

Defining the fan pressure ratio π_{lpc} and the fan isentropic efficiency η_{lpc} in the same way used for other compressors, it is possible to evaluate the total pressure at the fan outlet plane as

$$p_{10}^0 = \pi_{lpc} \cdot p_2^0 \quad (2.34)$$

and the total temperature at fan outlet plane as

$$T_{10}^0 = T_2^0 \cdot \left[1 + \frac{1}{\eta_{lpc}} \cdot \left(\pi_{lpc}^{\frac{k-1}{k}} - 1\right)\right] \quad (2.35)$$

Cold exhaust nozzle

Defining the isentropic efficiency of the fan cold nozzle makes possible to evaluate the cold jet velocity at exhaust in the same way used for the core exhaust nozzle.

It is possible to define the isentropic efficiency of the cold nozzle as

$$\eta_{mf} = \frac{T_{10}^0 - T_{11}}{T_{10}^0 - T_{11, is}} \quad (2.36)$$

Similarly it is possible to evaluate the critical pressure at cold nozzle exhaust from the equation

$$\frac{p_{10}^0}{p_c} = \frac{1}{\left[1 - \frac{1}{\eta_{mf}} \cdot \left(\frac{k-1}{k+1}\right)\right]^{\frac{k}{k-1}}} \quad (2.37)$$

If $p_c \geq p_a$ then the cold nozzle is choked and the exhaust velocity equals the local speed of sound

$$c_{ef} = \sqrt{k \cdot R \cdot T_{11}} \quad (2.38)$$

Hence $T_{11} = T_c$ and $p_{11} = p_c$.

When the cold nozzle is unchoked the exhaust pressure equals the ambient pressure (adapted exhaust) and the hot exhaust jet velocity c_{ef} can be calculated using the relation

$$c_{ef} = \sqrt{2 \cdot \eta_{mf} \cdot \frac{k}{k-1} \cdot R \cdot T_{10}^0 \left[1 - \left(\frac{p_a}{p_{10}^0}\right)^{\frac{k-1}{k}}\right]} \quad (2.39)$$

2.0.3 Thrust

Thrust can be evaluated by using the indirect method, which employs the mono-dimensional momentum balance at the engine control volume, and for a turbojet engine in evaluated as

$$F = \dot{m}_a \cdot [(1 + f) \cdot c_e - c_a] + A_e \cdot (p_e - p_a) \quad (2.40)$$

where c_a is the velocity of the airflow at the engine inlet, A_e is the nozzle outlet section area, p_e is the exhaust pressure and p_a is the ambient pressure. Usually c_a equals the flight speed of the airplane.

The thrust equation may be simplified in case of adapted nozzle (in this particular condition the exhaust pressure equals the ambient pressure) as

$$F = \dot{m}_a \cdot [(1 + f) \cdot c_e - c_a] \quad (2.41)$$

It is then possible to evaluate the specific thrust, defined as the ratio between the produced thrust and the air mass flow rate elaborated from the engine, as

$$F_s = \frac{R}{\dot{m}_a} = (1 + f) \cdot c_e - c_a \quad (2.42)$$

In a turbofan engine there are however two streams that produce thrust, the core (hot) flow and the bypass (cold) flow. The bypass flow has a low exhaust velocity while the core flow has higher jet velocity which is however lower than the one in the turbojet engine, because in this case the Low-Pressure turbine has to drive also the front fan. In an unmixed flow turbofan engine there are two separate exhaust nozzles which discharge the elaborated flows into the atmosphere.

Referring to the same calculations of the thrust made for the turbojet engine it is possible to rearrange the thrust equation (2.40) in the case of the turbofan engine, considering that now two jet velocities of the two exhaust nozzles have to be taken into account and that the air mass flow sucked into from the engine is the sum of the air flowing through the core and the air bypassing it.

It can be obtained that the thrust is in this case equal to

$$F = \dot{m}_a \cdot [(1 + f) \cdot c_e + BPR \cdot c_{ef} - (1 + BPR) \cdot c_a] + A_{11} \cdot (p_{11} - p_a) + A_9 \cdot (p_9 - p_a) \quad (2.43)$$

where the jet velocity of bypass flow at the cold nozzle exhaust c_{ef} is now taken into consideration together with the jet velocity of the core stream at the hot nozzle exhaust c_e .

In a turbofan engine from 30% to 80% of the total thrust is produced from the cold bypass flow.

The specific thrust which is defined as the thrust per total air mass flow rate ingested from the engine is

$$F_s = \frac{R}{\dot{m}_a \cdot (1 + BPR)} = \frac{(1 + f)}{(1 + BPR)} \cdot c_e + \frac{BPR}{(1 + BPR)} \cdot c_{ef} - c_a + \frac{1}{\dot{m}_a \cdot (1 + BPR)} \cdot [A_{11} \cdot (p_{11} - p_a) + A_9 \cdot (p_9 - p_a)] \quad (2.44)$$

2.0.4 Thrust Specific Fuel Consumption

Thrust specific fuel consumption is defined as

$$TSFC = \frac{\dot{m}_f}{F} = \frac{f}{F/\dot{m}_a} \quad (2.45)$$

2.0.5 Propulsive efficiency

Propulsive efficiency describes how efficiently the engine converts the energy spent in the acceleration of the elaborated airflow into propulsive power. Propulsive efficiency in a turbojet engine can be evaluated as the ratio between the propulsive power P_p and the jet power P_e

$$\eta_P = \frac{P_p}{P_e} = \frac{F \cdot c_a}{\dot{m}_a \cdot \left[(1 + f) \cdot \frac{c_e^2}{2} - \frac{c_a^2}{2} \right]} \quad (2.46)$$

which can be rearranged with the assumption that fuel-to-air ratio $f \ll 1$ in

$$\eta_p = \frac{2c_a/c_e}{1 + c_a/c_e} \quad (2.47)$$

which makes evident how the propulsive efficiency is function of the ratio between the flight velocity and the exhaust velocity.

As can be seen the propulsive efficiency is maximum when the ratio $c_a/c_e = 1$. However in this case the specific thrust would tend to zero and in order to create thrust the engine would require an infinite inlet mass flow which is impossible to obtain. In real engines the propulsive efficiency is accepted not to be maximum and the velocity ratio c_a/c_e is set to be near unity.

Compared to a turbojet engine, the turbofan engine produces a larger amount of air with a lower velocity while the turbojet engine generates a smaller amount of air but with higher velocity. For this reason a turbofan is characterized by lower specific thrust compared to a turbojet engine.

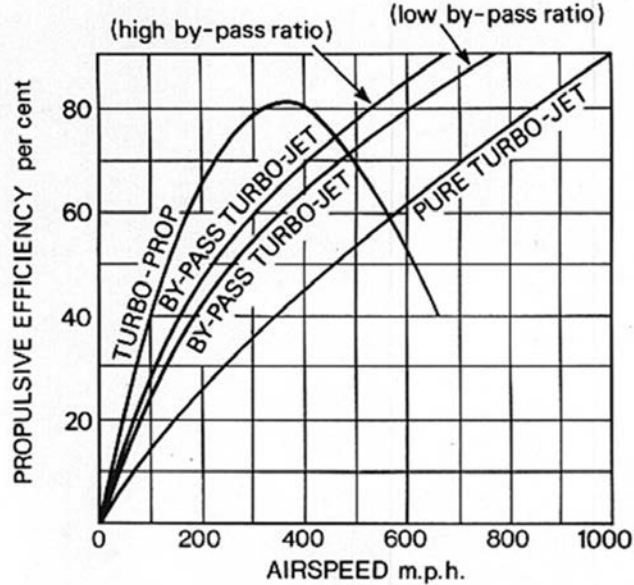
As seen before, propulsive efficiency is a function of the exhaust speed c_e and the flight speed c_a .

At flight speeds adopted usually by commercial aircrafts (500-1000 [km/h]) turbofans are the most efficient engines, while for lower speeds turbo-props are best suited and for higher speeds turbojets are preferred. In a turbo-prop in fact only 10% of the thrust is produced by the exhaust nozzle while in a turbojet all the thrust is produced by expanding turbine exhaust gases in the propelling nozzle.

Propulsive efficiency in a turbofan engine can be estimated using the following equation which is simplified for adapted exhaust nozzles

$$\eta_p = \frac{[(1 + f) \cdot c_e + BPR \cdot c_{ef} - (1 + BPR) \cdot c_a]}{(1 + f) \cdot \frac{c_e^2}{2} - \frac{c_a^2}{2} + BPR \cdot \left(\frac{c_{ef}^2}{2} - \frac{c_a^2}{2} \right)} \quad (2.48)$$

Fig. 2.5: Propulsive efficiency of different types of engine (Rolls-Royce, see [12])



In Figure 2.5, published by Rolls-Royce in [12], the propulsive efficiency of different types of engine is plotted as function of the flight speed. Turbofan engines are characterized however by additional components such as the fan, some bypass ducts, an increased number of turbine stages and a second exhaust nozzle which produce additional losses compared to a turbojet engine.

2.0.6 Unmixed flow turbofan

As far as unmixed flow turbofan engine is concerned, the core and the bypass flows do not mix together within a mixer but remain separate. The two streams with different jet velocities are discharged into the atmosphere through two distinct exhaust nozzles.

The gas turbine section of the turbofan generates a certain amount of power and bypass usually means transferring that power between the core and the bypass stream.

It is demonstrated theoretically that the ratio between the two exhaust jet velocities, which is called the Ideal Jet Velocity Ratio, could be properly set in order to achieve the lowest specific fuel consumption (SFC). In this case, the two jet velocities are optimally matched when the (ideal) ratio is equal to

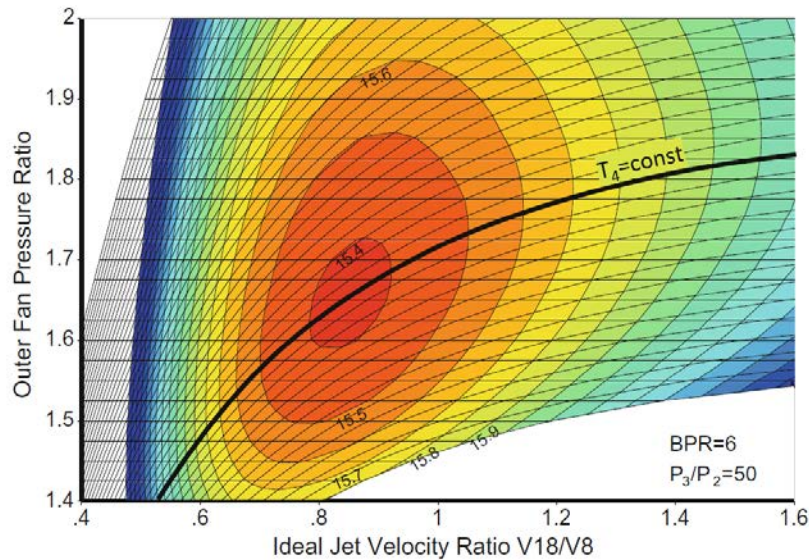
$$\frac{V_{11,id}}{V_{9,id}} = \eta_{p,f} \cdot \eta_{p,lp} \quad (2.49)$$

where $\eta_{p,f}$ is the fan polytropic efficiency and $\eta_{p,lpt}$ is the Low-Pressure turbine polytropic efficiency.

The Ideal Jet Velocity Ratio is a quantity which could be used in parametric studies of a turbofan engine since the fan pressure ratio now represents an additional design variable.

The Figure 2.6 from literature [2] reported below shows how an Ideal Jet Velocity Ratio of about ~ 0.8 minimizes the specific fuel consumption in a cycle parametric example carried out in GasTurb software, in which the fan and the Low-Pressure turbine efficiencies are ~ 0.9 as for most of modern turbofan engines.

Fig. 2.6: Contour lines for constant TSFC (Kurzke Halliwell, see [2])



2.0.7 Nozzles

In modern high-bypass turbofan engines the cold exhaust nozzle located downstream the short bypass duct typically is a convergent duct that during normal flight conditions is choked in order to generate a supersonic stream which flows around the core engine.

The core nozzle is instead more conventional and produces less thrust compared to the cold one.

Nozzles are designed also to reduce engine noise which is an important parameter in modern commercial aircrafts. For this purpose, it is possible to observe that modern engine configurations involve the implementation of particular serrated edges in the exhaust nozzle and the nacelle trailing edges, called chevrons.

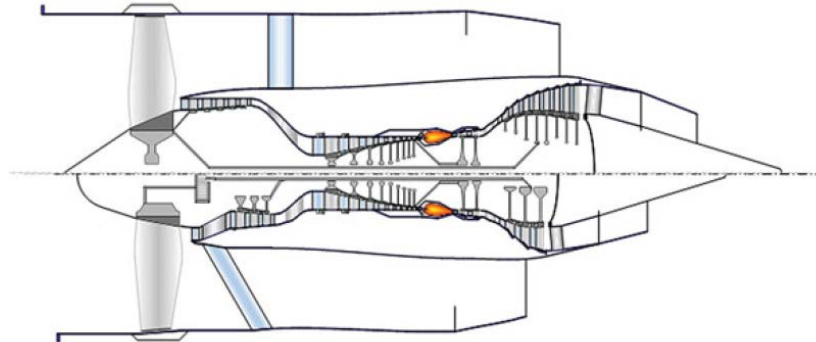
2.0.8 Geared turbofan

In the design of aircraft propulsion systems the engine's dimensions and weight are two important driving factors.

In the case of turbofan engines an high bypass ratio, especially when the BPR is higher than 12 as for the latest modern engines, requires an excessive number of Low-Pressure turbine stages. This is in contrast to weight and dimension design requirements.

In order to solve this drawback, a turbofan engine could be equipped with a gearbox. This device permits to make the fan rotational speed unrelated from the speed of both the booster (IPC) and the Low-Pressure turbine (LPT). In this case a lower number of IPC's and LPT's stages are required in addition to the fact that loading levels of turbo-machinery could be lower, thus obtaining higher component efficiency. Turbofan engines which are not equipped with a gearbox are called direct drive turbofans.

Fig. 2.7: Turbofan without and with gearbox, common core, BPR=12 (Kurzke Halliwell, see [2])



If the bypass ratio increases the dimensions of fan and Low-Pressure turbine increase, as reported in the figure above from literature [2]. In a direct drive turbofan the optimum rotational speed of the fan, which is lower than the one of the Low-Pressure turbine, implies additional Low-Pressure turbine stages in order to generate power requested to drive the fan. Moreover the booster pressure ratio in a direct drive turbofan is lower because of its lower rotational speed resulting in subsonic stages. By implementing a gearbox, however, higher pressure ratios could be achieved since booster stages could become transonic, leading to a lower stage count. At the same time the number of Low-Pressure turbine stages could be lowered because of the reduced required aerodynamic loading.

This additional device sets up optimal operational speeds for both the fan and

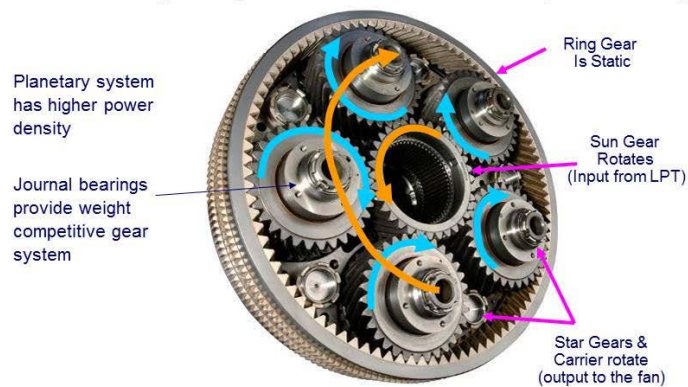
the Low-Pressure turbine. It is applied on the Low-Pressure spool between the fan and the Intermediate-Pressure compressor (booster). It consists of a planetary reduction gearbox characterized by an optimized gear ratio. A gear ratio equal to 3 is best suited to achieve lower fan tip speeds for reduced aerodynamical losses and to lower blade root stresses in last Low-Pressure turbine stages.

A modern implementation of this device is found in the recent Pratt & Whitney PW1000G engine family and the gear reduction system called Fan Drive Gear System (FDGS) is shown in the figure below.

Fig. 2.8: Pratt & Whitney gearbox system (Pratt & Whitney, see [25])

Planetary Fan Drive Gear System (FDGS)

Enables higher gear ratios; more compact design



Higher gear ratios Improve Propulsive η



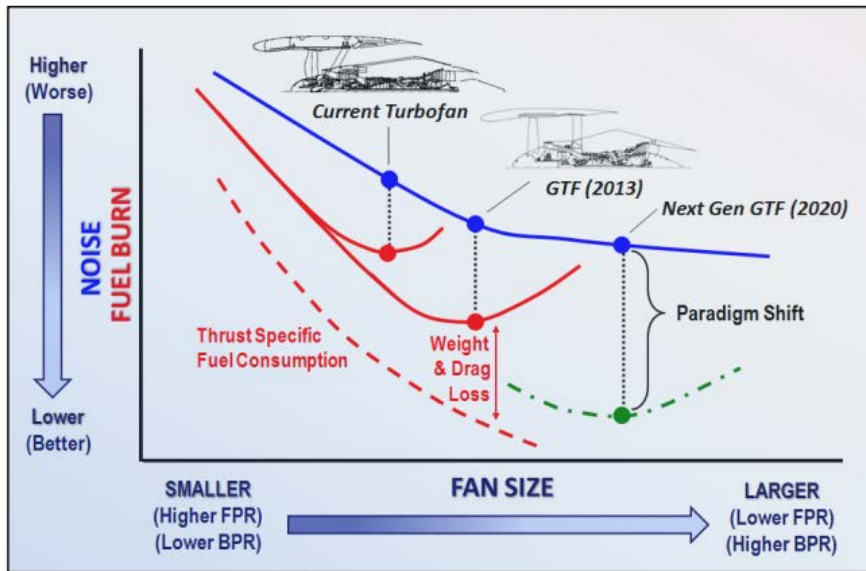
© 2015 United Technologies Corporation
This document has been publicly released

67

In Figure 2.9 below, retrieved from P&W commercial brochure dated back to 2015, it is possible to see the evolving trend in geared turbofans. As mentioned above, fan sizes in modern engines are constantly increasing in order to reduce specific fuel consumption and noise. Consequently together with the fan diameter also the bypass ratio increases and this modification brings to fans characterized by lower pressure ratios.

Fig. 2.9: Pratt & Whitney Geared Turbofan evolution (NASA, see [25])

Geared Turbofan Technology Enables Paradigm Shifts



3. SIMULATED ENGINE MODELS

3.1 *General Electric GE9X*

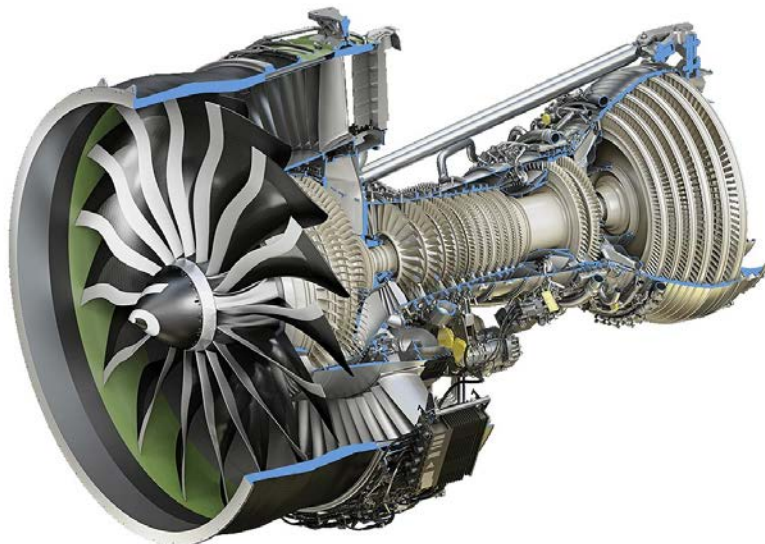
The General Electric GE9X is the latest model of high-bypass, unmixed, double spool turbofan engine produced by General Electric Aviation. It is currently under testing and first units have just been integrated on board the Boeing 777X prototype. The engine's first ground test which involved the FETT (First Engine To Test) unit occurred in April 2016 and a prototype flew for the first time on a Boeing 747 test plane in March 2018.

The GE9X is going to power the Boeing's new long-range, wide body airliner, the 777-9 variant. Its maiden flight is scheduled for 2019 and it is going to enter service later in 2020.

The engine is capable of producing 105000 [lbf] of thrust. From the baseline engine two derated variants that produce 102000 [lbf] and 93000 [lbf] of thrust will be available later.

The company invested more than 2 billion dollars for its entire development.

Fig. 3.1: GE9X cutaway (General Electric, see [18])



Its design is derived from the previous engine model, the General Electric GE90: major improvements concerning a larger fan, an higher bypass ratio, higher compression ratios, and the use of advanced materials like Ceramic Matrix Composites (CMC) allow to improve fuel efficiency by 10% over its predecessor.

The engine Overall Pressure Ratio (OPR) is now increased up to 61:1 in order to lower the thrust specific fuel consumption (TSFC) by 5% compared to the XWB-97 engine.

Maintenance costs are keep unchanged and are similar to those of the GE90-115B.

Such improvements are possible mainly thanks to the propulsion efficiency gain derived from the higher bypass ratio which is planned to be 10:1 .

In the new engine a number of titanium and nickel parts are replaced from newer parts made of carbon fibre and ceramic materials in order to achieve weight and strength advantages.

The huge fan has a diameter of 134 [in]. It is composed of only 16 blades, whereas the old GE90 has 22 blades and the GENx, which is the test-bed engine for technologies implemented in the GE9X and so similar to the latter, has 18 blades. This feature brings to a lighter engine and allows higher rotational speeds for both the fan and the booster that permit a better matching with the Low-Pressure turbine. The fan blades are made of glass-fibre trailing edges instead of carbon-fibre in order to improve their flexibility while the leading edges are made of steel. This combination leads to better bird strike shock absorption.

Fourth generation carbon fibre composite materials are employed in the bulk of the fan blades in order to improve strength and make possible to obtain blades which are lighter, thinner and more aerodynamically efficient.

Also the fan case is made of composites materials in order to reduce weight. The compressor and the High-Pressure turbine are made from powdered metal.

Fig. 3.2: Aerodynamics advantages (Credit: General Electric)

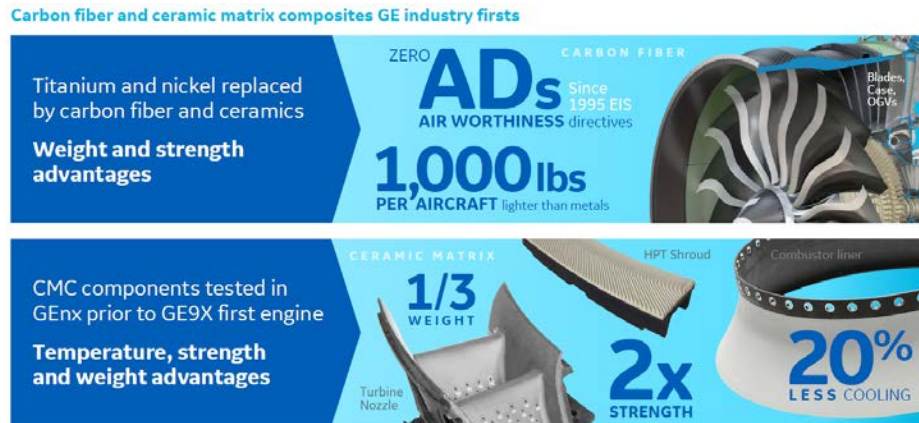
Aerodynamics enable engine efficiency

The efficiency of the High-Pressure compressor is increased up to 2% thanks to advanced 3D aerodynamic design. The engine Overall Pressure Ratio is increased from 40:1 in the GE90 to 61:1, since the HPC pressure ratio is increased from 19:1 in the GE90 to 27:1 by using additional compressor stages, which are now 11 instead of 9. The first five stages are composed by blisks, which are a combination of blades and disks.

CMC components was previously tested in the GENx engine and are now introduced in the new engine bringing temperature, strength and weight advantages. CMCs requires 20% less cooling, and are 1/3 lighter and 2 times stronger than metal. In the engine these materials are used to manufacture static components such as the outer combustor liners, the first- and the second-stage High-Pressure turbine nozzles and the first-stage High-Pressure turbine shroud, which could now operate 260 [°C] hotter than equivalent cooled components made of nickel alloys.

A new third-generation twin-annular pre-swirl (TAPS) combustor is introduced, substituting the previous dual annular combustor and assuring hotter combustor temperatures that permit higher efficiency and an increased 30% NOx margin to CAEP/8 regulation.

Fig. 3.3: Materials innovation (Credit: General Electric)



Low-Pressure turbine blades are made of titanium aluminide (TiAl) instead of nickel in order to be stronger, lightweight and enduring. Additive manufacturing is used to print components such as the combustor injector that would otherwise be impossible to produce using traditional manufacturing processes in order to reduce the number of parts, overall weight and to increase its operating life.

Fig. 3.4: Additive manufacturing (Credit: General Electric)



In the table below are reported the GE9X main characteristics.

<i>GE9X technical data</i>		<i>Notes</i>
Thrust	[lbf] 105000	
Bypass Ratio	10:1	
Overall Pressure Ratio	61:1	
HPC Pressure ratio	27:1	
LPT Expansion ratio	7:1	
T3 Redline	[°F] 1400	
Fan diameter	[in] 134	At fan tip
Fan blades	16	
Compressor stages	1/3/11	Fan/Booster/HPC
Turbine stages	3/5	HPT/LPT
Combustor	TAPS	
Transmission	Double-spool	Direct drive
Aircraft	Boeing 777-9	

Tab. 3.1: GE9X technical data

3.1.1 Geometrical information

General Electric has not disclosed precise geometrical data of the GE9X shape. Such information is useful to have an idea about the engine components properties. It is possible to estimate important performance information about its turbomachinery by mean of geometrical proportion by using the only one available cutaway image of the engine reported in Figure 3.1 and considering the fan diameter ($D_{tpc}=134$ [in]).

3.2 Pratt & Whitney PW1100G

The PW1000G is a high-bypass, unmixed, geared turbofan engine family produced by Pratt and Whitney.

The first P&W project of a geared turbofan dates back to 1998 with the PW8000. The engine was based on the PW6000 turbofan engine with an additional gearbox and a dual-stage fan. After some years of development the project was abandoned and the Advanced Technology Fan Integrator (ATFI) project took his place. The new design was a PW6000 based engine provided with a different gearbox system and a single-stage front fan. Then a new project started in collaboration with MTU Aero Engines and called Geared Turbofan (GTF) became definitive and led to the development of the current PW1000G PurePower family.

The family is going to power a wide variety of airliners like the Airbus A220, the Mitsubishi Regional Jet (MRJ), and the Embraer's second generation E-Jets, and it is currently an option on the Irkut MC-21 and the Airbus A320neo.

The engine initially flew aboard of a P&W Boeing 747SP but the first official test flight occurred in October 2008 in Toulouse aboard of an Airbus A340-600.

The first model to be produced was the PW1524G, that is going to power the Bombardier CSeries (Airbus A220), while the PW1000G engine produced for the Airbus A320 flew for the first time in May 2013.

The first PW1100G engine entered service on board the Lufthansa's first commercial Airbus A320neo back in January 2016.

Fig. 3.5: PW1000G engine (MTU, see [24])



Several derated engine models provide different levels of thrust in a range from 15000 [lbf] to 33000 [lbf], while sharing the same mechanical architecture.

Each model is denoted by the code PW1000G where the second digit indicates the customer that purchases the engine, and the last two digits indicates the thousands pounds of thrust generated. For example the PW1124G is the engine powering the Airbus A319neo which delivers 24000 [lbf] of thrust.

The engine could deliver fuel consumption and reduced ground noise when used in next-generation aircraft.

The PW1000G design provides a single-stage front fan, followed by a reduction gearbox that connects the fan to the two-stage Intermediate-Pressure compressor (booster) which allows optimum matching of rotating speeds for both the components, allowing the booster to run faster than the fan. Both the fan and the booster are driven by the 3-stage Low-Pressure turbine with advanced aerodynamics and reduced airfoil count. The fan has only 20 blades compared to the CFM56-5B fan which has 36 blades.

The fan case is made of composites materials in order to reduce weight.

The High-Pressure compressor provided by MTU, which consists of 8 stages, is driven by a 2-stage High-Pressure turbine designed using advanced aerodynamics and integrated blade rotors. The stage count of the PW1000G family results 1-G-3-8-2-3, with the G letter denoting the gear system.

The introduction of a 3:1 gearbox between the fan and the Low-Pressure spool allows both component to run at its optimal speed. The gearbox could transmit 30000 [hp] and is designed not to have life-limited parts, and in fact requires only oil changes across its operational lifetime.

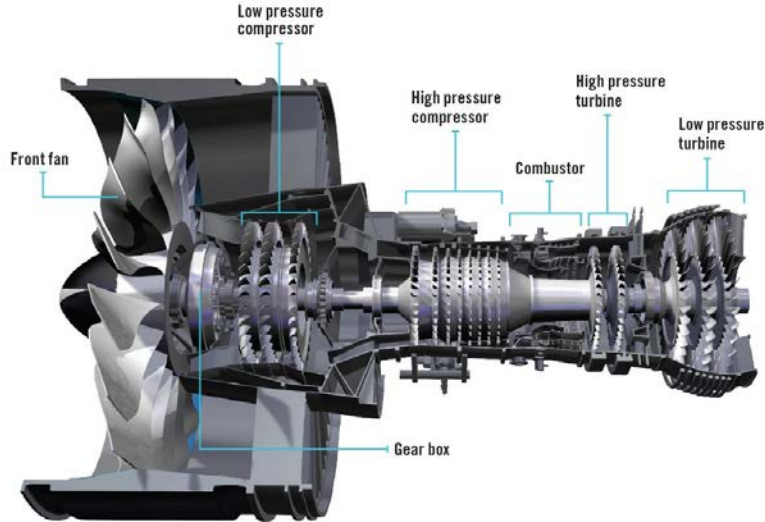
The 81 [in] diameter fan provides a higher bypass ratio which is set to be around 12:1, and together with gearbox contributes to deliver a higher propulsive efficiency. Consequently there is less need for a high performance engine core, ensuring constant improvements in terms of fuel consumption and gear design over the next decade.

The engine provides a 25% improvement in repairing cycles of Life-Limited Parts compared to similar engines, reducing overall maintenance costs.

The PW1000G engine is claimed to improve fuel burn up to 16% providing lower carbon emissions and the floatwall/TALON X combustor allows up to 50% margin in NOx emissions relative to CAEP/6 standards.

P&W says that the engine is also from 50% to 75% quieter.

Fig. 3.6: PW1000G cutaway (Credit: P&W)



In the table below are reported the PW1124G-JM main characteristics. The thesis is focused on this particular engine variant.

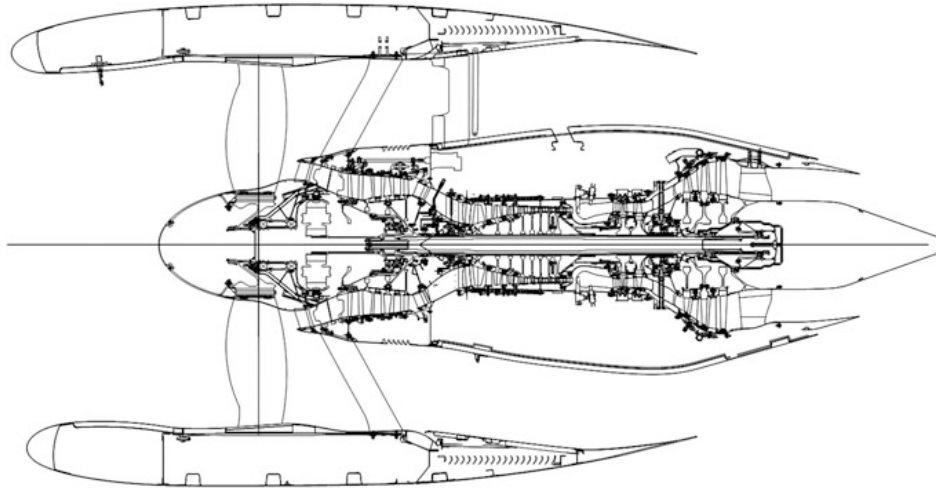
<i>PW1124G-JM technical data</i>			<i>Notes</i>
Thrust	[lbf]	24240	Take-Off
Bypass Ratio		12.5:1	
Fan diameter	[in]	81	At fan tip
Fan blades		20	
Compressor stages		1/3/8	Fan/Booster/HPC
Turbine stages		2/3	HPT/LPT
Combustor		TALON X	
Transmission		Double-spool	Geared
Aircraft		Airbus A319neo	

Tab. 3.2: PW1124G-JM technical data

3.2.1 Geometrical information

By using an available, fine detailed, cutaway image of the engine it is possible to evaluate by geometrical proportion a series of quantities which are useful for the engine analysis in GasTurb software. This is possible by taking into account the diameter of fan which is a known value. It is recalled that the fan diameter is 81 [in].

Fig. 3.7: Pratt & Whitney PW1000G cutaway (Kurzke Halliwell, see [2])



4. ENGINE RATINGS AND TECHNICAL DATA

4.1 *Engine Ratings*

The maximum amount of thrust that could be set at each operating condition during flight is established by engine ratings. Usually operating conditions refers to Take-Off, Maximum Continuous, Maximum Climb, Maximum Cruise and Idle.

Engine manufacturers establish ratings to ensure safe engine operations. These operating limits are declared to certifying authorities of each country. In the United States engine ratings are defined from the Federal Aviation Administration (FAA) and are published in the Definitions and Abbreviations document of the Federal Aviation Regulations.

Ratings for Take-Off and Maximum Continuous operations are given by the manufacturer and then published for each engine series and specific model. Once approved by FAA these ratings expressed in terms of pounds of thrust are reported in the FAA Type Certificate Data Sheet.

While Take-Off and Maximum Continuous ratings requires the approval from the certifying authority, the Maximum Climb and Maximum Cruise ratings for a commercial engine are values set by the engine manufacturer and not subjected to regulation.

Literature [8] gives detailed information of thrust ratings and general instructions for Pratt & Whitney turbojet and turbofan engines as reported below.

Engine ratings are taken into account in order to build a reasonable engine model in GasTurb software, which can best simulate the real performance of the engine in terms of delivered thrust during specific flight conditions. Thrust values are needed to set up the thermodynamic cycle of the engine.

Maximum Take-Off (MTO)

This is the maximum value of thrust certified for take-off and this setting produces the maximum Turbine Entry Temperature (TET). This rating is time-limited usually for 5 minutes as specified in the TCDS documentation in order to ensure adequate engine lifetime, and is intended to be used only

during take-off, go around and for reverse thrust operation during landing when aircraft certification allows it.

Usually it is selected by setting the aircraft throttle to obtain the computed Take-Off rating thrust in terms of Engine Pressure Ratio (EPR) for the current ambient conditions.

The maximum value of thrust is obtained for an engine when it is running at fixed point ($M=0$). However for a turbofan engine during take-off the most critical condition is obtained at around $M=0.25$ when lift off occurs at the end of the runway. In that situation the engine is subjected to high temperatures and stresses which determine the maximum 5-minute time limitation of this rating.

Maximum Continuous (MCT)

This is the maximum value of thrust certified for continuous use at all operating conditions.

This rating is not time-limited as for the previous one but it is intended to be used in emergency conditions in order to not reduce engine lifetime.

Engine must operate within operating limits in terms of temperatures and spool speed while producing this rated level of thrust in order to be considered airworthy.

Maximum Climb (MCL)

This is the maximum thrust allowed for normal climb. It is not regulated by FAA so it is not available in the TCDS documentation. This thrust setting is obtained by setting throttle position in order to obtain a predetermined EPR value.

The top-of-climb condition achieved at the end of the climb phase is one of the more critical operating point for a turbofan engine and it represents an important design condition.

Maximum Cruise (MCR)

This is the maximum thrust approved for cruise operation.

Flight Idle

This rating sets the minimum value of thrust during normal flight operation. Usually it is determined to avoid aircraft flutter and to comply with surge margin requirements. In this condition the engine is still running and is

able to provide the required auxiliary services such as cabin pressurization or hydraulic power.

Ground Idle

The engine is running and the minimum thrust configuration is used for ground operations and taxiing. Usually it is set to guarantee the functioning of secondary services to the aircraft.

Flat Rating

As reported in literature [8] flat rating is defined as an engine rating schedule which offers a constant level of engine thrust over a range of ambient or compressor inlet temperature.

4.2 Type Certificate Data Sheet

A type certificate is a document issued by the regulating body of each country which establishes that the engine is certified for flight.

The purpose is to establish that the engine design is approved and responds to all airworthiness requirements. Once issued the design cannot be modified.

Airworthiness requirements are usually described as the Minimum Operating Performance Standards (MOPS) for every aircraft equipment, including additional components or secondary units whose performance must be guaranteed during all aircraft operations.

Regulating authorities are, for example, the European Aviation Safety Agency (EASA) or the Federal Aviation Administration (FAA).

Engine design parameters are required in order to simulate a model representing each engine in GasTurb software. However, this type of information is hard to find. A wide variety of parameters could be obtained from the Type Certificate Data Sheet of the engine.

Useful information involving measured quantities during engine certification process could be found in the TCDS for different operating conditions corresponding to engine ratings. These quantities make possible to set the thermodynamic cycle of the engine in GasTurb software so that the simulated engine model represents with high fidelity the real engine.

The following PW1100G TCDS is taken into consideration for this thesis.

4.2.1 Example of TCDS: PW1124G-JM

This engine belongs to P&W PW1000G Family and it is indeed one of the derated versions of the engine family.

The TCDS in this case is the same for all the listed PW1100G engines. The only one difference is that the flat rating temperature could vary for different engine variants.

At the beginning of the Pratt & Whitney PW1100G Type Certificate Data Sheet a general description of the engine is initially introduced:

"High bypass ratio, axial-airflow, dual-spool, turbofan engine controlled by a Full Authority Digital Engine Control (FADEC). The Low-Pressure spool consists of a three-stage Low-Pressure turbine that drives a three-stage Low-Pressure compressor, and a single stage high bypass ratio fan drive gear speed reduction system. The High-Pressure compressor has eight axial stages driven by a two-stage cooled High-Pressure turbine".

Engine equipment, dimensions and dry weight are then introduced.

The following section reports engine ratings for all the engine variants. Ambient condition during test procedures are specified as "Sea level static, standard pressure 1.01 bar (14.696 psia), up to the flat rating ambient temperature."

Another test condition is the "Ideal inlet" assumption which brings to a 100% ram (pressure) recovery.

There are also information about the fuel described from the Fuel lower heating value of 42798 [kJ/kg].

Two engine ratings are reported and involve the Take-Off and the Maximum Continuous thrust settings at Sea level static conditions.

Fig. 4.1: TCDS thrust ratings (EASA, see [16])

6. Ratings

The engine ratings are based on calibrated test stand performance under the following conditions:

- Sea level static, standard pressure 1.01 bar (14.696 psia), up to the flat rating ambient temperature.
- No customer bleed or customer horsepower extraction.
- Ideal inlet, 100% ram recovery.
- Production aircraft flight cowlng.
- Production instrumentation.
- Fuel lower heating value 42798 kJ/kg (18400 BTU/lb).

Model	Sea Level Static Thrust	
	Take-Off (5 min.)	Maximum Continuous
PW1133G-JM	147.28 kN (33110 lbf)	145.81 kN (32780 lbf)
PW1133GA-JM	147.28 kN (33110 lbf)	145.81 kN (32780 lbf)
PW1130G-JM	147.28 kN (33110 lbf)	145.81 kN (32780 lbf)
PW1127G-JM	120.43 kN (27075 lbf)	117.18 kN (26345 lbf)
PW1127GA-JM	120.43 kN (27075 lbf)	117.18 kN (26345 lbf)
PW1127G1-JM	120.43 kN (27075 lbf)	117.18 kN (26345 lbf)
PW1124G-JM	107.82 kN (24240 lbf)	106.91 kN (24035 lbf)
PW1124G1-JM	107.82 kN (24240 lbf)	106.91 kN (24035 lbf)
PW1122G-JM	107.82 kN (24240 lbf)	106.91 kN (24035 lbf)
PW1431G-JM	140.39 kN (31572 lbf)	138.19 kN (31068 lbf)
PW1129G-JM	130.00 kN (29245 lbf)	117.19 kN (26345 lbf)
PW1431GA-JM	140.44 kN (31572 lbf)	138.20 kN (31068 lbf)
PW1431GH-JM	140.44 kN (31572 lbf)	138.20 kN (31068 lbf)
PW1428G-JM	132.38 kN (29761 lbf)	126.55 kN (28450 lbf)
PW1428GA-JM	132.38 kN (29761 lbf)	126.55 kN (28450 lbf)
PW1428GH-JM	132.38 kN (29761 lbf)	126.55 kN (28450 lbf)
-Flat rating ambient temperature Takeoff:		
30°C/86°F for models PW1133G-JM, PW1133GA-JM, PW1130G-JM, PW1431G-JM, PW1428G-JM, PW1428GA-JM, PW1428GH-JM, PW1431GA-JM, PW1431GH-JM		
47°C/117°F for models PW1127G-JM, PW1127GA-JM and PW1127G1-JM		
51°C/123°C for models PW1124G-JM, PW1124G1-JM and PW1122G-JM		
44°C/111°F for PW1129G-JM		
-Flat rating ambient temperature Maximum Continuous: 25°C/77°F for all models		

Ambient temperature during tests is defined as the Flat rating ambient temperature for Take-Off:

30 [°C] / 86 [°F] for models PW1133G-JM, PW1133GA-JM, PW1130G-JM, PW1431G-JM, PW1428G-JM, PW1428GA-JM, PW1428GH-JM, PW1431GA-JM, PW1431GH-JM.

This rating provides the engine thrust during static conditions which is a main simulation parameter in GasTurb.

In the following TCDS section the air mass flow rates for nacelle anti-ice and customer services are measured as a fraction of the engine core air mass flow rate.

Fig. 4.2: TCDS air bleed limits (EASA, see [16])

10. Maximum Permissible Air Bleed Extraction

Customer ECS/WAI:	18.2% W25
Nacelle Anti Ice:	1.2% W25

Subsequently limits involving maximum temperatures and maximum rotational speeds of the spools are set. Temperature limits are indicated in terms of ITT (Indicated Turbine Temperature) for different operating conditions. As far as P&W engines are concerned, the maximum ITT temperature is usually measured in the interstage between the High-Pressure turbine and the Low-Pressure turbine.

Fig. 4.3: TCDS temperature limits (EASA, see [16])

1. Temperature Limits

Maximum permissible Indicated Turbine Temperatures (ITT), °C(°F):

Take-Off (5 minutes)*	Maximum Continuous	At start-up
1083 (1982)	1043 (1909)	1083 (1982)
*: The normal 5 minute takeoff rating may be extended to 10 minutes for engine out contingency.		

Operating limits concerning the maximum rotational speeds for both the Low-Pressure (N1) and the High-Pressure (N2) spool are defined for different conditions. Reference is also made to the gear ratio which is 1:3.0625 .

Fig. 4.4: TCDS speed limits (EASA, see [16])

2. Speed Limits

Low Pressure Rotor (N1) rpm			High Pressure Rotor (N2) rpm		
Maximum permissible	Minimum at Ground Idle	Minimum at Flight Idle	Maximum permissible	Minimum at Ground Idle	Minimum at Flight Idle
10047	1750	1801	22300	12400	12400
Notes: -Power setting, power checks, and control of engine thrust output in all operations are based on Low Rotor Speed (N1). The Fan Speed (NFAN) is directly proportional to N1 by a gear ratio of 1:3.0625. -The minimum N1 certified for in-flight operation in icing conditions is 1801 rpm. The Electronic Engine Control will prevent rotor speeds below this value while in flight.					

4.2.2 No TCDS: GE9X

The engine is currently under testing. No TCDS is available for this engine at the moment.

In the thesis TCDS from similar engines are used to make assumptions on some engine parameters. In particular I considered TCDS information of the General Electric GE90-115B and Genx engines.

4.3 *ICAO Aircraft Engine Emissions Databank*

Other useful information, concerning real engine parameters involving the GasTurb model used during simulation, could be found also in the ICAO Aircraft Engine Emissions Databank. It is a database containing engine exhaust emissions in terms of various combustion gaseous products that are limited to standard levels by the Convention on International Civil Aviation. Information about all modern certified engines can be found there.

This type of documentation is useful because information about Overall Pressure Ratio of the engine and the fuel consumption for different operating conditions could be retrieved.

An example of the data-sheet contained in the databank is reported below for the Pratt & Whitney PW1124G-JM engine.

In the first part of the document useful information concerns engine bypass ratio, overall pressure ratio and rated thrust. Subsequently the measured data about fuel consumption, in terms of fuel flow, for different engine thrust settings along with emission indices of combustion products are reported. A reference about ambient test conditions is provided.

Fig. 4.5: PW1124G-JM datasheet (ICAO, see [17])



ICAO ENGINE EXHAUST EMISSIONS DATA BANK

SUBSONIC ENGINES

ENGINE IDENTIFICATION: PW1124G-JM BYPASS RATIO: 12.7
 UNIQUE ID NUMBER: 18PW119 PRESSURE RATIO (π_{c2}): 29.8
 ENGINE TYPE: TF RATED OUTPUT (F_{30}) (kN): 107.8

REGULATORY DATA

CHARACTERISTIC VALUE:	HC	CO	NOX	SMOKE NUMBER
D_p/F_{30} (g/kN) or SN	0.9	40.3	25.7	12.7
AS % OF ORIGINAL LIMIT	5.0 %	34.0 %	26.0 %	55.0 %
AS % OF CAEP/2 LIMIT (NOx)			33.0 %	
AS % OF CAEP/4 LIMIT (NOx)			40.0 %	
AS % OF CAEP/6 LIMIT (NOx)			45.0 %	
AS % OF CAEP/8 LIMIT (NOx)			53.0 %	

DATA STATUS

- PRE-REGULATION
 x CERTIFICATION
 - REVISED (SEE REMARKS)

TEST ENGINE STATUS

- NEWLY MANUFACTURED ENGINES
 x DEDICATED ENGINES TO PRODUCTION STANDARD
 - OTHER (SEE REMARKS)

EMISSIONS STATUS

x DATA CORRECTED TO REFERENCE
 (ANNEX 16 VOLUME II)

CURRENT ENGINE STATUS

(IN PRODUCTION, IN SERVICE UNLESS OTHERWISE NOTED)
 - OUT OF PRODUCTION
 - OUT OF SERVICE

MEASURED DATA

MODE	POWER SETTING (% F_{30})	TIME minutes	FUEL FLOW kg/s	EMISSIONS INDICES (g/kg)			
				HC	CO	NOX	SMOKE NUMBER
TAKE-OFF	100	0.7	0.710	0.1	0.26	16.47	11.57748933
CLIMB OUT	85	2.2	0.600	0.1	0.38	13.85	7.874611069
APPROACH	30	4.0	0.210	0.02	6.39	8.92	0.419800002
IDLE	7	26.0	0.080	0.55	29.78	4.72	1.233194106
LTO TOTAL FUEL (kg) or EMISSIONS (g)			284	80	4076	2626	-
NUMBER OF ENGINES				3	3	3	3
NUMBER OF TESTS				9	9	9	9
AVERAGE D_p/F_{30} (g/kN) or AVERAGE SN (MAX)				0.77	37.22	23.8	11.57748933
SIGMA (D_p/F_{30} in g/kN, or SN)				-	-	-	-
RANGE (D_p/F_{30} in g/kN, or SN)				-	-	-	-

ACCESSORY LOADS

POWER EXTRACTION 0 (kW) AT - POWER SETTINGS
 STAGE BLEED 0 % CORE FLOW AT - POWER SETTINGS

ATMOSPHERIC CONDITIONS

BAROMETER (kPa)	99.56 - 101.71
TEMPERATURE (K)	265.6 - 278.15
ABS HUMIDITY (kg/kg)	0.00071 - 0.00203

FUEL

SPEC	Jet-A
H/C	1.86
AROM (%)	15.1% - 16.6%

MANUFACTURER: Pratt & Whitney
 TEST ORGANIZATION: Pratt & Whitney
 TEST LOCATION: X8 Test Stand, East Hartford, CT
 TEST DATES: FROM 11 Mar 14 TO 14 Mar 14

REMARKS

- Data from Certification Report PWA-11521, 3 engines tested, block C combustor
- Certification in accordance with Part III, Chapter 2, of Amendment 8 of ICAO Annex 16 Vol. II.
- NOx levels in accordance with Part III, Chapter 2, 2.3.2 e) (CAEP/8)□

4.4 Engine components efficiency and losses

With this data regarding real engine functioning it is not possible to simulate the thermodynamic cycle operated into the engine.

In order to create a thermodynamic cycle, also the efficiencies and the total pressure losses of the engine components like fan, Intermediate-Pressure compressor, High-Pressure compressor, High-Pressure turbine and Low-Pressure turbine have to be taken into account. Engine manufacturers do not disclose such relevant data about their turbomachinery.

The efficiency, in terms of isentropic or polytropic efficiency, and the total pressure loss for the various turbo-machinery however are reported in literature. In the following tables there are listed all the polytropic efficiencies and total pressure losses than can be considered during engine design for particular operating conditions.

In particular in Figure 4.6, for a turbofan engine, Mattingly in [3] summarizes component polytropic efficiencies and total pressure losses based on the level of technology of the component. In this case the fourth level of technology has to be considered as the engine simulated are produced in the years after 2005.

In Figure 4.7 by literature [2], Kurzke provides loss assumptions in terms of polytropic efficiency and total pressure loss for all the engine components during cruise conditions at Mach number $M=0.8$ at an altitude of 36000 [ft]. It is now possible with such data to reconstruct the thermodynamic cycle reproduced inside the engine using the GasTurb software.

Fig. 4.6: Component polytropic efficiencies and total pressure losses (Mattingly Heiser Pratt, see [3])

Component	Figure of merit	Type	Level of technology			
			1	2	3	4
Diffuser	$\pi_{d \max}$	A ^a	0.90	0.95	0.98	0.995
		B ^b	0.88	0.93	0.96	0.97
		C ^c	0.85	0.90	0.94	0.96
Compressor	e_c	—	0.80	0.84	0.88	0.90
Fan	e_f	—	0.78	0.82	0.86	0.89
Burner	π_b	—	0.90	0.92	0.94	0.96
	η_b	—	0.88	0.94	0.99	0.995
Turbine	e_t	Uncooled	0.80	0.85	0.89	0.91
		Cooled	—	0.83	0.87	0.89
Afterburner	π_{AB}	—	0.90	0.92	0.94	0.95
	η_{AB}	—	0.85	0.91	0.96	0.97
Nozzle	π_n	D ^d	0.95	0.97	0.98	0.995
		E ^e	0.93	0.96	0.97	0.985
		F ^f	0.90	0.93	0.95	0.98
Maximum T_{t4}		(K)	1110	1390	1780	2000
		(°R)	2000	2500	3200	3600
Maximum T_{t7}		(K)	1390	1670	2000	2220
		(°R)	2500	3000	3600	4000

^aA = subsonic aircraft with engines in nacelles.

^bB = subsonic aircraft with engine(s) in airframe.

^cC = supersonic aircraft with engine(s) in airframe.

^dD = fixed-area convergent nozzle.

^eE = variable-area convergent nozzle.

^fF = variable-area convergent-divergent nozzle.

^gStealth may reduce $\pi_{d \max}$, π_{AB} , and π_n .

Note: The levels of technology can be thought of as representing the technical capability for 20-year increments in time beginning in 1945. Thus level 3 technology presents typical component design values for the time period 1985–2005.

Fig. 4.7: Loss assumptions for the turbofan at cruise conditions 35000ft and M=0.8
(Kurzke Halliwell, see [2])

Fan	$\eta_{\text{pol}} = 0.91$
Compressor interduct	$P_{25}/P_{21} = 0.98$
Compressor	$\eta_{\text{pol}} = 0.9$
Combustor total pressure loss	$P_4/P_3 = 0.95$
HP turbine	$\eta_{\text{pol}} = 1.0625 - 0.000125 * T_4$
Turbine interduct	$P_{45}/P_{44} = 0.98$
LP turbine	$\eta_{\text{pol}} = 0.91$
Turbine exit duct	$P_6/P_5 = 0.98$
Bypass duct pressure loss	$\frac{P_{16}}{P_{13}} = 1 - \frac{0.05}{(BPR+1)^{0.4}}$
Gas generator mechanical efficiency (represents accessory drive)	$\eta_{\text{mech}} = 0.98$
High pressure air leakage to bypass	0.5% of W_{25}
High pressure air leakage to LPT exit	1% of W_{25}
High pressure air to overboard	1% of W_{25}

4.5 Engine components pressure ratios

Pressure ratio in all the engine components must be known in order to simulate the engine design cycle once the component efficiencies are set.

4.5.1 GE9X

IP compressor pressure ratio

There are no available data regarding the Intermediate-Pressure compressor pressure ratio but it must be estimated in order to simulate the engine design cycle.

From a cutaway image of the engine it is possible to deduce the IP compressor inlet diameter considering that the fan diameter is 134 [in].

By proportion the IP compressor inlet diameter evaluated at blade tip is roughly 0.5 times the one of the fan so its diameter results

$$D_{ipc,in} = 0.5 \cdot D_{lpc} = 67 \text{ [in]} = 1.702 \text{ [m]}$$

Considering an hypothetical maximum Low-Pressure spool speed (N1) of 2400 [rpm], derived from TCDS spool speeds data of both the GE90 and GENx engines, the angular velocity of the shaft is

$$\omega_{LP} = 2400 \cdot \frac{2\pi}{60} = 251.327 \text{ [rad/s]}$$

It is now possible to evaluate the linear velocity of the compressor blade tip at estimated radius as

$$u_{tip} = \omega_{LP} \cdot \frac{D_{ipc,in}}{2} = 213.855 \text{ [m/s]}$$

From initial simulations we can consider a IP compressor inlet static temperature T_{22} that ranges from 313 [K] to 323 [K] according to a possible fan pressure ratio $\pi_{lpc} \sim 1.3$ and once finally assumed that $T_{22} = 318$ [K].

Evaluating the corresponding Mach number as

$$M_u = \frac{u_{tip}}{\sqrt{k \cdot R \cdot T_{22}}} = 0.598$$

and assuming an inlet Mach number of 0.4 for the absolute flow M_a which is considered to be purely axial, it is possible to obtain the inlet relative Mach number at blade tip as

$$M_w = \sqrt{M_u^2 + M_a^2} = 0.719$$

and it is possible to assume that the compressor has to be a subsonic unit. Statistically by literature [1] subsonic axial compressor stages can achieve a maximum pressure ratio of about $\pi_C = 1.3$.

Considering a mean compression ratio of 1.2 for each of the three IP compressor stages, a minimum value for the IP compressor pressure ratio is calculated as

$$\pi_{ipc,max} = (1.2)^3 = 1.728$$

while considering a mean compression ratio of 1.15 for each stage of the IP compressor pressure ratio brings to an IPC pressure ratio of about

$$\pi_{ipc,min} = (1.15)^3 = 1.521$$

This is the range assumed for the IP compressor pressure ratio in the optimization process of the Design Cycle.

HP compressor pressure ratio

No information is available in order to estimate the HP compressor pressure ratio.

From a cutaway image of the engine it is possible to deduce the HP compressor inlet diameter considering that the fan diameter is 134 [in]. By proportion the HP compressor inlet diameter evaluated at blade tip is equal to

$$D_{hpc,in} = 0.264 \cdot D_{ipc} = 35.327 [in] = 0.897 [m]$$

Considering a maximum High-Pressure spool speed (N2) of 10600 [rpm] deduced from similar considerations on the GE90's and GENx's TCDS reported spool speeds, it is possible to calculate the angular velocity of the High-Pressure spool moving the HP compressor

$$\omega_{HP} = 10600 \cdot \frac{2\pi}{60} = 1110.029 [rad/s]$$

It is possible to calculate the compressor blade linear velocity at tip radius as

$$u_{tip} = \omega_{HP} \cdot \frac{D_{hpc,in}}{2} = 498.022 [m/s]$$

which is a value that could indicate that the compressor is a transonic unit since statistically the blade tip linear velocity of a axial-flow transonic compressor at inlet section usually varies from 500 to 550 [m/s]. From initial simulations it is possible to consider an HP compressor inlet static temperature T_{25} of about 400 [K].

The corresponding Mach number is then

$$M_u = \frac{u_{tip}}{\sqrt{k \cdot R \cdot T_{25}}} = 1.242$$

and assuming an inlet Mach number of 0.35 for the absolute flow M_a which is considered to be purely axial, it is possible to obtain the inlet relative Mach number at blade tip as

$$M_w = \sqrt{M_u^2 + M_a^2} = 1.290$$

which confirms that the compressor has to be a 11-stage transonic unit since statistically inlet relative Mach numbers at blade tip for transonic axial compressors usually range from 1.25 to 1.35 .

Statistically, by literature [1] while subsonic axial compressors can achieve pressure ratios of about $\pi_C = 1.3$, for a transonic axial compressor stage the compression ratio ranges from $\pi_C = 1.4$ up to $\pi_C = 2.4$.

Considering a mean compression ratio equal to 1.3 for each of the eleven HP compressor stages, we obtain a minimum value for the HP compressor pressure ratio as

$$\pi_{C,min} = (1.3)^{11} = 17.92$$

If we consider a mean compression ratio equal to 1.35 for each of the eleven HP compressor stages it could be obtained a maximum HP compressor pressure ratio of about

$$\pi_{C,max} = (1.35)^{11} = 27.14$$

In General Electric brochures about the GE9X engine the company claims an outstanding HPC pressure ratio of about 27:1. The operating condition at which this value is referred is not known. This information is however in line with the assumption stated above.

Finally I assumed that the HP compressor pressure ratio in our optimization process varies within the range of values calculated above.

Overall Pressure Ratio

In the GE9X information sheet it is also reported that the engine is characterized by an Overall Pressure Ratio (OPR) of about 61:1. Although it is still not known at which operating condition it refers, it is possible to assume that this high value is obtained only at cruise condition while at take-off the Overall Pressure Ratio should be lower.

In this case referring to the numbering scheme for the engine thermodynamic

stations reported in Figure 5.21, the Overall Pressure Ratio represents the ratio between the total pressure at the High-Pressure compressor outlet and the total pressure at the fan inlet.

It results in particular

$$OPR = \frac{p_3^\circ}{p_2^\circ}$$

The value of the Overall Pressure Ratio is used in order to find the proper Cycle Design point of the engine.

HP turbine expansion ratio

Information about the expansion ratio of the High-Pressure turbine are not available for the engine. The expansion ratio of the HP turbine needs to be estimated in order to evaluate the expansion ratio obtained from the optimization.

As far as turbines are concerned, we define the work coefficient ψ of the turbine stage as

$$\psi = \frac{L}{u^2}$$

where

L : work extracted from the turbine

u : blade linear velocity at mean radius

Considering that the maximum rotational speed assumed for the High-Pressure spool (N2) which is 10600 [rpm], the angular velocity of the High-Pressure spool was previously calculated as

$$\omega_{HP} = 10600 \cdot \frac{2\pi}{60} = 1110.029 \text{ [rad/s]}$$

Using the cutaway image of the engine we can estimate the mean diameter of the High-Pressure turbine related to the diameter of the fan (which is 134 [in]). We can calculate the mean radius as

$$D_{hpt,mean} = 0.273 \cdot D_{lpc} = 35.327 \text{ [in]} = 0.897 \text{ [m]}$$

Now it is possible to estimate the blade linear velocity u at mean radius as

$$u_{mean} = \omega_{HP} \cdot \frac{D_{hpt,mean}}{2} = 498.022 \text{ [m/s]}$$

It is possible to estimate the expansion ratio of a turbine if we consider the expression for the turbine extracted work

$$L = c_p \cdot (T_{IN}^\circ - T_{OUT}^\circ) \quad (4.1)$$

together with the expression valid for a polytropic transformation, which associates the difference of total pressure to the difference of total temperature and also the polytropic efficiency

$$\frac{T_{OUT}^\circ}{T_{IN}^\circ} = \left(\frac{p_{OUT}^\circ}{p_{IN}^\circ} \right)^{\frac{k}{\eta_{pol}(k-1)}} \quad (4.2)$$

and considering that the expansion ratio of the turbine is defined as the ratio between the total pressure of the flow at the turbine inlet and the total pressure of the flow at the turbine outlet

$$\pi_e = \frac{p_{IN}^\circ}{p_{OUT}^\circ} \quad (4.3)$$

The following expression is then obtained

$$L = \psi \cdot u^2 = \frac{k \cdot R \cdot T_{IN}^\circ}{k-1} \left[1 - \left(\frac{1}{\pi_e} \right)^{\frac{\eta_{pol}(k-1)}{k}} \right] \quad (4.4)$$

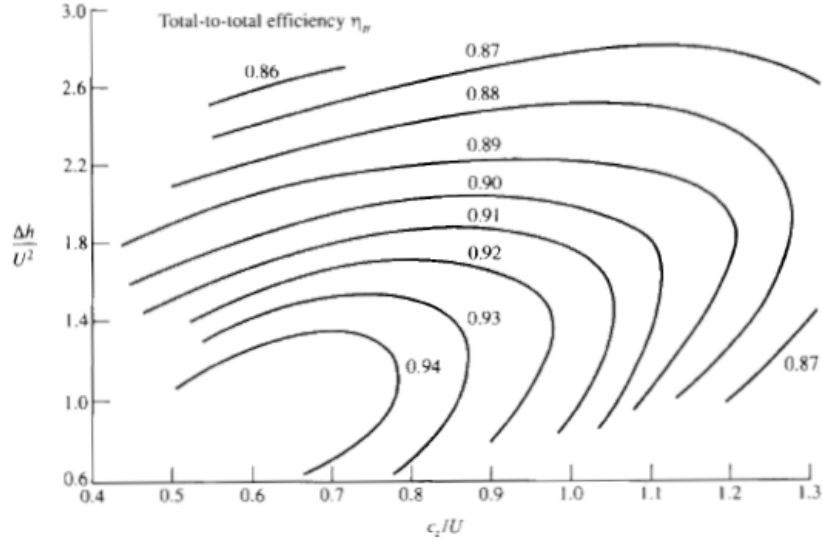
and now the expansion ratio π_e of the turbine can be evaluated and results

$$\pi_e = \left\{ 1 - \left[\frac{\psi \cdot u^2 \cdot (k-1)}{k \cdot R \cdot T_{IN}^\circ} \right] \right\}^{\frac{k}{\eta_{pol}(1-k)}} \quad (4.5)$$

In this equation the blade linear velocity u was previously calculated taking into account geometrical considerations. The constant k of the gas is known and the polytropic efficiency was supposed from literature [2]. The work coefficient ψ must be discovered.

From literature [14] it is possible to use the Kacker and Okapuu diagram which summarizes performance of several gas turbines working in design conditions. It represents the isentropic total-total efficiency of the turbine in function of the work coefficient ψ and the flow coefficient ϕ . As it can be seen, in order to obtain maximum isentropic efficiencies the work coefficient has to be ~ 1 while the flow coefficient has to be ~ 0.6 .

Fig. 4.8: Kacker & Okapuu diagram (Benini, see [1])



However, as reported in literature [1], in an aeronautical engine turbines with a lower number of stages are preferred in order to minimize the weight of the component. This results in heavy loaded turbines with lower efficiencies and in this case the work flow coefficient can also be as high as 2 or even more.

Considering the following assumptions:

$\psi = 1.6$ suggested from literature [1] and [2]

$k = 1.33$

$T_{IN}^\circ = 2000$ [K] from literature [3]

$R = 287.15$ [J/kgK]

$\eta_{pol} = 0.89$ from literature [2] for cooled turbine stages

It is possible to obtain the mean expansion ratio for each stage of the High-Pressure turbine $\pi_e = 2.344$.

The following stages while considering the same work coefficient ψ will have a lower expansion ratio due to the fact that the velocity at tip increases as the mean radius of the turbine stage increases and the stage inlet total temperature decreases as the flow is expanded.

Considering a mean expansion ratio for all the stages it is possible to finally estimate the expansion ratio of the High-Pressure turbine as

$$\pi_e = (2.344)^2 = 5.493$$

It is possible to assume an EGT temperature value, which could be evaluated

from the TCDSs of the GE90 and the GENx engines. EGT in this case is defined as the total temperature measured at LPT inlet and its maximum value is reported in the engine TCDS. It varies (at Take-Off) from 1060 [°C] in the GENx-2B67 engine to 1090 [°C] in the GE90-115B engine.

Considering the assumptions

$$k = 1.33$$

$$T_{IN}^{\circ} = 2000 [K] \text{ from literature [3]}$$

$$T_{OUT}^{\circ} = 1363.15 [K] \text{ evaluated from GE90 TCDS}$$

$$R = 287.15 [J/kg/K]$$

$$\eta_{pol} = 0.89 \text{ from literature [2] for cooled turbine stages}$$

it is possible to evaluate the maximum achievable turbine expansion ratio which results

$$\pi_e = \left(\frac{T_{IN}^0}{T_{OUT}^0} \right)^{\frac{k}{\eta_{pol}^{k-1}}} = 5.677$$

which makes the previous calculated value acceptable.

LP turbine expansion ratio

Similar considerations can be done to evaluate the Low-Pressure turbine expansion ratio.

In this case there is no information about the Interstage Turbine Temperature (ITT) at the turbine inlet section.

From the assumed maximum Low-Pressure spool speed (N1) of 2400 [rpm] which gives the angular velocity of the Low-Pressure spool as

$$\omega_{LP} = 2400 \cdot \frac{2\pi}{60} = 251.329 [rad/s]$$

From the cutaway section of the engine the mean diameter of the Low-Pressure turbine can be estimated by comparing it to the fan diameter, and it results

$$D_{lpt,mean} = 0.5 \cdot D_{lpc} = 67 [in] = 1.702 [m]$$

Now it is possible to estimate the blade linear velocity u at mean radius as

$$u_{mean} = \omega_{LP} \cdot \frac{D_{lpt,mean}}{2} = 213.855 [m/s]$$

It is possible to evaluate the expansion ratio π_e using equation (4.5).

Considering the following assumptions:

$$\psi = 2.5 \text{ allowed from literature [1] and [2]}$$

$$k = 1.33$$

$T_{IN}^{\circ} = T_{45}^0 = 1363.15 [K]$ evaluated from GE90 TCDS
 $R = 287.15 [J/kg/K]$
 $\eta_{pol} = 0.91$ from literature [2] for uncooled turbine stages

Finally it is possible to obtain the mean expansion ratio for each stage of the low-Pressure turbine $\pi_e = 1.395$.

Taking into account the value calculated, the expansion ratio of the Low-Pressure turbine would be equal to

$$\pi_e = (1.395)^6 = 7.384$$

while considering a constant mean expansion ratio for all the turbine stages. From literature [2] it is possible to see that temperature at LPT outlet usually ranges from 850 [K] to 870 [K]. This value allows to calculate the maximum expansion ratio achievable considering that

$$k = 1.33$$

$T_{IN}^{\circ} = 1363.15 [K]$ from literature [3]

$T_{OUT}^{\circ} = 860 [K]$ evaluated from literature

$R = 287.15 [J/kg/K]$

$\eta_{pol} = 0.91$ from literature [2] for uncooled turbine stages

so the expansion ratio results

$$\pi_e = \left(\frac{T_{IN}^0}{T_{OUT}^0} \right)^{\frac{k}{\eta_{pol}(k-1)}} = 7.691$$

which makes the previous calculated value acceptable.

4.5.2 PW1124G-JM

IP Compressor pressure ratio

There are no information about the Intermediate-Pressure compressor pressure ratio but it is necessary to estimate it in order to simulate the engine model.

From a cutaway image of the engine one can deduce the IP compressor inlet diameter considering that the fan diameter is 81 [in].

By proportion the IP compressor inlet diameter is roughly 0.4 times the one of the fan. The same is possible for the outlet section of the IP compressor. The estimated diameter of the IPC can be obtained as:

$$D_{ipc,tip} = 0.373 \cdot D_{lpc} = 32.4 [in] = 0.823 [m]$$

Considering the maximum Low-Pressure spool speed (N1) reported in the TCDS, the angular velocity of the Low-Pressure spool moving the IP compressor

$$\omega_{LP} = 10047 \cdot \frac{2\pi}{60} = 1052.12 [rad/s]$$

It is possible to calculate the velocity of the IP compressor blade at tip radius as

$$u_{tip} = \omega_{LP} \cdot \frac{D_{ipc,tip}}{2} = 432.947 [m/s]$$

From initial simulations it is possible to consider an IP compressor inlet temperature T_{22} that ranges from 320 [K] to 323 [K]. It is assumed that $T_{22} = 318 [K]$.

The related Mach number results

$$M_u = \frac{u_{tip}}{\sqrt{k \cdot R \cdot T_{22}}} = 1.211$$

and assuming an inlet Mach number of 0.4 for the absolute flow M_a which is considered to be purely axial, it is possible to obtain the inlet relative Mach number at blade tip as

$$M_w = \sqrt{M_u^2 + M_a^2} = 1.275$$

and it is possible to assume that the compressor has to be a transonic unit. Considering a mean compression ratio of 1.2 for each one of the three IP compressor stages, a minimum value for the IP compressor pressure ratio could be

$$\pi_{C,min} = (1.2)^3 = 1.728$$

Considering a mean compression ratio of 1.35 for each one of the three IP compressor stages leads to a maximum value for the IP compressor pressure ratio equal to

$$\pi_{C,max} = (1.35)^3 = 2.460$$

Finally the IP compressor pressure ratio in the optimization process has to be chosen within this range of values.

HP Compressor pressure ratio

No data regarding the High-Pressure compressor pressure ratio is available, but it is necessary to estimate it in order to simulate the engine model.

From a cutaway image of the engine one can deduce the HP compressor inlet diameter considering that the fan diameter is 81 [in].

By proportion the HP compressor inlet diameter is roughly half the one of the fan. It is possible to obtain the mean diameter of the HPC:

$$D_{hpc,tip} = 0,248 \cdot D_{lpc} = 18 [in] = 0.457 [m]$$

Considering the maximum High-Pressure spool speed (N2) reported in the TCDS, the angular velocity of the High-Pressure spool moving the HP compressor

$$\omega_{HP} = 22300 \cdot \frac{2\pi}{60} = 2335.25 [rad/s]$$

It is possible to calculate the linear velocity of the compressor blade at tip radius as

$$u_{tip} = \omega_{HP} \cdot \frac{D_{hpc,tip}}{2} = 533.838 [m/s]$$

From initial simulations it is possible to consider a HP compressor inlet temperature T_{45} that ranges from 375 [K] to 395 [K]. I considered T_{45} equal to 385 [K].

Evaluating the corresponding Mach number as

$$M_u = \frac{u_{tip}}{\sqrt{k \cdot R \cdot T_{45}}} = 1.357$$

and assuming an inlet Mach number of 0.35 for the absolute flow M_a which is considered to be purely axial, it is possible to obtain the inlet relative Mach number at blade tip as

$$M_w = \sqrt{M_u^2 + M_a^2} = 1.401$$

which confirms that the compressor has to be a transonic unit since statistically inlet relative Mach numbers at blade tip for transonic axial compressors usually range from 1.25 to 1.35 .

Statistically, while subsonic axial compressor stages can achieve pressure ratios of about $\pi_C = 1.3$, for a transonic axial compressor stage the compression ratio ranges from $\pi_C = 1.4$ up to $\pi_C = 2.4$.

Considering a mean compression ratio equal to 1.4 for each of the eight HP compressor stages, a minimum value for the HP compressor pressure ratio as

$$\pi_{C,min} = (1.4)^8 = 14.76$$

If it is considered a mean compression ratio equal to 1.45 for each of the eight HP compressor stages it is possible to obtain a maximum value for the HP compressor pressure ratio as

$$\pi_{C,max} = (1.45)^8 = 19.54$$

Finally it is assumed that the HP compressor pressure ratio in the optimization process varies within this range of values.

HPT expansion ratio

Information about the expansion ratio of the High-Pressure turbine are not available for the engine. The expansion ratio of the HP turbine need to be discovered to evaluate the expansion ratio obtained from the optimization.

The same procedure used to calculate the turbine expansion ratio in the GE9X engine case is now implemented. TCDS gives the maximum speed for the High-Pressure spool (N2) which is 22300 [rpm] and so the maximum angular velocity of the High-Pressure spool is

$$\omega_{HP} = 22300 \cdot \frac{2\pi}{60} = 2335.25 [rad/s]$$

Using the cutaway image of the engine it is possible to estimate the mean diameter of the High-Pressure turbine which results ~ 0.245 times the diameter of the fan (which is 81 [in]). The mean radius could be calculated as

$$D_{hpt,mean} = 0.245 \cdot D_{lpc} = 18.9 [in] = 0.480 [m]$$

Now it is possible to estimate the linear velocity u at mean radius as

$$u_{mean} = \omega_{HP} \cdot \frac{D_{hpt,mean}}{2} = 560.5305 [m/s]$$

Considering the procedure used for the same calculation in the GE9X case, in particular the equation (4.5) together with the Kacker and Okapuu diagram reported in Figure 4.8 and taking into account the following assumptions:

$$\psi = 1.6$$

$$k = 1.33$$

$$T_{IN}^{\circ} = 1770 [K]$$

$$R = 287.15 [J/kg/K]$$

$$\eta_{pol} = 0.89 \text{ from literature [2] for cooled turbine stages}$$

Using equation (4.5) it is possible to obtain the expansion ratio for the High-Pressure turbine $\pi_e = 5.912$.

It is possible to evaluate the maximum expansion ratio achievable since the inlet and the outlet turbine total temperature could be evaluated from literature and TCDS information.

Considering the assumptions

$$k = 1.33$$

$$T_{IN}^{\circ} = 2000 [K] \text{ from literature [3]}$$

$$T_{OUT}^{\circ} = 1356.15 [K] \text{ evaluated from TCDS}$$

$$R = 287.15 [J/kg/K]$$

$$\eta_{pol} = 0.89 \text{ from literature [2] for cooled turbine stages}$$

it is possible to evaluate the maximum achievable turbine expansion ratio which results

$$\pi_e = \left(\frac{T_{IN}^0}{T_{OUT}^0} \right)^{\frac{k}{\eta_{pol}(k-1)}} = 5.808$$

which makes the previous calculated value acceptable.

LPT expansion ratio

Similar considerations can be done to evaluate the Low-Pressure turbine expansion ratio.

In this case from TCDS the inlet turbine temperature is represented by the interstage turbine temperature (ITT) which is $T_{IN}^0 = T_{45}^0 = 1083 [^{\circ}C]$. From the TCDS the maximum Low-Pressure spool speed (N1) is 10047 [rpm] which gives the angular velocity of the Low-Pressure spool as

$$\omega_{LP} = 10047 \cdot \frac{2\pi}{60} = 1052.119 \text{ [rad/s]}$$

From the cutaway section of the engine one could estimate the mean diameter of the Low-Pressure turbine in relation to the fan diameter and it results

$$D_{lpt,mean} = 0.544 \cdot D_{lpc} = 33.75 \text{ [in]} = 0.857 \text{ [m]}$$

Now it is possible to estimate the linear velocity u at mean radius as

$$u_{mean} = \omega_{LP} \cdot \frac{D_{lpt,mean}}{2} = 450.965 \text{ [m/s]}$$

It is now possible to evaluate the expansion ratio π_e of the turbine using the equation (4.5) and considering the following assumptions:

$$\psi = 1.7$$

$$k = 1.33$$

$$T_{IN}^\circ = T_{45}^0 = 1356.15 \text{ [K]} \text{ from TCDS}$$

$$R = 287.15 \text{ [J/kg/K]}$$

$$\eta_{pol} = 0.91 \text{ from literature [2] for uncooled turbine stages}$$

The estimated expansion ratio for the Low-Pressure turbine is $\pi_e = 8.075$.

From literature [2] it is possible to see that temperature at LPT outlet usually ranges from 850 [K] to 870 [K]. This value allow to calculate the maximum expansion ratio achievable considering that

$$k = 1.33$$

$$T_{IN}^\circ = 1356.15 \text{ [K]} \text{ from literature [3]}$$

$$T_{OUT}^\circ = 860 \text{ [K]} \text{ evaluated from literature}$$

$$R = 287.15 \text{ [J/kg/K]}$$

$$\eta_{pol} = 0.91 \text{ from literature [2] for uncooled turbine stages}$$

so the expansion ratio results

$$\pi_e = \left(\frac{T_{IN}^0}{T_{OUT}^0} \right)^{\frac{k}{\eta_{pol}(k-1)}} = 7.518$$

which makes the previous calculated value acceptable.

5. GASTURB SOFTWARE

GasTurb consists of a gas turbine cycle software allowing calculations of gas turbine performance for both design and off-design conditions. It features built-in simulation models of common types of aircraft propulsion systems and power generation gas turbines.

The program is able to perform parametric studies and optimization calculations. Additional functions such as plotting the temperature-entropy diagrams or showing the engine thermodynamic stations are easy to handle within the software.

A series of real component maps is provided in order to simulate off-design performance of the engines with more accuracy. It is also possible to define a flight envelope or a multi-point mission schedule which are automatically calculated in a single run.

5.1 *Introduction and basic functions*

5.1.1 *Program scope*

In GasTurb software it is possible to choose between different scopes that are characterized by an increasing simulation accuracy and details. The software features:

Basic Thermodynamics This mode is useful to analyse only basic aspects of the gas turbine cycle.

Basic thermodynamics section is split into two main menus: the Cycle Design menu, which involves only the cycle design point, and the Off Design one involving all the other possible operational conditions of the engine. A few input properties are taken into consideration for this scope because they are required only for the initial definition of the cycle. At this point, quantities like the burner inlet temperature and all the component's pressure ratios and efficiencies are requested.

Performance This mode is useful to study realistic gas turbine cycles more in depth. The mode could be set in the Engine design section and in Off

Design section there are additional options that can be used along this type of calculation.

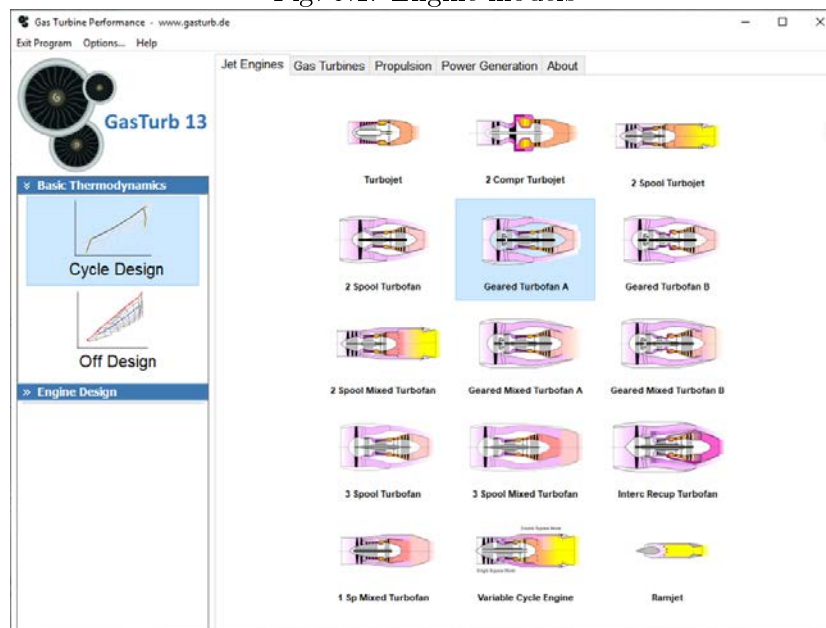
This scope is suitable for early engine design process because it takes into account further considerations required for professional performance simulations. In this case it is possible, for example, to consider also secondary air streams and turbine cooling system.

Different scopes could be set in the software main window by selecting the desired mode button in the left column.

5.1.2 Engine models

First of all the user have to select the type of gas turbine he want to simulate before starting the calculation. A wide variety of aircraft propulsion systems like turbojet engines, turbofan or even ramjet are available along with multiple gas turbines configurations. All the implemented simulation models are collected in separate tabs at the top of the main window as showed in Figure 5.1 below.

Fig. 5.1: Engine models



5.1.3 Setting up the calculation

Once the user selected the gas turbine type and the program scope, it is possible to set up the calculation.

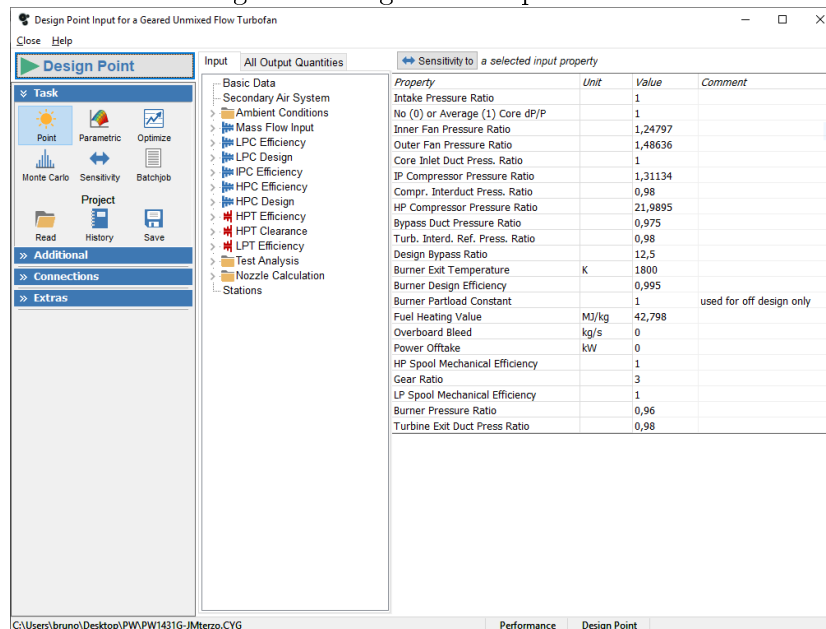
In GasTurb, all the input data are usually organized into tables. Moreover

only required quantities for the selected scope are reported in the window. Contents of this table vary according to the desired function which can be selected in the left part of the window.

Once all the required input quantities are filled in by the user, by clicking the button "Design Point" the calculation of the thermodynamic cycle begins. All input data is analysed and, if the resulting calculated cycle is correct, the data is then saved automatically in a file with extension .CY... .

It is possible that the software doesn't find a solution (a proper cycle) for the input data defined by the user. In this case GasTurb 13 supports the user by detecting possible errors involving wrong magnitudes of the input values.

Fig. 5.2: Design Point input menu



In the summary cycle page, where all calculated quantities referring to the calculated cycle are reported, the user can also use a slider in order to set up to three variables to the slider. By moving the slider the user can analyse the variation of the cycle data caused by the modified quantity.

Fig. 5.3: Summary cycle page

Station	W kg/s	T K	P kPa	WRstd kg/s		
amb						
2	214,918	223,15	26,436		FN =	29,44 kN
13	198,998	251,77	40,309	504,997	TSFC =	16,9764 g/(kN*s)
21	15,920	270,14	59,913	335,280	WF =	0,49984 kg/s
22	15,920	270,14	50,304	31,049	s NOX =	0,6129
24	15,920	294,74	65,965	24,731	Core Eff =	0,5643
25	15,920	294,74	64,946	25,236	Prop Eff =	0,7785
3	15,920	765,27	1421,532	1,849	BPR =	12,3000
31	15,522	765,27	1421,532		P2/P1 =	1,0000
4	16,022	1800,00	1364,671	2,973	P3/P2 =	35,27
41	16,022	1800,00	1364,671	2,973	P5/P2 =	2,3106
43	16,022	1424,35	417,121		P16/P13 =	0,9750
44	16,022	1424,35	417,121		P16/P6 =	0,64000
45	16,022	1424,35	408,778	8,829	P16/P2 =	1,44920
49	16,022	1046,91	93,136		P6/P5 =	0,98000
5	16,022	1046,91	93,136	33,224	AS =	0,14772 m ²
8	16,181	1044,35	91,273	34,197	A18 =	1,46136 m ²
18	199,078	286,18	58,415	344,134	XM8 =	1,00000
Bleed	0,159	765,27	1421,531		XM18 =	1,00000
Efficiency	isen	polytr	RNI	P/P	WB1d/w2 =	7,4074E-4
Outer LPC	0,8837	0,8900	0,466	1,486	CD8 =	0,98000
Inner LPC	0,8968	0,9000	0,466	1,248	CD18 =	0,97600
IP Compressor	0,8857	0,8900	0,536	1,311	PwX =	0,0
HP Compressor	0,8526	0,9000	0,621	21,989	W18/V8,1d =	0,42607
Burner	0,9950			0,960	WBLD/w22 =	0,00000
HP Turbine	0,9025	0,8900	1,582	3,272	Wreci/w25 =	0,00000
LP Turbine	0,9148	0,9000	0,622	4,389	Loading =	100,00 %
HP Spool mech Eff	1,0000	Nom Spd	22300 rpm		WCHN/w25 =	0,00000
LP Spool mech Eff	1,0000	Nom Spd	3349 rpm		WCHR/w25 =	0,00000
IPC & LPT		Nom Spd	10047 rpm		WCLN/w25 =	0,00000
P22/P21=1,0000	P25/P24=0,9800	P45/P44=0,9800			WCLP/w25 =	0,00000
hum [%]	war0	FHV	Fuel		WBLD/w25 =	0,01000
0,0	0,00000	42,798	Generic		Gear Rat =	3,00000
					WkBy/w25 =	0,00500
					WkLP/w25 =	0,01000

5.1.4 Additional functions: Formulas and Iterations

Formulas

A wide variety of properties could be calculated within GasTurb software by selecting them in the standard output list. However, if the user is interested in a quantity which is not implemented by default, it is possible to manually define a composed value.

This can be achieved by selecting the "Formulas" button from the tree selection menu on the left. The composed value could be defined using the formula editor which permits to add user defined functions to standard GasTurb quantities. In order to describe a composed value it is possible to employ any input or output quantity already implemented in GasTurb and also to use numbers as multiplying coefficients.

Iterations

The software allows the user to employ additional iterations to the default ones. This method allows to calculate a result cycle in which some quantities are forced to assume a specific value from the user. The option could be set by clicking the "Iterations" button.

During iteration process it is possible to involve up to 99 variables while forcing up to 99 output quantities to assume a user defined value bringing

anyway to an acceptable desired cycle. However, it is possible that iterations converge or not, depending on the problem imposed.

It is expected that the user sets a suitable range of variation for the variables by setting minimum and maximum values for each variable.

5.1.5 *Parametric analysis*

Once calculated the Design Point of the cycle in Performance mode, it is also possible to study the variation of specified variables by setting up a parametric study. This function have to be selected using the "Parametric" button in the left column.

In the parameter selection window that opens, it is possible to choose which parameters the user want to vary during the study. Parameters are calculated starting from the Start Value and are arranged by imposing the Number of Values and the Step Size desired from the user.

The parametric study could be started by clicking on the "2 Parameters" button. Once the calculation is completed it is possible to plot the requested property. If a parameter do not change value during the parametric study, it will not be visible in the parameter list.

It is possible to parameters by selecting different contour lines and also plot boundaries. The user could repeat the parametric study with another parameter in order to plot in the same graph the additional result. The plot will be characterized by more y-axes and a common x-axis.

Fig. 5.4: Parametric selection window

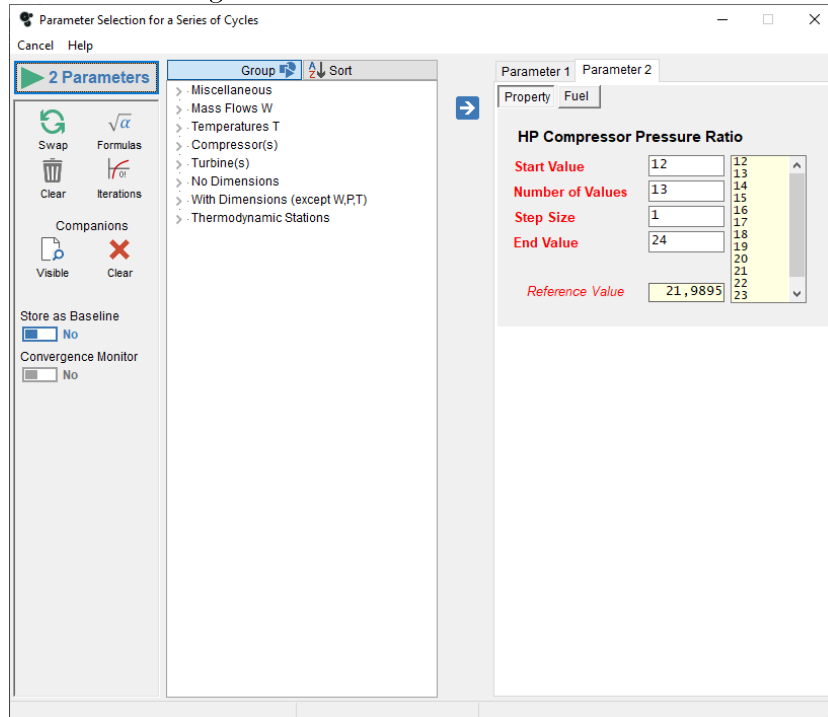
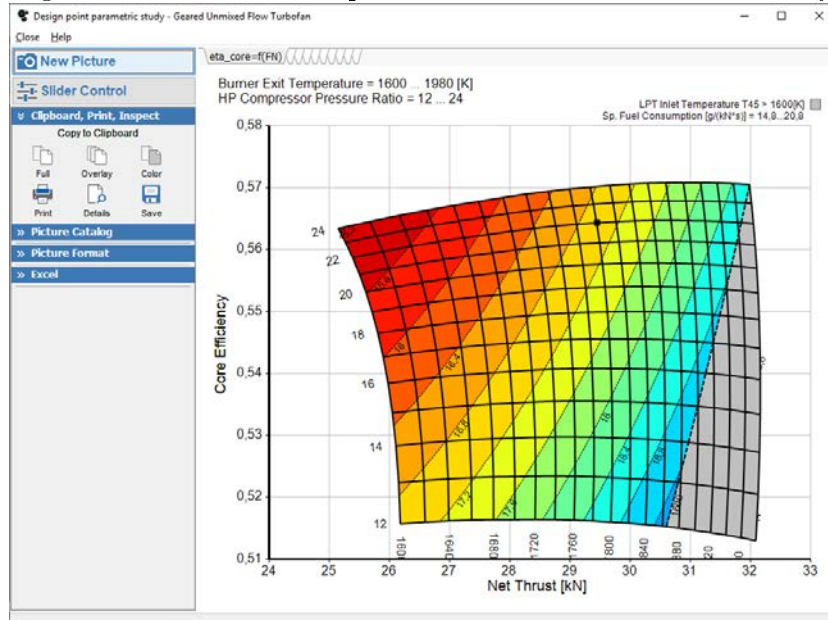


Fig. 5.5: Parametric example with contour lines and a boundary



5.1.6 Cycle Optimization

Another useful function available in GasTurb is the automated numerical optimization.

Optimization involves the calculated cycle design point and could be started by clicking on the "Optimize" button in the left menu. Optimization could also be combined with iteration.

During the optimization process some variables are used for the optimization and others are imposed from the user as constraints. Every variable and constraint is defined in a range that goes from a minimum value to a maximum value set by the user, and also composed values could be selected. Each variable's value calculated in the design point cycle must lie in that interval.

Finally the tab "Figure of Merit" is used to define the quantity the user want to maximize (e.g. Net Thrust) or minimize (e.g. Specific Fuel Consumption) during the optimization procedure, which can be selected from the output variables list.

In addition to the properties of the cycle design point you can consider several off-design operating points which are defined in a mission schedule. Data from each different mission points can be used as constraints and it can be employed as figure of merit.

In the optimization window, on the left side there are horizontal gauges which represent the range of values set for the optimization variables while on the right side there are gauges representing the ranges set for the optimization constrains. In the bottom part of the window, the figure of merit diagram calculated during every optimization run is reported.

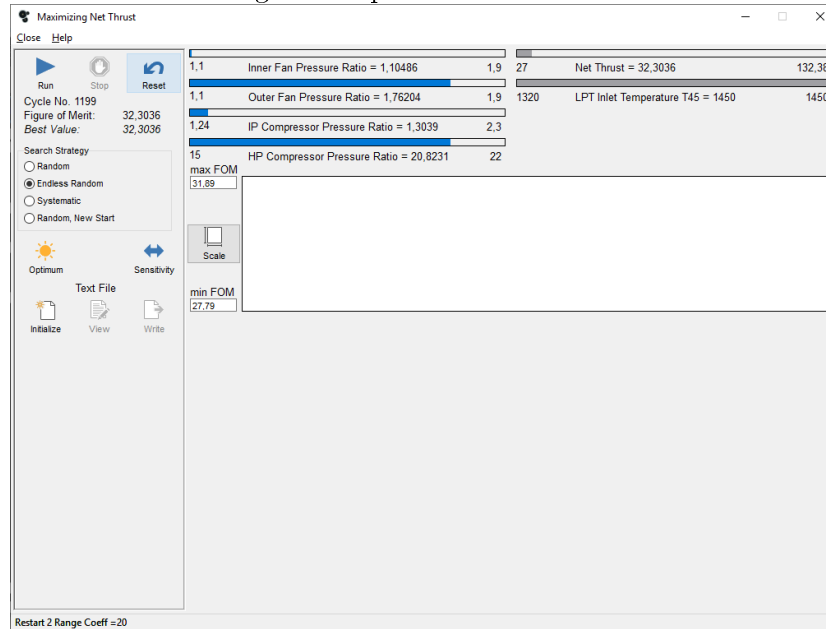
In GasTurb there are implemented multiple strategies of optimization procedures, such as Random search strategies as well as a Systematic strategy.

By clicking the "Optimum" button the user can access all the results of the optimized cycle. Once the calculation is finished the user have to check whether the found optimum is local or global. If the same optimum is calculated at each run signifies that it is a global optimum. If the result of each optimization changes continuously the user could try using the Endless Random strategy which automatically restarts after each run.

In the optimization procedure the user can define up to 12 optimization variables.

Each variable could vary within minimum and maximum boundaries set by the user. This range have to be wide enough in order to obtain possible solutions that could be found away from the limits. When the range is too wide it is possible to find a solution involving a cycle that is however not physically correct.

Fig. 5.7: Optimization window



5.1.7 Sensitivity analysis

The user is able to use another function embedded in GasTurb available clicking the "Sensitivity" button which allows to discover the influence of different quantities in the simulated cycle.

It is possible to select parameters the user wants to study from a provided list. The user have to define input and output quantities by selecting the buttons "Show the effect of..." and "Result for..."

Results consist on a table containing exchange rates of the requested quantities. The resulting rates are described as percentage values referred to the initial quantities of the cycle.

5.2 The cycle design point

The analysis of a gas turbine starts with the calculation of the thermodynamic cycle for a particular design point which constitutes the cycle design point (cycle reference point) of the gas turbine. The engine geometry is fixed because, for this particular operating point, mass flow rates, total pressures and total temperatures at the inlet and outlet sections of all components of the engine assume known values. The simulation of the engine model is at component level.

This point refers to design conditions of the engine and, when an existing engine is simulated, real data measured during testing, must coincide with the data obtained from the simulated model.

5.2.1 Input data

In this section all input quantities required to start a GasTurb simulation and contained in the Design Point input window will be introduced and analysed.

Basic Data

GasTurb provide a series of pre-compiled engine data sets for each available engine type that are used in case a new engine model is simulated. User cannot start a new simulation based on a blank data set.

Once the user have selected the engine type in the main menu and the program have opened the simulation window, reported in Figure 5.2, the first quantity that can be found in the property list concerns multiple definitions used to describe the intake pressure loss.

The Burner Partload Constant is used only during off-design simulations, and is set to its standard value by default.

The fuel type selected for the simulation is described in terms of its Fuel Heating Value (FHV). A list of available fuel types could also be found in the "Connections" menu.

If the engine is equipped with multiple components (e.g. compressors or turbines), pressure losses that occur in component inter-ducts can be also taken into account.

In the same table the user also find design pressure ratios for engine components. As far as the turbofan engine is concerned, different pressure ratios for both the inner and the outer fan flow, together with the design bypass ratio could be found in the Property list. Here the user define also the Burner Exit Temperature, the maximum temperature found in all cycle stations, along with Overboard Bleed or Power Off-take option. Also mechanical efficien-

cies for both Low-Pressure and High-Pressure spools are requested. If the turbofan is a geared model the table provides also the Gear Ratio of the gearbox.

Secondary Air System

Secondary Air Systems (SAS) guarantee reliable engine component operations. Secondary air consists on bleed air extracted from handling bleed valves or cooling air used for components cooling (e.g. HPT cooling air) as well as other type of airflow bleed that occurs inside the engine. Overboard bleed, for example, is used to provide cabin air ventilation or nacelle de-icing. In order to avoid compressor surge a handling bleed valve is usually opened thus lowering the compressor operating line. The bleed valve can be situated downstream the compressor or it can be situated in a interstage position within the compressor.

In order to set bleed valves position inside the engine, the relative enthalpy rise definition is used. For example, if the bleed valve in a 10-stage compressor is positioned between the third and the fourth stage, relative enthalpy rise of the bleed would be equal to $3/10=0.3$.

Fig. 5.8: Secondary Air System window

The screenshot shows the 'Design Point Input for a Geared Unmixed Flow Turbofan' window. The 'Secondary Air System' is selected in the tree view. The table below lists various properties and their values:

Property	Unit	Value	Comment
Rel. Handling Bleed to Bypass		0	
Rel. HP Leakage to Bypass		0,005	
Rel. Overboard Bleed W _{Bld} /W ₂₅		0,01	
Rel. Enthalpy of Overb. Bleed		1	
Recirculating Bleed W _{recirc} /W ₂₅		0	Off Design Input Only
Rel. Enthalpy of Recirc bleed		1	
Number of HP Turbine Stages		2	
HPT NGV 1 Cooling Air / W ₂₅		0	
HPT Rotor 1 Cooling Air / W ₂₅		0	
HPT NGV 2 Cooling Air / W ₂₅		0	
HPT Rotor 2 Cooling Air / W ₂₅		0	
HPT Cooling Air Pumping Dia	in	0	
Number of LP Turbine Stages		3	
LPT NGV 1 Cooling Air / W ₂₅		0	
LPT Rotor 1 Cooling Air / W ₂₅		0	
LPT NGV 2 Cooling Air / W ₂₅		0	
LPT Rotor 2 Cooling Air / W ₂₅		0	
Rel. Enth. LPT NGV Cooling Air		0,6	
Rel. Enth. of LPT Cooling Air		0,6	
Rel. HP Leakage to LPT exit		0,01	
Rel. Fan Overb. Bleed W _{Bld} /W ₁₃		0	
Core Byp Heat Transf Effectiven		0	
Coolg Air Cooling Effectiveness		0	
Bleed Air Cooling Effectiveness		0	

The schematic diagram at the bottom shows a cross-section of the engine with numbered bleed points (1-13) and arrows indicating the flow of secondary air.

Ambient Conditions

Ambient conditions are specified in terms of altitude, flight Mach number and temperature variation from the International Standard Atmosphere (ISA) model and must be accurately specified for each simulated flight condition. Definition of ambient condition could also be set by means of total temperature, total pressure and static ambient pressure.

The (Sea Level) standard day ambient conditions are $T=288.15$ [K] and $P=101.325$ [kPa]. The gas constant of dry air is 287.05 [J/(kg K)].

Mass Flow Input

Mass flow rate represents an input quantity during the analysis of a gas turbine cycle. In GasTurb software different definitions of the engine inlet mass flow rate are available.

By selecting the option 1 the user could set the standard day corrected inlet flow $W2Rstd$ at fan face.

Using the second option the user set the core inlet corrected flow rate $W25Rstd$ upstream the High-Pressure compressor. Thus the fan inlet mass flow rate is retrieved from the design bypass ratio.

The third option also retrieves the core mass flow rate but by reading a High-Pressure compressor map.

However, corrected mass flow rate is defined as

$$W_{cor} = W \cdot \frac{\sqrt{\frac{R}{R_{std}} \cdot \frac{T}{T_{std}}}}{\frac{p}{p_{std}}} = W \cdot \frac{\sqrt{\frac{R}{R_{std}} \cdot \Theta}}{\delta} \quad (5.1)$$

with

W Mass flow rate

T Total temperature

p Total pressure

R Gas constant

T_{std} Standard day temperature

p_{std} Standard day pressure

R_{std} Gas constant of dry air

Compressors Efficiency

Compressor efficiency must be set by the user for the cycle design point as isentropic or polytropic. However, during off-design simulations only the isentropic efficiency is employed because the efficiency is read from the compressor map.

The efficiencies set for the cycle design point in all compressors and fan were determined in section 4.4 .

Turbines Efficiency

In the same way applied for compressors, the user have to set turbine efficiency in terms of isentropic or polytropic efficiency during cycle design point calculation. Values retrieved from literature were introduced in in section 4.4 .

Efficiencies of uncooled turbines are easier to calculate. If the turbine is cooled, its efficiency could be calculated in a more complicated way as described in literature [4]. Values from the same table are used in this case because the Preliminary Turbine Design calculation is not employed.

Thermodynamic Stations

In order to calculate the thermodynamic cycle of a gas turbine, total pressures and total temperatures at each component's inlet and outlet section have to be set. Static quantities are required only for exhaust nozzle calculations.

The user can also provide Mach numbers or flow areas for each component boundary section in order to set the geometrical shape of the engine, which is not required to complete thermodynamic cycle calculations-

In section 5.5 a complete list of the thermodynamic stations employed in the GasTurb analysis of a specific model of turbofan engine is reported.

External Load and Power Off-take

External Load or Power Off-take could be used in order to represent an external equipment which absorbs a certain amount of power, such as for auxiliary onboard aircraft services.

An External Load could be connected to any spool in the simulation of every engine type.

An example of common external load is represented by connecting a constant load considering it as a Power Off-take.

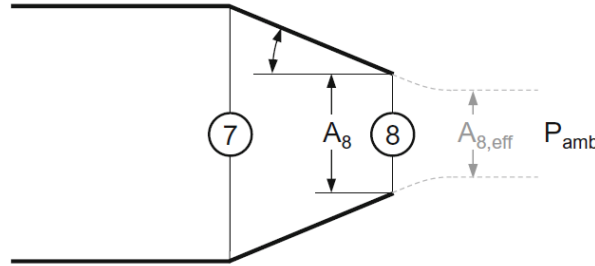
Nozzle Calculation

Turbojet and turbofan engines adopted for subsonic civil transport are usually employ convergent conical nozzles.

In GasTurb software both convergent and convergent-divergent nozzles are implemented for different engine models.

The user can choose between a standard modeling setting and a user-defined one. In the former the input quantities required are the nozzle thrust coefficient and the nozzle petal angle, while in the latter the gross thrust coefficient and the discharge coefficient are requested.

Fig. 5.9: Conical convergent nozzle (Kurzke Halliwell, see [2])



The thrust coefficient is defined as the ratio between the actual thrust and the ideal thrust, which would be produced in case of an ideal expansion to ambient pressure or an expansion without losses. These two conditions defines two thrust coefficients, respectively the C_{fg} and the $C_{fg,id}$, which are the same if the exhaust velocity V_e is subsonic.

The gross thrust can be obtained as

$$F_g = w_8 \cdot c_8 \cdot C_{fg} + A_8 (p_8 - p_{amb}) \quad (5.2)$$

The ideal thrust coefficient $C_{fg,id}$ is defined as

$$C_{fg,id} = \frac{F_g}{w_8 \cdot c_8} \quad (5.3)$$

The discharge coefficient C_d relates the actual mass flow rate with the theoretical one.

Once the geometry of the nozzle is known, the petal (cone) angle, the outlet to inlet nozzle area ratio and the pressure ratio define the discharge coefficient, as can be found in literature [2].

5.3 *Off-Design Calculations*

5.3.1 *Input Data*

In order to initialize an off-design calculation, the cycle design point must be previously calculated using the Performance scope. This calculation, as mentioned above, defines the geometry of the engine. Off-design analysis concerns different operating conditions once the engine cycle design point is set.

The calculation can be started by selecting either the "Standard Maps" button or the "Selected Maps" button. By clicking the "Standard Maps" button the program adapts and scales automatically the standard component maps to the cycle design point previously calculated. Alternatively, by clicking the "Selected Maps" button the user has the ability to select component maps from a provided list of maps which are available for each component and included in the software. Scaling map procedure is important to produce more accurate and realistic results as far as the component off-design performance is concerned. Special Maps are then scaled using settings chosen by the user in order and made consistent with the cycle design point.

Alternative maps that differs from the standard ones can also be selected once the Off-Design input window opens by clicking on the "Special" button in the "Maps and Connections" button group on the left side of the window. As done in section 5.2, a brief introduction about all input quantities available in the off-design input window is shown below.

Basic data

Basic Data contained in the Off-Design input window changes according to which function the user has selected from the tree view on the left side of the page.

In the basic data list the setting "ZNX given (1) or ZT4 given (2)" allows the user to choose which quantity is used to define the engine off-design operating condition. Setting (1) means that the operating point is defined by the relative High-Pressure spool speed ZNX while setting (2) sets the Burner Temperature ZT4 as the quantity that defines the off-design point of the engine.

Off-design calculations require less input data compared to design point calculations because engine model and characteristics are already defined by the engine cycle design point.

Fig. 5.10: Off-Design input window

Off Design Input for a Geared Unmixed Flow Turbofan

Cycle Design Main Window Exit Program Help

Off Design Point

Task

OD Point Operat Line Parametric

Mission Flight Envel Monte Carlo

Analysis Sensitivity Int Trans

Batchjob Transient

Project

Read Engine Model Save

Off-Design Point Input Data

Read File History Save

Additional

Controls

Extras

Maps and Connections

Basic Data Distortion No

Property	Unit	Value	Comment
Intake Pressure Ratio		1	
No (0) or Average (1) Core dP/P		1	
Fuel Heating Value	MJ/kg	42.798	
Overboard Bleed	kg/s	0	
Rel. Overboard Bleed W_Bld/W25		0,01	
Recirculating Bleed W_reci/W25		0	
Power Offtake	kW	0	
ZXN given (1) or ZT4 given (2)		1	
HPC Spool Speed ZXNH		1	
Compressor Delta VG Setting		0	inactive
d_HPT Efficiency / d_XN_HP		0	
d_LPT Efficiency / d_XN_LP		0	

C:\Users\bruno\Desktop\PW\PW1431Q-JMterzo.CYG Off Design Point

Controls: Maximum and Minimum Limiters

The engine operating cycle is defined within certain limits and its performance are strongly affected from those constraints. Common limits are defined for example by maximum temperature, maximum pressure and maximum spool speed allowed for each component. These structural limits affect the maximum thrust achievable by the engine and are essentially imposed from the operating condition of the engine, such as ambient conditions.

There are also minimum limiters concerning the minimum spool speed at engine idle or minimum fuel flow.

The user can set both maximum or minimum limiters from the "Controls" menu on the left part of the Off-Design input window. The software allows to select a set of minimum limiters (Min Limits) or a set of maximum limiters (Max Limits). It is also possible to run the calculation between minimum and maximum limits that can act at the same time.

Fig. 5.11: Max Limiters window

	Value	Maximum	On/Off
Low Press Spool Speed NL [%]	100,0	0	Off <input type="checkbox"/>
Corr Low Spool Speed NLR [%]	100,0	0	Off <input type="checkbox"/>
High Press Spool Speed NH [%]	100,0	100	On <input checked="" type="checkbox"/>
Corr High Spool Speed NHR [%]	100,0	105	On <input checked="" type="checkbox"/>
Comp Exit Temperature T3 [K]	765	0	Off <input type="checkbox"/>
Compr Exit Pressure P3 [kPa]	1422	0	Off <input type="checkbox"/>
HPT Rotor Inlet Temp T41 [K]	1800	0	Off <input type="checkbox"/>
LPT Inlet Temp T45 [K]	1424	1500	On <input checked="" type="checkbox"/>
Turb Exit Temperature T5 [K]	1047	0	Off <input type="checkbox"/>
Fuel Flow [kg/s]	0,4998	0	Off <input type="checkbox"/>
Net Thrust [kN]	29,4435	0	Off <input type="checkbox"/>
Engine Pressure Ratio EPR	2,3106	0	Off <input type="checkbox"/>

5.3.2 *Operating Line*

Clicking on the "Operating Line" button in the Task menu opens the Operating Line window in order to generate component's operating lines. The operating line is plotted in the component map and it is formed by a series of operating points starting from the off-design point previously calculated. In fact, the user have to set the step size of the High-Pressure spool speed in order to define the operating points that are going to form the operating line, and the number of desired points. It is possible to calculate the operating line either by increasing or decreasing the spool speed.

User can decide to create the operating line by setting thrust steps instead of choosing spool speed steps. By default the program uses High-Pressure spool speed steps of 0.025 .

Once calculated the operating line, the software asks to calculate more operating lines. The user could answer negatively in order to get the calculated operating line for each component in the component map. All the equispaced points requested and previously calculated are highlighted in the operating line and user is able to visualize cycle details for each point by selecting the desired point.

If the user answer positively the program allows to calculate a series of operating lines starting from a specified list of operating points. The desired list of points could be set in a window analogue to the Mission Input one. Several columns are available in order to specify different points that constitutes the starting points of the additional operating lines. By clicking the "Run" button GasTurb calculates an operating line for each data set contained in each column and, once the process is completed, all the different operating lines are plotted in the same component map in order to compare results.

Fig. 5.12: HPC Operating line window

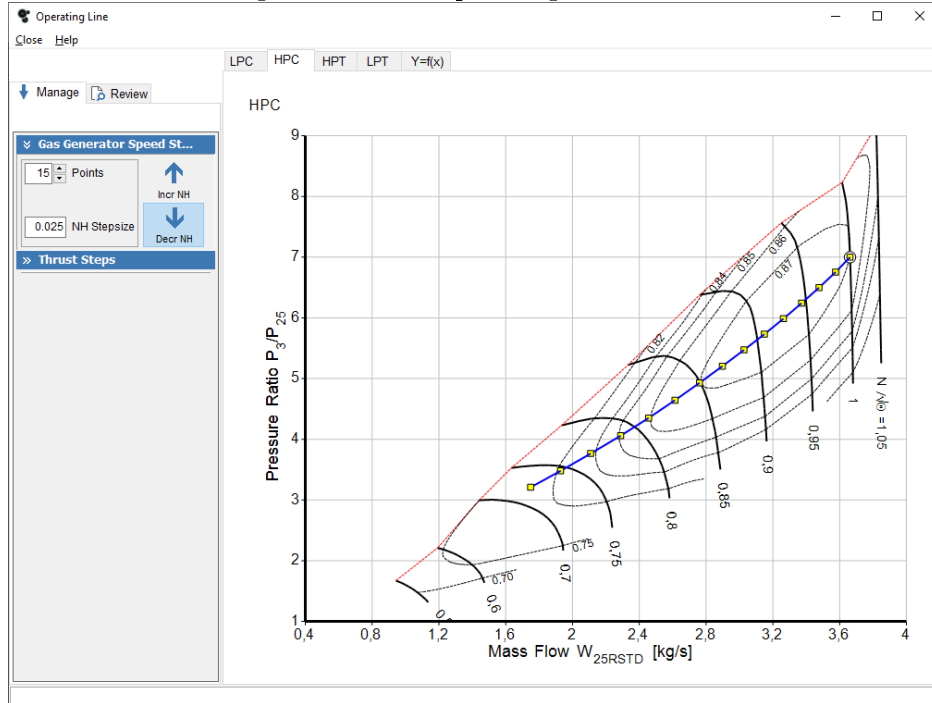
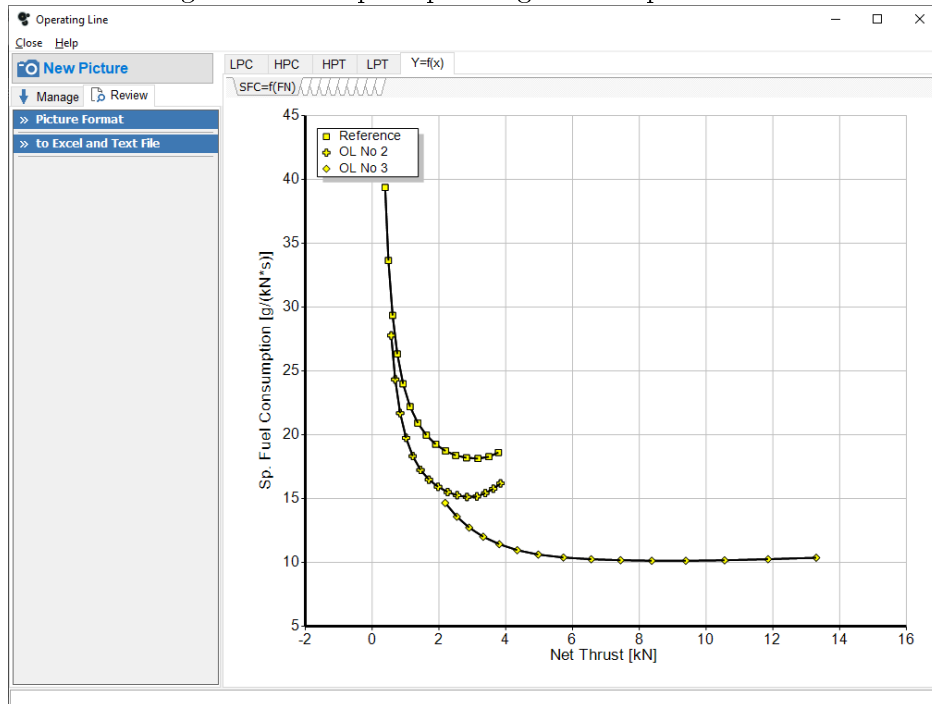


Fig. 5.13: Multiple Operating line Output window



5.3.3 *Operating Line errors*

Once the operating line is created it is possible to encounter problems involving surge. In particular it is possible that the just created operating line lies above the surge line. For example frequently the booster operating line could be almost horizontal and thus intersecting the surge line and extending beyond it.

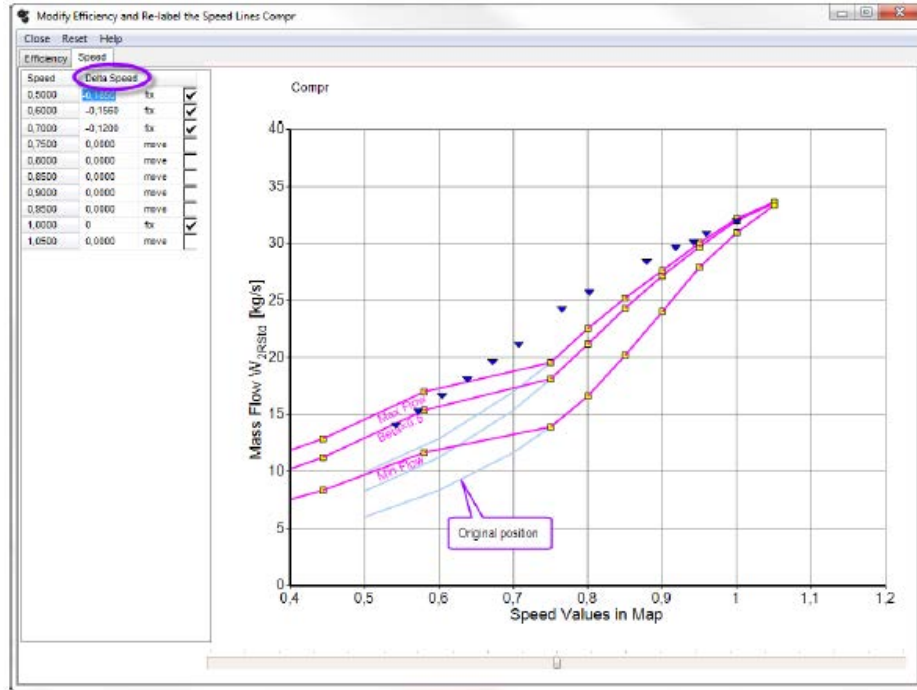
This is a common problem and could be solved by re-labeling the speed lines in the component map. This procedure requires that the user has a set of comparative data which consists of corrected flow and relative corrected speed of real measured operating points of the engine component. It is possible also to relabel speed lines without comparative data, however, it is highly not recommended. In this thesis, for example, comparative data was not available and thus not used.

The user has to click the "Edit Compr Map" button in the Compressor Map button group. Then a window containing a graph opens. In the graph along the x-axis there are the Speed Values contained in the map while along the y-axis there are the corrected Mass Flows. There are three lines that represent the trend of the properties for three different values of the Beta_{ds} parameter, in particular for $\text{Beta}_{ds}=0$, $\text{Beta}_{ds}=0.5$ and $\text{Beta}_{ds}=1$, which therefore represent the boundaries of the component map.

There is also a table on the left side of the window containing the original Speed Values of the map along with a Delta Speed column and a list of checkboxes. Each checkbox if set fixes the corresponding Speed Value of the map, allowing the user to modify the other unchecked values using the cursor at the bottom of the page.

Moving the cursor to the right allows to lower the operating points in the component map, and once the procedure is done for all the required points, the resulting operating line will no longer be affected by the surge problem. It is possible that although the Speed Lines are now re-labeled, the operating line continues to intersect the surge line especially at low corrected mass flows. It is then possible to set up an automatic bleed schedule.

Fig. 5.14: Relabel Speed Lines (GasTurb, see [4])



5.3.4 Automatic Bleed schedule

In order to guarantee an adequate safety margin against compressor stall, its operating line must be kept away from the surge line during all operating conditions. However, islands of high efficiency in a map of an axial compressor are situated near the surge line and the operating line should pass through these areas to maintain high efficiency levels.

Compressor surge usually occurs when the pilot suddenly requires more thrust. In this situation more fuel is injected into the combustor, leading to a turbine inlet temperature (TIT) increase. However, the compressor does not accelerate instantaneously because of its massive inertia. The operating point in this case shifts towards the surge line along a constant speed line.

The software includes an automatic handling bleed schedule, which can be set from the user, that allows to restrain the surge margin of the compressor. First of all, surge margin (SM) can be defined in several ways and in GasTurb 13, as reported in literature [4], it is calculated by considering that usually the pressure ratio is greater than 1. Thus results

$$SM = 100 \cdot \frac{PR_{surge} - PR_{operatingline}}{PR_{operatingline} - 1} \quad (5.4)$$

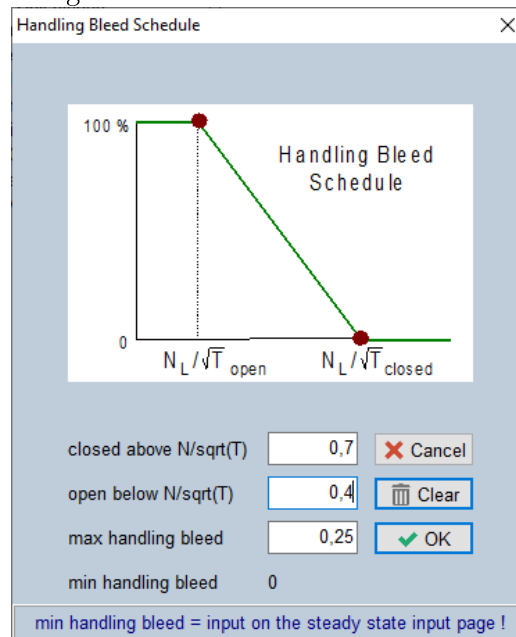
The necessary SM depends on the engine configuration and varies according to acceleration and deceleration times, inlet distortion and the compressor type. From literature [22]. a surge margin of 10-20% is required for fans, while a 10-25% SM is requested for Low-Pressure compressors and a higher 15-30% SM is used in High-Pressure compressors.

This system consists on bleed valves that eject a certain amount of compressed air in order to lower the operating line and avoid the compressor surge. The air is usually extracted from a position that is located downstream the compressor or between two compressor stages, and discharged into the bypass duct or overboard.

The bleed schedule can be defined by the user by selecting the spool corrected speed at which the valve starts to open and the spool corrected speed at which the valve is fully opened. The user sets also the maximum handling bleed mass flow rate quantity.

Automatic bleed schedule in case of cycle design calculation is the last expedient to overcome the compressor stall issue.

Fig. 5.15: Automatic Bleed schedule



5.3.5 Off-Design Parametric analysis

Parametric studies carried out during Off-Design analysis allow to calculate a series of operating points in a similar way as done for the operating line. In this case the operating points that were previously calculated for equal

spool speed steps are in this case calculated, for example, for different amounts of power off-take.

All the operating points calculated during the parametric study are then plotted in the same component map.

5.3.6 Mission analysis (flight)

Another useful function in GasTurb helps the user to analyse a series of different off-design points of the gas turbine. It can be activated using the "Mission" button.

In a study involving aeronautical engines this is a common task because usually it is requested to calculate operating condition of the engine at different flight altitudes.

The user can set a list of operating points, each one characterized by a different off-design conditions, which constitute the Design Table. A maximum of 49 different points are analysed at the same time.

The user defines different operating conditions for each point in the mission input table. In the same table there are specified also the available defined limiters for each operating condition, so the user is able to turn on them quickly and easily.

All points contained in the list are calculated simultaneously and results are provided in the form of tables containing all the points cycle data.

In the mission scope it is also possible to define the composed value *MissionAvg(...)* in order to calculate the average value of a quantity or to consider the sum of values by setting the composed value *MissionSum(...)*.

For this study it would be useful to calculate the fuel burnt during the entire flight (mission). This is possible by defining two composed values:

$$SegmentFuel = InPar1 \cdot wf \quad (5.5)$$

$$MissionSum(SegmentFuel) \quad (5.6)$$

where *InPar1* represents the time spent at each off-design point (each segment of flight).

5.3.7 Flight Envelope

The Flight Envelope setup is used to calculate a series of points with different altitudes and Mach numbers that are contained in the flight envelope.

The user has to previously activate one or more maximum limiters in order to calculate the flight envelope.

By definition, a flight envelope ranges from sea level altitude up to a specified

altitude.

The envelope is defined within two speed boundaries. These flight speeds must be expressed in terms of Equivalent Air Speed (EAS) which is defined as the speed at which the plane have to fly at different altitudes in order to produce the same dynamic pressure delivered at sea level altitude, and it is calculated as

$$EAS = TAS \cdot \sqrt{\frac{\rho}{\rho_0}} \quad (5.7)$$

The first point to be calculated from the software is sea level static conditions. The cycle solution of this point must converge in order to calculate the flight envelope.

5.4 Off-Design component modeling

Off-design studies involve performance of the engine running at operating conditions that differ from the design point conditions. The software performs a cycle design simulation in background if the user starts an off-design simulation immediately after the program startup.

The most important part of the off-design study is the map scaling. Each component design point must be associated to component maps so that the points are correctly matched. This procedure can be done automatically by using Standard Maps that are scaled autonomously by the software before the calculation process. The user can also manually set and scale component maps by selecting the Special Maps function, depending on the level of accuracy of the analysis he want to achieve.

In this section properties employed in the engine component modeling, as well as the gas model used in GasTurb and the component losses, are introduced together with the map scaling procedure and the Reynolds effect corrections.

5.4.1 Gas Properties

While simulating engine performance it is important to employ an adequate model of the gas properties. In this case the working fluid is considered as an half-ideal gas.

In this model specific heat, enthalpy, entropy and gas constant are a function of temperature and gas composition, and they are not function of pressure.

5.4.2 Standard Atmosphere

A brief introduction to atmosphere model implemented in GasTurb software is reported below for completeness.

In order to describe environment conditions, the model of the International Standard Atmosphere is adopted and makes possible to estimate the ambient temperature and pressure.

In case of severe weather conditions it is possible to use the US Military Standard 210 (MIL210) which defines atmosphere conditions for standard hot and cold days.

By ISA definition it is possible to calculate static pressure and temperature at a given altitude for different ranges.

Below 11000 [m] the ISA temperature and pressure are defined as

$$T_{amb,ISA} = 288.15 [K] - 6.5 \cdot \frac{alt [m]}{1000 [m]} \quad (5.8)$$

$$p_{amb,ISA} = 101.325 [kPa] \cdot \left(1 - \frac{0.0225577 \cdot alt [m]}{1000 [m]}\right)^{5.25588} \quad (5.9)$$

For an altitude range between 11000 [m] and 25000 [m] temperature is constant and pressure is calculated as

$$T_{amb,ISA} = 216.65[K] \quad (5.10)$$

$$p_{amb,ISA} = 22.632 [kPa] \cdot e^{\frac{11000 [m] - alt [m]}{6341.62 [m]}} \quad (5.11)$$

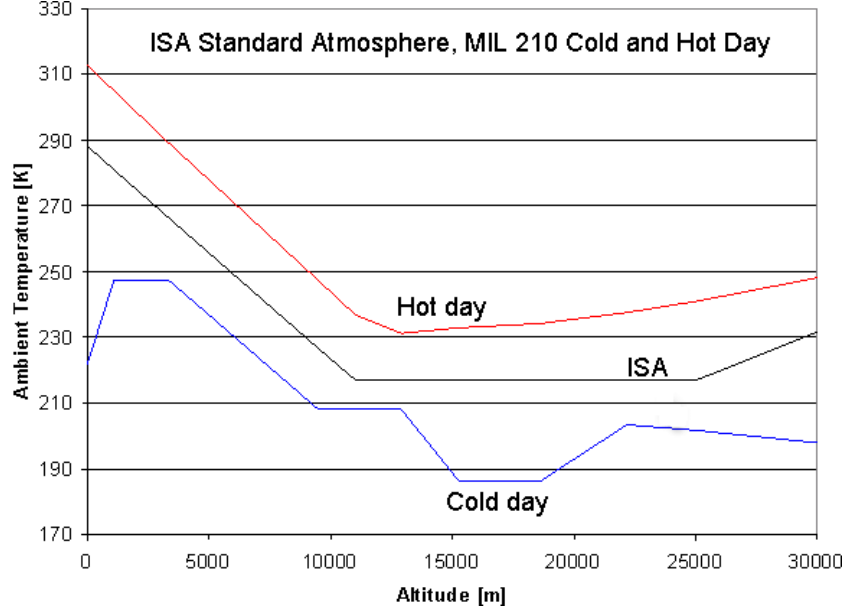
Finally above 25000 [m] temperature and pressure are obtained from

$$T_{amb,ISA} = 216.65 [K] + \frac{alt [m] - 25000[m]}{1000 [m]} \cdot 3 [K] \quad (5.12)$$

$$p_{amb,ISA} = 2.4886 [kPa] \cdot \left(\frac{216.15 [K]}{T_{amb,ISA} [K]}\right)^{11.8} \quad (5.13)$$

In GasTurb 13 MIL210 standards for hot and cold day can be retrieved by setting the ambient temperature to +999 in case of hot day and -999 in case of cold day.

Fig. 5.16: Temperature profile in ISA atmosphere and MIL210 conditions (Gasturb GmbH, see [4])



5.4.3 Component modeling

During off-design simulations some quantities employed to describe a particular component, such as the pressure loss at the intake for example, differ from the constant value set during cycle design point analysis.

Below are introduced those corrections used in component modeling during off-design simulation.

Intake losses

A variety of methods could be selected while defining the pressure recovery obtained at the engine intake.

The intake pressure ratio could be described by any positive value of p_2/p_1 . Setting a value of 2 implies that an intake map is used for this scope.

A negative p_2/p_1 ratio is used when shock losses occur during supersonic flight and set by employing the definition reported in the document MIL-E-5007 and valid up to Mach 5.

$$\frac{p_2}{p_1} = - \left(\frac{p_2}{p_1} \right)_{input} \cdot [1 - 0.075 \cdot (M - 1)^{1.35}] \quad (5.14)$$

When flying above Mach 5 the intake pressure recovery can be evaluated as

$$\frac{p_2}{p_1} = - \left(\frac{p_2}{p_1} \right)_{input} \cdot \frac{800}{M^4 + 935} \quad (5.15)$$

While simulating a turbofan engine, it is possible to define a radial pressure profile at the engine inlet by selecting the input property No (0) or Average (1) Core dp/p in the main off-design input menu. By setting the property to 0 the core pressure loss will be zero and a mass averaged pressure loss is calculated for the bypass stream in order to obtain the input pressure ratio p_2/p_1 for the bypass flow. If the property is set by default to 1 the intake pressure loss is the same for both the core and the bypass flows. Values that range from 0 to 1 is used to define the radial pressure loss at the engine intake.

Compressor performance

Input data at the compressor inlet are usually the inlet temperature T_1 , the design pressure ratio p_2/p_1 and the compressor efficiency in terms of isentropic or polytropic efficiency. The user has to remember that during off-design studies only isentropic efficiency read from component map is used during the simulation while during cycle design analysis both isentropic and

polytropic efficiencies could be equally employed.

Calculation allows to evaluate the outlet temperature T_2 and the required specific work dH_{21} .

First of all entropy at the outlet station ψ_2 is calculated from the inlet temperature and the input pressure ratio as

$$\Psi_2 = \Psi_1 + \ln(p_2/p_1) \quad (5.16)$$

Inverting the entropy function permits to calculate the outlet temperature T_2 .

Using the definition of isentropic efficiency

$$\eta_{is} = \frac{h(T_{2is}) - h(T_1)}{h(T_2) - h(T_1)} \quad (5.17)$$

it is possible to evaluate the requested specific work as

$$dH_{1,2} = \frac{h(T_{2is}) - h(T_1)}{\eta_{is}} \quad (5.18)$$

Polytropic efficiency could be however evaluated as

$$\eta_{pol} = \frac{\ln(p_2/p_1)}{\ln(p_{2is}/p_1)} \quad (5.19)$$

Gearbox losses

In order to take into account gearbox losses the user has to include these losses in the mechanical efficiency of the spool at which the gearbox is connected.

Duct pressure losses

Pressure losses that occur in ducts are taken into consideration by defining a pressure ratio $(P_2/P_1)_{ds}$ during cycle design calculation.

However, during off-design simulation ducts pressure losses are considered using the equation

$$\frac{1 - \frac{p_2}{p_1}}{1 - \left(\frac{p_2}{p_1}\right)_{ds}} = \left(\frac{\frac{W \cdot \sqrt{R \cdot T}}{P}}{\left(\frac{W \cdot \sqrt{R \cdot T}}{p}\right)_{ds}} \right)^2 \quad (5.20)$$

The ratio p_2/p_1 during off-design simulation can be calculated using the equation (5.20) above.

Combustor performance and losses

Nowadays combustors are characterized by very high efficiencies when working at design conditions, while their efficiency at off-design operating points could drop considerably.

During off-design simulation the burner efficiency could be expressed in terms of the "burner loading" quantity which is defined as

$$\Omega = \frac{W_{31}}{p_3^{1.8} \cdot e^{T_3[K]/300[K]} \cdot Vol} \quad (5.21)$$

where w_{31} is the inlet mass flow rate, p_3 is the inlet pressure expressed in [bar], T_3 is the inlet temperature in [K] and Vol is the combustor volume in [m^3].

During cycle design the burner efficiency is set by the user and the burner loading is equal to 1. During off-design condition the relative burner loading Ω/Ω_{ds} is calculated. The volume of the combustor chamber, which could be an unknown parameter, remains constant so calculation could be done anyway.

Change in burner efficiency could be correlated to burner load as

$$\log(1 - \eta) = a + b \cdot \log(\Omega/\Omega_{ds}) \quad (5.22)$$

where the constant a is a property of the design cycle efficiency as

$$a = \log(1 - \eta_{ds}) \quad (5.23)$$

Finally, burner part load efficiency can be estimated using the only one remaining parameter, the burner part load constant b , which is set by default in GasTurb 13 to 1.6 .

Pressure losses that occurs in the combustor, which are caused by friction and heat addition phenomena, are calculated as pressure duct losses in the same way described in the previous section.

Turbine performance

Similarly to what was introduced for a compressor, input quantities at the turbine inlet are the inlet temperature T_1 , the design expansion ratio p_1/p_2 and the turbine efficiency in terms of isentropic or polytropic efficiency.

Calculation permits to estimate the isentropic exit temperature $T_{2,is}$, since the extracted isentropic specific work dH_{21} and the isentropic turbine efficiency are known, using the following equation

$$h(T_{2,is}) = h(T_1) - \frac{dH_{1,2}}{\eta_{is}} \quad (5.24)$$

The expansion ratio is a function of entropy calculated for T_1 and $T_{2,is}$ as follows

$$p_2 = p_1 \cdot e^{\Psi(T_{2,is}) - \Psi(T_1)} \quad (5.25)$$

and the exit temperature T_2 could be found using the enthalpy

$$h_2 = h_1 - dH_{1,2} \quad (5.26)$$

Polytropic efficiency could be evaluated as

$$\eta_{pol} = \frac{\ln(p_1/p_{2,is})}{\ln(p_1/p_2)} \quad (5.27)$$

while isentropic efficiency is equal to

$$\eta_{is} = \frac{h(T_1) - h(T_2)}{h(T_1) - h(T_{2,is})} \quad (5.28)$$

5.4.4 Component Maps

Once the user has set the desired cycle design point it is possible to begin with the off-design calculations in order to analyse other engine operating conditions.

This is possible once the cycle design point is correctly matched and positioned within the component maps.

The accuracy of off-design simulation derive from how the selected component map approximates the real functioning of the modelled component. In order to predict component performance, in terms of component efficiency, at conditions that differ from the design ones, the user have to recreate maps that represents the component behaviour since the original component ones are not available.

The software provides a list of preselected maps which offers multiple different maps for all components, based on the type of the component (subsonic, transonic) and its pressure ratio.

Component maps usually need to be scaled so the initial design point matches to a specific point in the map which is called the Map Scaling Point. This operation is automatically carried out when the user clicks the "Standard Maps" button in the program main window.

In case Standard maps are not suitable for engine components or in case better maps are available, the user can select these maps by using the "Special Maps" button. It is obvious that the use of the best maps available produces the most accurate result.

Standard Maps

The software provides a list of compressor and turbine maps which is implemented and available to be used by default.

A standard map suitable for common calculations is delivered for all the components. These maps are derived from literature and involves axial flow turbo-machinery and axial-radial compressors.

All the maps are retrieved from real machines and could be scaled in order to be suitable for similar components. However, simulations that need to be more accurate and realistic require high quality maps, especially for the compressors.

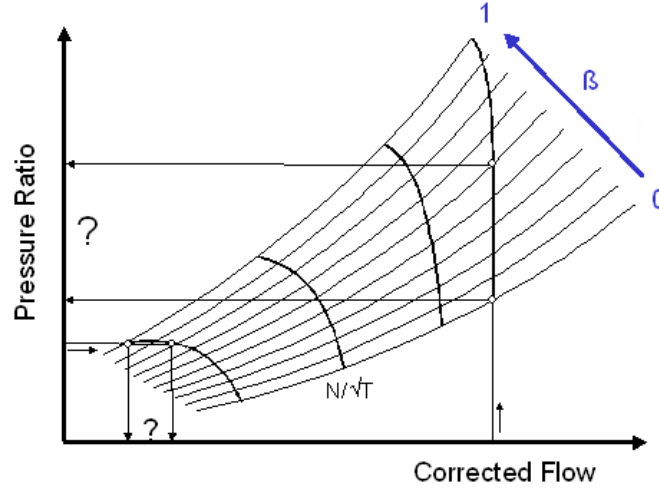
All maps are automatically scaled using the default scaling point in order to assure a good match with the cycle design point. Scaling procedure is done before starting off-design calculations.

Special Maps

With the "Special Maps" function the user can manually scale component maps by manually selecting the position of the Map Scaling Point. In the compressor Standard Map the Map Scaling Point is set by default to speed line $N/\sqrt{\Theta} = 1$ and auxiliary coordinate $\beta = 0.5$. This point is matched with the cycle design point and highlighted by a yellow square. Its coordinates are reported in a table on the left side of the window.

Two x-axes are available in the component map, one reporting the corrected flow and a second one referring to the compressor inlet Mach number. This is because engine dimensions are not required during a pure thermodynamic cycle study, so Mach numbers are not required.

Fig. 5.17: Beta, ds definition in a compressor map (Kurzke Halliwell, see [2])



It is possible that the default Map Scaling Point is not positioned correctly. The user can set its position by clicking on the yellow square, which represent the Map Scaling Point, and dragging it to a more suitable and effective place in order to increase the surge margin, for example. User is also able to move the Map Scaling Point by typing its coordinates in terms of N/\sqrt{T} , ds and $Beta, ds$ in the table on the left.

Varying the map scaling point location in the map implies that all efficiency contours and the map peak efficiency assume different values. Displacing the design point to a map region where the efficiency is lower leads to a higher peak efficiency in the scaled map. This is because the efficiency of the cycle reference point, by definition, must remain constant.

Reynolds Number Index

Performance of engine components is described in the component map as function of dimensionless parameters which indeed reflects, once the geometry of the engine is set, the machine Mach number.

Performance of turbo-machinery is also affected from compressibility effects of the air and thereby from the Reynolds number of the flow. This parameter is important for aircraft engine simulation since pressure and temperature during flight are very variable and then the Reynolds number have to be considered.

Usually the Reynolds number is employed, and it is defined as

$$Re = \frac{L \cdot V}{\nu} = \frac{\rho \cdot V \cdot L}{\mu} \quad (5.29)$$

where L is the blade chord length, V is the relative velocity to the blade, ν is the kinematic viscosity and μ is the dynamic viscosity, while in GasTurb the Reynolds Number Index (RNI) is considered. The RNI is defined as the ratio between the actual Reynolds number and a reference Reynolds number adopted at the same Mach number.

$$RNI = \frac{\rho \cdot L \cdot V}{\rho_{ref} \cdot L_{ref} \cdot V_{ref}} \cdot \frac{\mu_{ref}}{\mu} \quad (5.30)$$

Considering that the length quantity is the same for actual and reference conditions $L = L_{ref}$ and assuming the fluid as an ideal gas which behaviour is described by the law $p_s/\rho = R \cdot T_s$ (where the subscript s stands for static), the RNI can be obtained as

$$\begin{aligned} RNI &= \frac{p_s}{R \cdot T_s} \cdot \frac{R_{ref} \cdot T_{s,ref}}{p_{s,ref}} \cdot \frac{V}{V_{ref}} \cdot \frac{\mu_{ref}}{\mu} = \\ &= \frac{p_s}{p_{s,ref}} \cdot \frac{V}{\sqrt{k \cdot R \cdot T_s}} \cdot \frac{\sqrt{k}}{R \cdot T_s} \cdot \frac{\sqrt{k_{ref} \cdot R_{ref} \cdot T_{s,ref}}}{V_{ref}} \cdot \frac{\sqrt{R_{ref} \cdot T_{s,ref}}}{k_{ref}} \cdot \frac{\mu_{ref}}{\mu} \end{aligned} \quad (5.31)$$

Since the Reynolds Number Index associates conditions with the same Mach number, the equation (5.31) can be simplified as

$$RNI = \frac{p_s}{p_{s,ref}} \cdot \sqrt{\frac{T_{s,ref}}{T_s}} \cdot \sqrt{\frac{R_{ref}}{R} \frac{k}{k_{ref}}} \cdot \frac{\mu_{ref}}{\mu} \quad (5.32)$$

Introducing the total pressure p_t and the total temperature T_t for both the actual and reference state the equation (5.32) becomes

$$RNI = \frac{p_s/p_t}{p_{s,ref}/p_{t,ref}} \cdot \frac{p_t}{p_{t,ref}} \cdot \sqrt{\frac{T_{s,ref}/T_{t,ref}}{T_s/T_t} \cdot \frac{T_{t,ref}}{T_t}} \cdot \sqrt{\frac{R_{ref}}{R} \frac{k}{k_{ref}}} \cdot \frac{\mu_{ref}}{\mu} \quad (5.33)$$

The equation can be rearranged considering that the ratio between total pressure and total temperature are the same for both the considered conditions since the Mach number is the same. Assuming that the heat capacity ratio k remains constant, it is possible to finally evaluate the RNI from equation (5.33) as

$$RNI = \frac{p}{p_{ref}} \cdot \frac{R_{ref} \cdot T_{ref}}{R \cdot T} \cdot \frac{\mu_{ref}}{\mu} \quad (5.34)$$

Reference condition are ISA Sea Level, thus $p_{ref} = 101.325$ [kPa], $T_{ref} = 288.15$ [K] and $R_{ref} = 287.15$ [J/(kg · K)] and RNI in this case is equal to 1.

is done by considering the quantities $f_{\eta,RNI}$ and $f_{W,RNI}$:

$$\eta_{dp,map} = \eta_{R,map} \cdot f_{\eta,RNI} \quad (5.35)$$

$$\left(W \sqrt{\Theta_R/\delta} \right)_{dp,map} = \left(W \sqrt{\Theta_R/\delta} \right)_{R,map} \cdot f_{W,RNI} \quad (5.36)$$

Reynolds correction factors for efficiency $f_{\eta,RNI}$ and flow $f_{W,RNI}$ can be defined in the GasTurb Special Components Map window.

The efficiency correction factor varies linearly with the RNI, which is however reported in a logarithmic scale. The mass flow correction factor is then defined to be a specified fraction of the efficiency correction factor. In this study the default definition of the Reynolds correction factors based on efficiency is used.

Factors can be computed in different ways by modifying the Reynolds number correction algorithm. It is possible to evaluate the factor by using efficiencies, by using losses or even by considering the geometry of the engine. It is also possible to switch off this type of correction. In the figures below these multiple settings are reported.

Fig. 5.19: Efficiency and flow factors based on efficiency

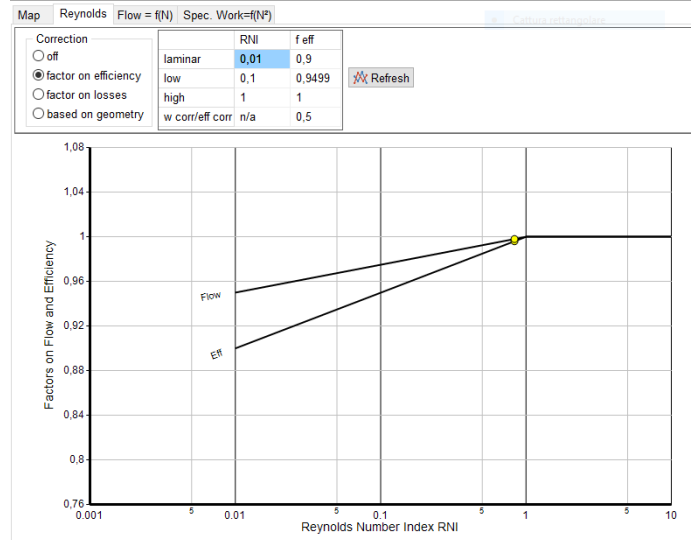
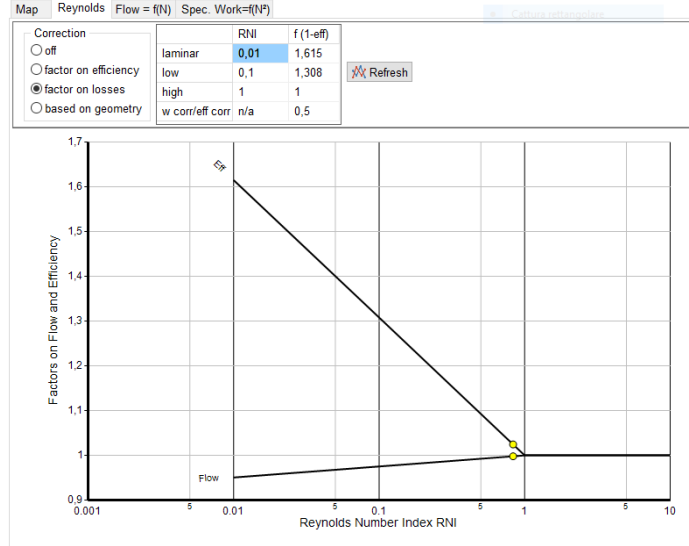


Fig. 5.20: Efficiency and flow factors based on losses



Map scaling factors can be finally evaluated as

$$f_{mass} = \frac{(W \sqrt{\Theta_R / \delta})_{dp}}{(W \sqrt{\Theta_R / \delta})_{R, map} \cdot f_{W, RNI}} \quad (5.37)$$

$$f_{eff} = \frac{\eta_{dp}}{\eta_{R, map} \cdot f_{\eta, RNI}} \quad (5.38)$$

$$f_{P_3/P_2} = \frac{(p_3/p_2)_{dp} - 1}{(p_3/p_2)_{R, map} - 1} \quad (5.39)$$

$$f_{speed} = \frac{N_{dp}}{N_{R, map}} \quad (5.40)$$

in order to scale corrected mass flow rates, efficiencies, pressure ratios and spool speeds between design point conditions and unscaled maps conditions. These scaling factors are employed to match component map with the cycle design point and are consequently applied to the quantities contained in the unscaled map.

Turbine map scaling is similar to compressor map scaling.

5.5 Engine model and stations

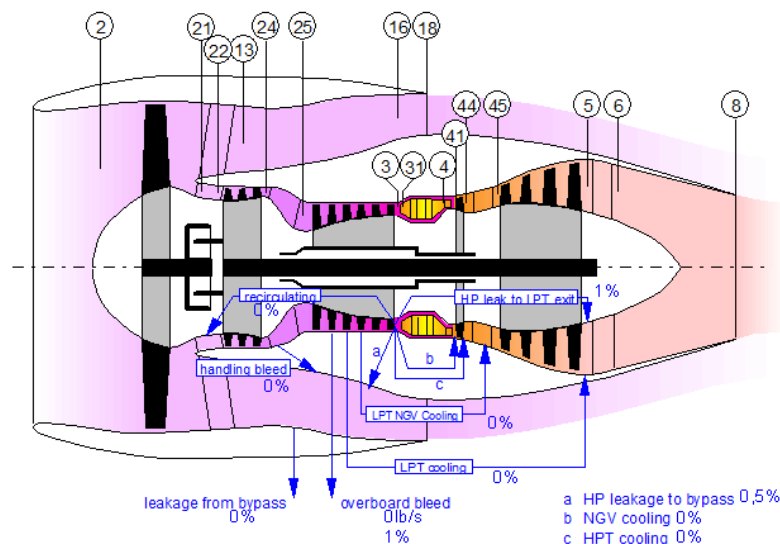
During the analysis it is important to consider the value of a given property at different locations along the engine.

In the software the engine is divided into stations which are normally positioned at each component's inlet or outlet. The nomenclature implemented in GasTurb is the international standard one, developed by the Society of Automotive Engineers SAE and published in the ARP 755C document, which describes station designation and nomenclature systems for aircraft propulsion systems.

First of all one has to choose the type of gas turbine he wants to simulate in the GasTurb main menu. I decided to carry out the analysis by selecting the "Geared Turbofan A" engine model from the engine list provided in the main window of the software. This model is used to analyse a geared unmixed flow turbofan engine. Geared turbofan engines must be simulated with this engine model and even ungeared turbofan engines, like the General Electric GE9X, can be adapted to this engine model if the gear ratio is set to be equal to 1, and gearbox losses are not be taken into account.

Below in Figure 5.21 it is shown the engine model reproduced in GasTurb software with reference to station numbering. The engine cross section could be produced from the cycle design point result window.

Fig. 5.21: GasTurb "Geared Turbofan A" model



As can be seen from Figure 5.21 above, the more relevant thermodynamic stations in this study are also reported in the table below. From GasTurb manual [4] the station designation results

<i>Station</i>	<i>Component</i>
0	Ambient
1	Aircraft-engine interface
2	First compressor inlet
21	Inner stream fan exit
13	Outer stream fan exit
16	Bypass exit
161	Cold side mixer inlet
163	Bypass nozzle throat
24	Intermediate-Pressure compressor exit
25	High-Pressure compressor inlet
3	Last compressor exit
31	Burner inlet
4	Burner exit
41	First turbine stator exit = rotor inlet
43	High-Pressure turbine exit before addition of cooling air
44	High-Pressure turbine exit after addition of cooling air
45	Low-Pressure turbine inlet
49	Low-Pressure turbine exit before addition of cooling air
5	Low-Pressure turbine exit after addition of cooling air
6	Jet pipe inlet
8	Nozzle throat

Tab. 5.1: Station numbering

Other intermediate stations not summarized in the table above are useful to take into consideration losses that occurs in ducts that connect each component to the others. Stations are also defined in order to consider the leakage of air between different engine zones.

Symbols used to describe quantities in GasTurb software are those defined in the same ARP 755 document published by SAE.

Symbols used in the software and in the manual consist of the station name and some leading letters. The complete symbol list could be found in the chapter XI of the GasTurb 13 manual [4] and it is not summarized below.

6. DESIGN CYCLE

For each engine it is important at the beginning of the analysis to define its cycle Design Point. This particular condition defines all the basic information regarding mass flows, total pressures and total temperatures at each engine component's inlet or outlet station.

Basically this consists on establishing the thermodynamic cycle actually reproduced inside the engine at these particular operating conditions. In this section this procedure is reported for the two selected engines.

It is possible to consider a wide variety of Cycle Design points. However in each case of the engines analysed in this study, the Cycle Design point refers to the Take-Off condition at fixed point operation. This choice is due to the amount of experimental information available for this specific operating condition and is made in order to obtain an accurate cycle model.

6.1 GE9X

6.1.1 Design Point: Take-Off

It is possible to take into consideration all the data disclosed by General Electric and other assets by mean of brochures and to derive other important parameters from the predecessor of the GE9X , the GEnx engine, which was the test-bed for the technologies used later in the GE9X project.

The cycle design point for the General Electric GE9X is chosen at Take-Off, thus a sea level altitude running at fixed point ($M=0$) when the engine produces the maximum Net Thrust.

Available data

In the table below I summarised all the gathered information about the engine, useful for the simulation set up.

<i>Quantity</i>	<i>Notes</i>	
OPR	61:1	
HPC Pressure Ratio	27:1	
HPT Expansion Ratio	7:1	
BPR	10:1	
Thrust	105000 [lbf]	
Fuel Flow at 100% power setting	4.221 [kg/s]	-10% of GE90-115B
Fuel Flow at 85% power setting	3.303 [kg/s]	-10% of GE90-115B
Fuel Flow at 30% power setting	1.017 [kg/s]	-10% of GE90-115B
Fuel Flow at 7% power setting	0.342 [kg/s]	-10% of GE90-115B
TSFC at 100% power setting	7.629 [g/kN/s]	-5% of XWB-97 TSFC
TSFC at 85% power setting	7.179 [g/kN/s]	-5% of XWB-97 TSFC
TSFC at 30% power setting	6.577 [g/kN/s]	-5% of XWB-97 TSFC
TSFC at 7% power setting	10.100 [g/kN/s]	-5% of XWB-97 TSFC
T3 Redline	1033.15 [K]	

Fuel flows and TSFC values are obtained from the ICAO Emission Data-bank sheets of the General Electric GE90-115B and the Rolls Royce XWB-97 engines. These engines are in this case tested at ground, while no accessory loads (power offtake) are applied.

6.1.2 Ambient Conditions

First of all we have to select Ambient Conditions for the selected Design Point: during Take-Off I considered Sea Level altitude at 0 [m], while the

engine is running at fixed point ($M=0$) and ambient temperature is defined as ISA+15 [$^{\circ}\text{C}$]. There is no TCDS for the engine which provides detailed information about testing environment, however this condition is commonly used for engine certification at take-off conditions.

Fig. 6.1: GE9X design ambient conditions

The screenshot displays the 'Design Point Input for a Geared Unmixed Flow Turbopan' software window. The interface is divided into several sections:

- Task Panel:** Contains icons for Point, Parametric, Optimize, Monte Carlo, Sensitivity, Batchjob, Project, Read, History, and Save.
- Input Panel:** Shows a tree view of the design model. Under 'Ambient Conditions', 'alt. Mach. dtamb' is selected.
- Property Table:** A table with columns 'Property', 'Unit', 'Value', and 'Comment'. It lists the following inputs:

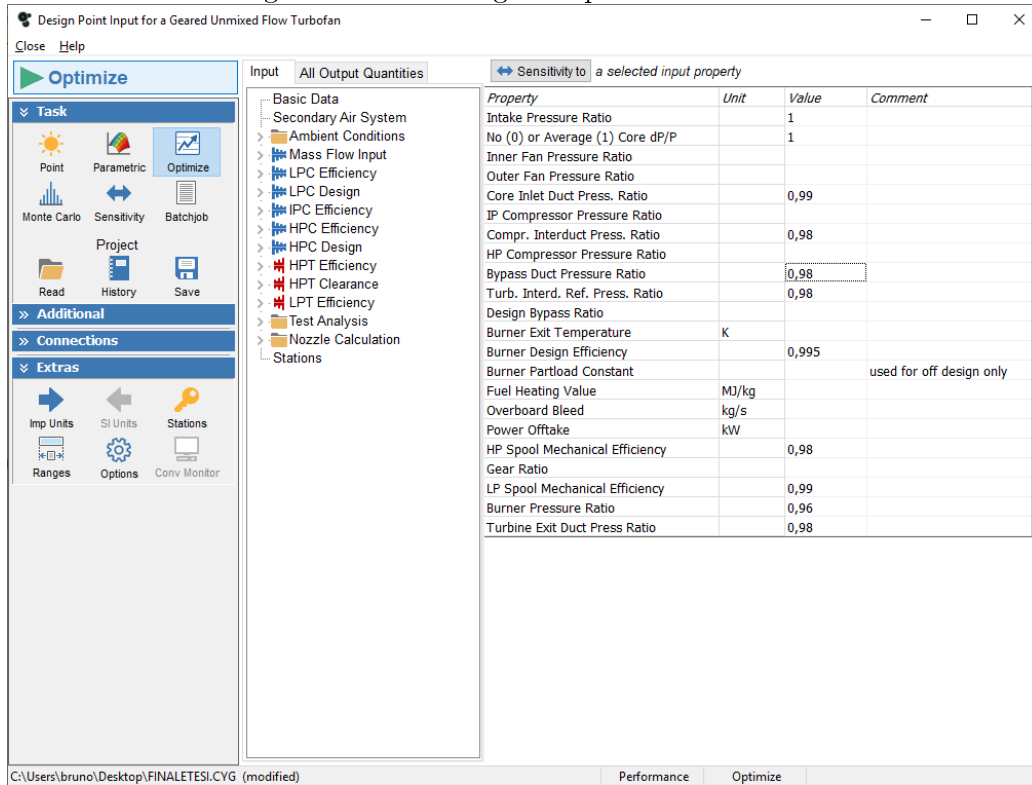
Property	Unit	Value	Comment
Altitude	m	0	
Delta T from ISA	K	15	
Relative Humidity [%]		0	
Mach Number		0	

The status bar at the bottom shows the file path 'C:\Users\bruno\Desktop\FINALETESI.CYG' and active tabs for 'Performance' and 'Design Point'.

6.1.3 Component's efficiency and pressure ratio

In order to set the General Electric GE9X design cycle every component's polytropic efficiency must be fixed for the design operating conditions. These values can be retrieved in literature and in this case the table below, provided by Kurzke in [2] and reported in Figure 4.6, is used.

Fig. 6.2: GE9X design component efficiencies



Pressure ratios of compressors have to be set from the user, together with the burner pressure ratio and pressure losses that occur in the component's interducts. Turbine's expansion ratios are output values and they should only be checked by the user at the end of the analysis. Hypothetical and acceptable values have been previously assumed and are now used as a design constraint.

6.1.4 TCDS Data

No TCDS information is available for this engine since it is currently under development and testing.

Useful information can be assumed from the TCDS of the GENx engine or from the TCDS of the GE90 engine which is the previous generation GE engine.

As mentioned before, in subsection 4.5.1 the maximum allowable temperature T_{45}^0 at Low-Pressure turbine inlet was used to evaluate both the High-Pressure and Low-Pressure turbine expansion ratios. This information was attained from the GE90-115B and the GENx-2B67 TCDSs. These temperature values

are used now as constraints in order to set up the optimization process of the design cycle.

6.1.5 *Thrust*

Information about the thrust produced by the engine could be attained in General Electric commercial brochures of the engine. The engine is reported to be capable of producing 105 [klbf] of Net Thrust. However again there is no reference about the operating condition at which this value of thrust is obtained.

Usually this is the maximum value of net thrust that the engine could provide. The maximum value of thrust is also obtained for an engine at fixed point configuration which corresponds to the (Take-Off) Design Cycle point.

This value is used as constraint during the Cycle Design point analysis in order to retrieve the proper simulated model of the engine.

6.1.6 *Cycle optimization*

During the estimation of the engine design cycle a series of variables and constraints are taken into consideration in order to obtain an acceptable and realistic engine thermodynamic cycle.

Variables and constraints are shown below in each GasTurb window:

Fig. 6.3: GE9X design optimization variables

The screenshot shows the 'Input for Optimization' dialog box with the 'Variables' tab selected. The left pane lists various design categories, and the right pane displays a table of optimization variables.

Variables	Min Value	Start Value	Max Value
Inner Fan Pressure Ratio	1,1	1,34284	1,9
Outer Fan Pressure Ratio	1,1	1,58718	1,9
IP Compressor Pressure Ratio	1,4	1,68514	1,7
HP Compressor Pressure Ratio	20	25,3668	27
Design Bypass Ratio	10	10,0763	10,5
Burner Exit Temperature	1800	1899,84	2000

Fig. 6.4: GE9X design optimization constraints

The screenshot shows the 'Input for Optimization' dialog box with the 'Constraints' tab selected. The left pane lists various design categories, and the right pane displays a table of optimization constraints.

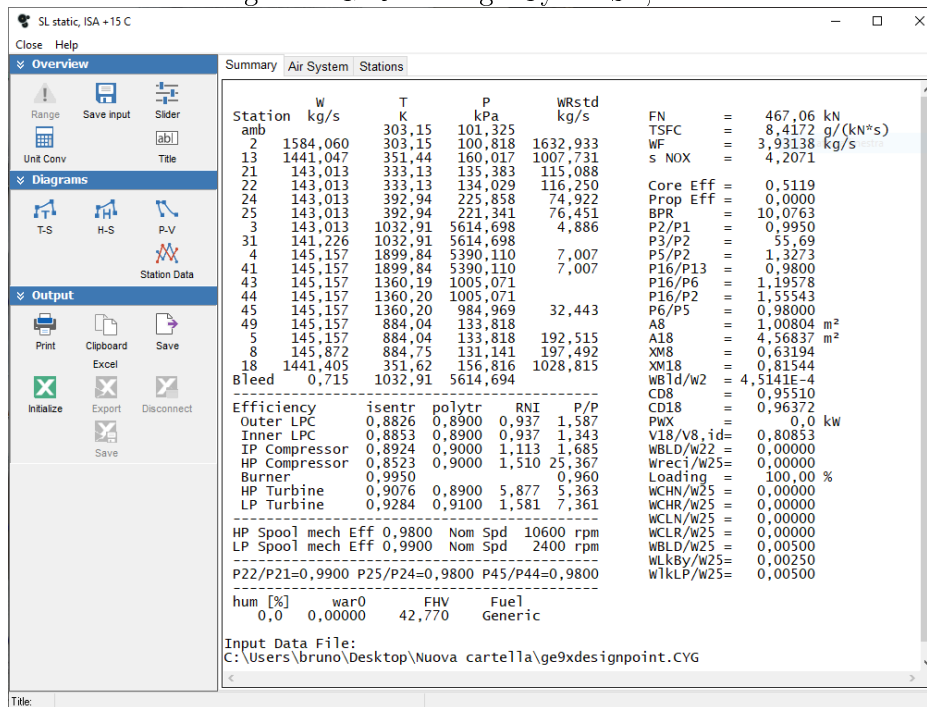
Constraints	Min Value	Start Value	Max Value
HPC Exit Temperature T3	1000	1032,91	1033,15
Overall Pressure Ratio P3/P2	54	55,6912	61
Net Thrust	467,063	467,064	467,152
LPT Inlet Temperature T45	1300	1360,2	1363,15
HPT Pressure Ratio	4	5,36292	5,65
LPT Pressure Ratio	7,3	7,36054	7,65

... on how to consider constraints from an off-design point during cycle design

6.1.7 Results

Finally the engine design cycle summary page from GasTurb is shown below:

Fig. 6.5: GE9X Design Cycle: SL, static



6.2 PW1124G-JM

6.2.1 Design Point: Cruise

In the Design Cycle analysis of this particular version of the PW1000G family engine, component polytropic efficiencies from literature [2] are used along real performance data contained in its TCDS.

6.2.2 Ambient Conditions

First of all Ambient Conditions for the Design Point must be set: during average cruise it is considered an altitude of 10973 [m] at a flight speed corresponding to a Mach number equal to 0.85 .

Fig. 6.6: PW1124G-JM design ambient conditions

The screenshot shows the 'Design Point Input for a Geared Unmixed Flow Turbofan' software interface. The window title is 'Design Point Input for a Geared Unmixed Flow Turbofan'. The interface includes a 'Task' panel on the left with options like Point, Parametric, Optimize, Monte Carlo, Sensitivity, Batchjob, Project, Read, History, and Save. The main area is divided into 'Input' and 'All Output Quantities' tabs. The 'Input' tab is active, showing a tree view of the design model. The 'Ambient Conditions' folder is expanded, showing 'alt, Mach, dtamb' and 'T1, P1, Pamb' as selected inputs. A table on the right displays the input values for these properties.

Property	Unit	Value	Comment
Altitude	m	10972,8	
Delta T from ISA	K	8,88889	
Relative Humidity [%]		0	
Mach Number		0,85	

The status bar at the bottom shows the file path 'C:\...PW1124G-JM - Copia - Copia\pw1124g-jm1cruisemassecorrette-fanV2.MYG' and the current view 'Performance Design Point'.

6.2.3 Component's efficiency and pressure ratios

Then the efficiency of all engine components have to be considered. I took into account polytropic efficiency for engine components like fan (LPC), booster (IPC), High-Pressure compressor (HPC), High-Pressure turbine (HPT) and Low-Pressure turbine (LPT). Also total pressure losses due to wall friction effects in the combustion chamber, in ducts connecting each component and in bypass ducts are taken into consideration. Taking into consideration literature [3], polytropic efficiencies and total pressure losses are summarized in table of Figure 4.7 .

Fig. 6.7: PW1124G-JM design component pressure losses and efficiencies

The screenshot shows a software window titled "Design Point Input for a Geared Unmixed Flow Turbofan". The interface is divided into several sections:

- Task Menu:** Includes options for Point, Parametric, Optimize, Monte Carlo, Sensitivity, Batchjob, Project, Read, History, and Save.
- Input Tree:** A hierarchical tree view showing various input properties such as Basic Data, Secondary Air System, Ambient Conditions, Mass Flow Input, LPC Efficiency, LPC Design, IPC Efficiency, HPC Efficiency, HPC Design, HPT Efficiency, HPT Clearance, LPT Efficiency, Test Analysis, Nozzle Calculation, and Stations.
- Output Table:** A table with columns for Property, Unit, Value, and Comment. It lists various performance metrics and their values.

Property	Unit	Value	Comment
Intake Pressure Ratio		-1	
No (0) or Average (1) Core dP/P		1	
Inner Fan Pressure Ratio			
Outer Fan Pressure Ratio			
Core Inlet Duct Press. Ratio		0,98	
IP Compressor Pressure Ratio			
Compr. Interduct Press. Ratio		0,98	
HP Compressor Pressure Ratio			
Bypass Duct Pressure Ratio		0,982187	
Turb. Interd. Ref. Press. Ratio		0,98	
Design Bypass Ratio			
Burner Exit Temperature	K		
Burner Design Efficiency		0,995	
Burner Partload Constant			used for off design only
Fuel Heating Value	MJ/kg		
Overboard Bleed	kg/s		
Power Offtake	kW		
HP Spool Mechanical Efficiency		0,99	
Gear Ratio			
LP Spool Mechanical Efficiency		0,995	
Burner Pressure Ratio		0,96	
Turbine Exit Duct Press Ratio		0,98	

The status bar at the bottom shows the file path: C:\...PW1124G-JM - Copia - Copia\pw1124g-jm1cruiseassecorrette-fanV2.MYG (modified) and the current view: Performance Design Point.

Available data

The table below summarizes the known data concerning real, measured, engine performance parameters during average cruise flight:

<i>Measured data</i>		
Thrust	[lbf]	4729
Fan face corr. Flow	[lbm/s]	1429.4
Fan OD corr. Flow	[lbm/s]	1322.6
Fan face physical flow	[lbm/s]	502.7
First speed (power turbine)	[rpm]	8416
Engine Unit Thrust Parameter		0.05

Tab. 6.1: PW1124G-JM avg. cruise known data

Usually the average cruise is set to an altitude that ranges from 10000 to 11000 [m] while the flight Mach number usually ranges from 0.8 to 0.85 . It is possible to obtain the average cruise bypass ratio as

$$BPR = \frac{1322.6}{1429.4 - 1322.6} = 12.384 \quad (6.1)$$

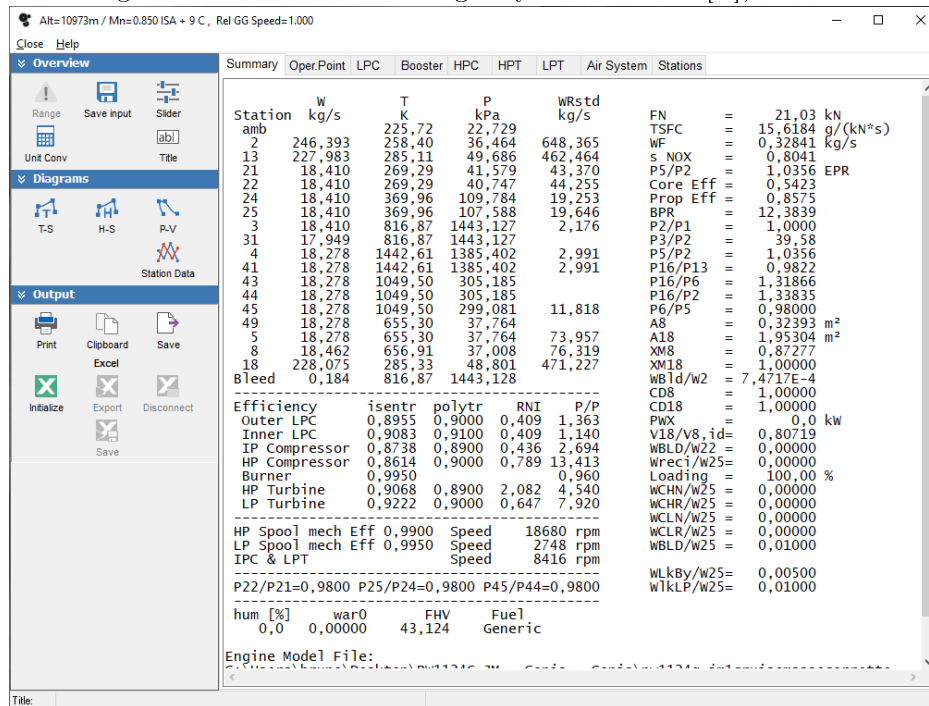
6.2.4 Cycle optimization

During the estimation of the engine design cycle a series of variables and constraints are taken into consideration in order to obtain an acceptable and realistic engine thermodynamic cycle in the same way used for the GE9X engine cycle design optimization.

6.2.5 Results

Finally the engine design cycle summary page from GasTurb is shown below:

Fig. 6.8: PW1124G-JM Design Cycle: h=36000 [ft], M=0.85



7. OFF-DESIGN CYCLE AND COMPONENT MAPS

The user can consider multiple important off-design point.

First of all one should consider cruise, the situation at which the plane flies for most of the time. At cruise it is important for a civil turbofan engine the thrust specific fuel consumption (TSFC) for fuel economy aspects of the flight, which is so important for airlines.

7.1 GE9X

7.1.1 Off-Design Point: Cruise

Estimated thrust

As today there are no technical information about the Boeing 777X which will be equipped with the GE9X engine, so it is difficult to take into consideration and to assume its Maximum Take-Off Weight (MTOW), aerodynamic drag during cruise and aerodynamic efficiency in order to calculate the required cruise thrust.

During cruise operations although it is possible to consider the following simplified equation from literature [21] which makes possible to evaluate the ratio between the required cruise thrust and the take-off thrust for conventional cruise Mach numbers ($M \approx 0.8$) of jet transport aircrafts

$$\frac{F_{CR}}{F_{TO}} = (0.0013 \cdot BPR - 0.0397) \cdot h_{CR} - 0.0248 \cdot BPR + 0.7125 \quad (7.1)$$

where F_{CR} is the thrust produced in cruise condition, F_{TO} is the thrust during take-off, BPR is the bypass ratio and h_{CR} is the cruise altitude in [km].

Assuming that:

$$F_{CR} = 105000 \text{ [lbf]}$$

$$BPR = 10.25$$

$$h_{CR} = 36000 \text{ [ft]} \sim 10.9728 \text{ [km]}$$

Finally the cruise thrust results $F_{CR}=17734$ [lbf]. This value is useful for

off-design calculation in cruise conditions. From engine off-design simulation this thrust value is going to be set within a reasonable margin.

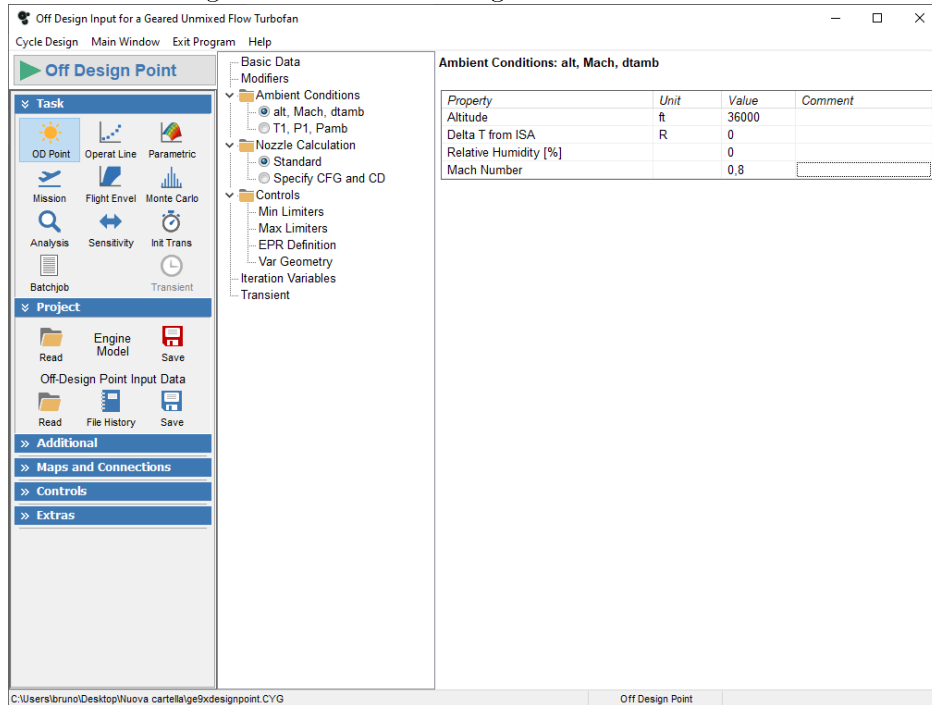
Another simplified equation useful to estimate the cruise thrust can be found in literature [31] and it is reported below

$$F_{CR}[lbf] = 200 + (0.2 \cdot F_{TO}[lbf]) \quad (7.2)$$

which permits to evaluate the cruise thrust $F_{CR}=21200$ [lbf].

GasTurb: Ambient Conditions

Fig. 7.1: GE9X Off-Design ambient conditions



Component maps

It is now possible to obtain components maps by selecting the Off-Design program scope. Special maps provided with GasTurb are used instead of standard maps in order to simulate more accurately the engine operation. I selected the following maps for the components running at cycle design point which is by default set at High-Pressure spool speed of 1 (which is 10600 [rpm] for the GE9X):

Component	Map type	Map description
LPC	GasTurb Special Map	Single-stage fan
IPC	GasTurb Special Map	Subsonic compressor
HPC	GasTurb Special Map	High-pressure ratio compressor
HPT	GasTurb Special Map	Two-stage turbine
LPT	GasTurb Special Map	High-pressure ratio turbine

Tab. 7.1: GE9X selected GasTurb maps

All maps are shown below with their scaling on the left side of the window.

Fig. 7.2: GE9X LPC map settings

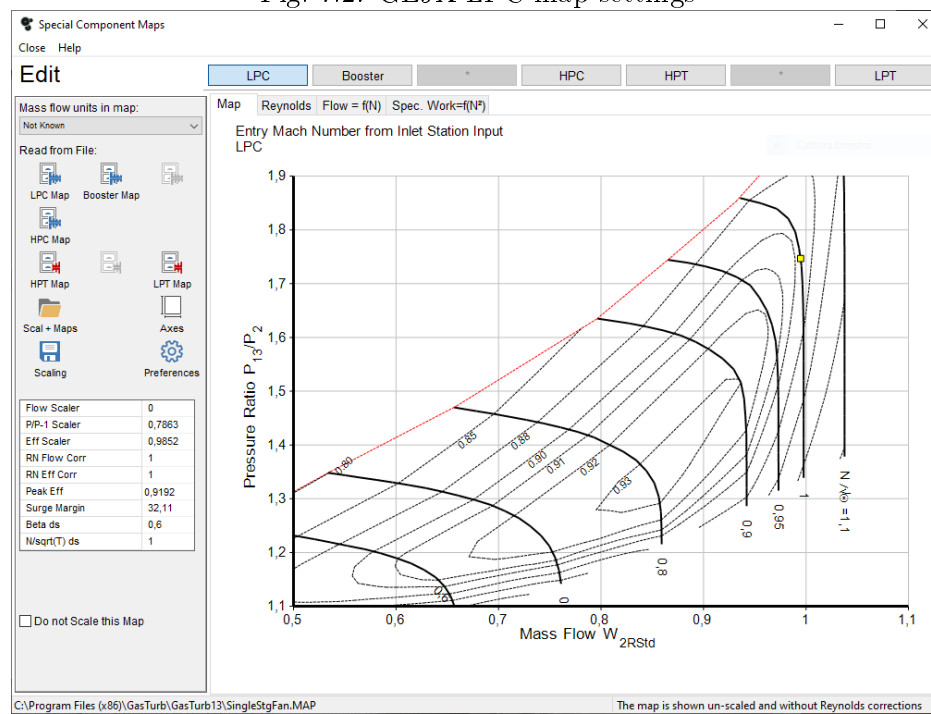


Fig. 7.3: GE9X IPC map settings

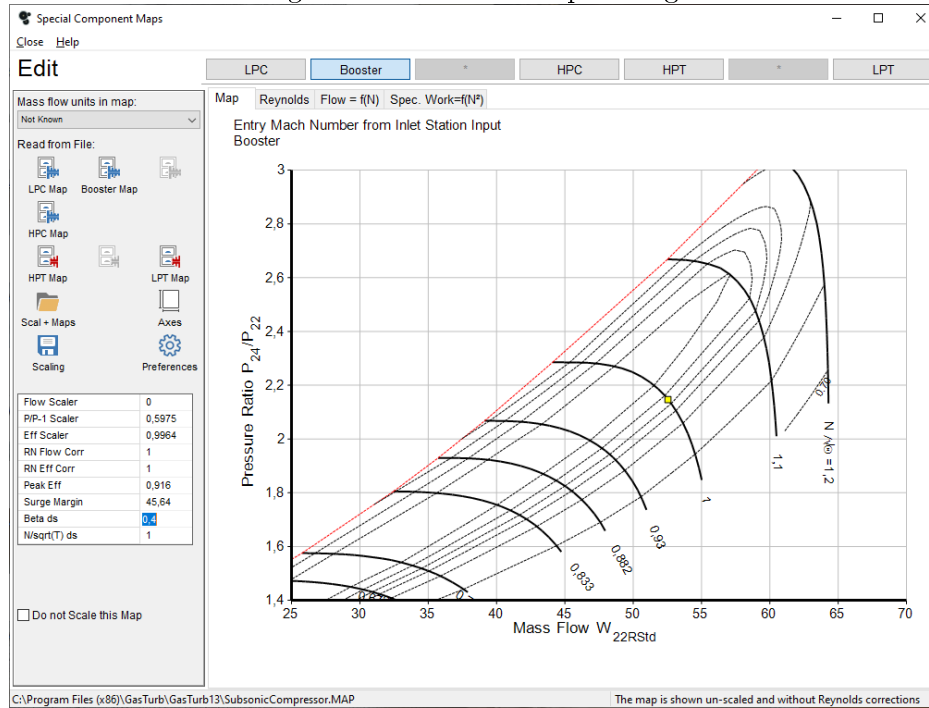


Fig. 7.4: GE9X HPC map settings

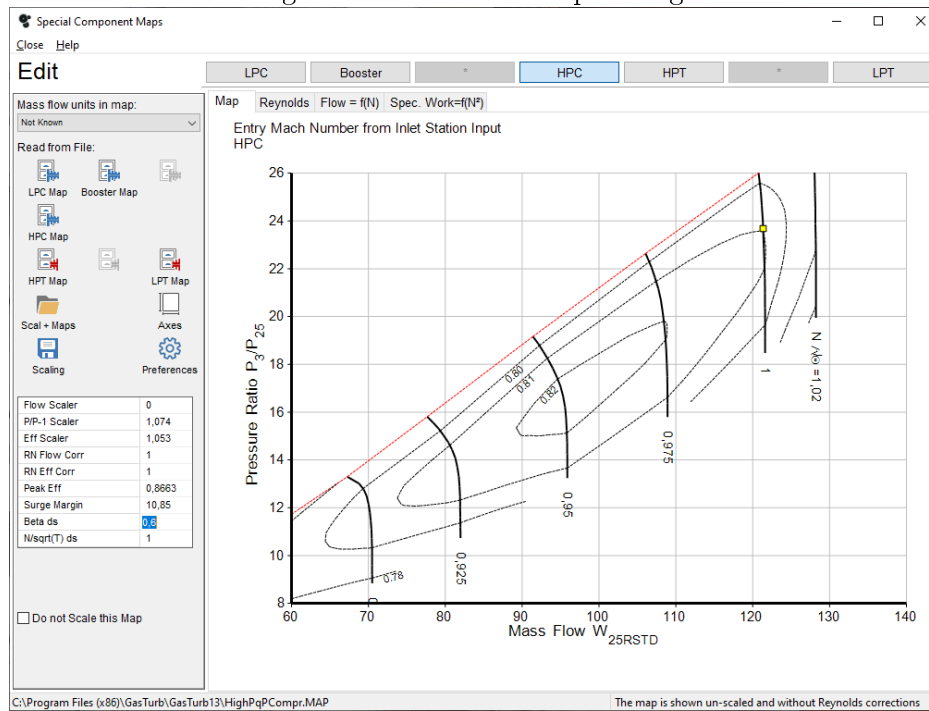


Fig. 7.5: GE9X HPT map settings

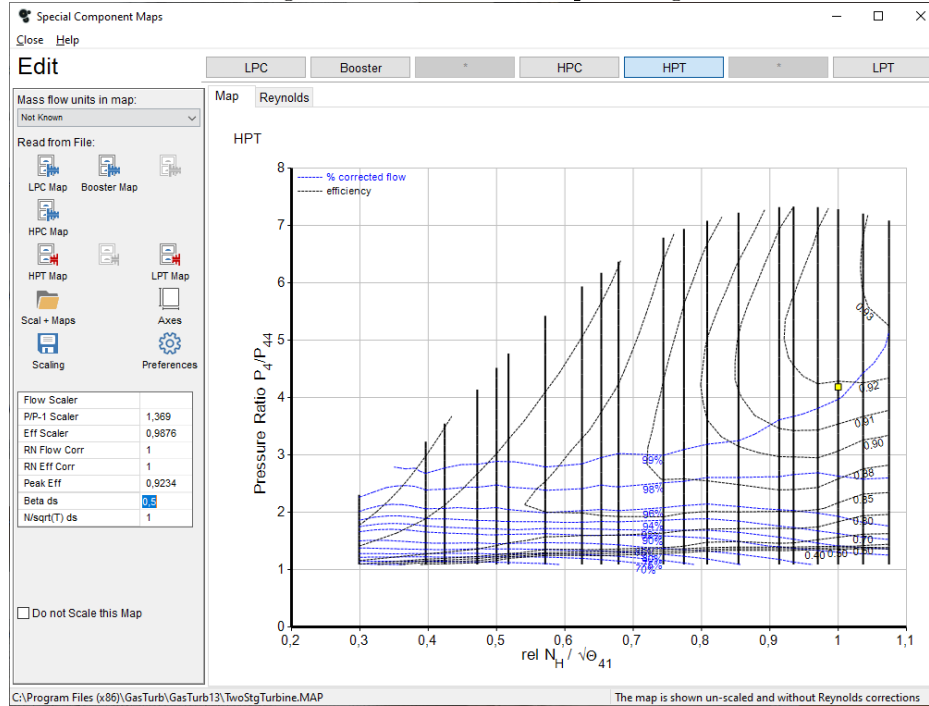
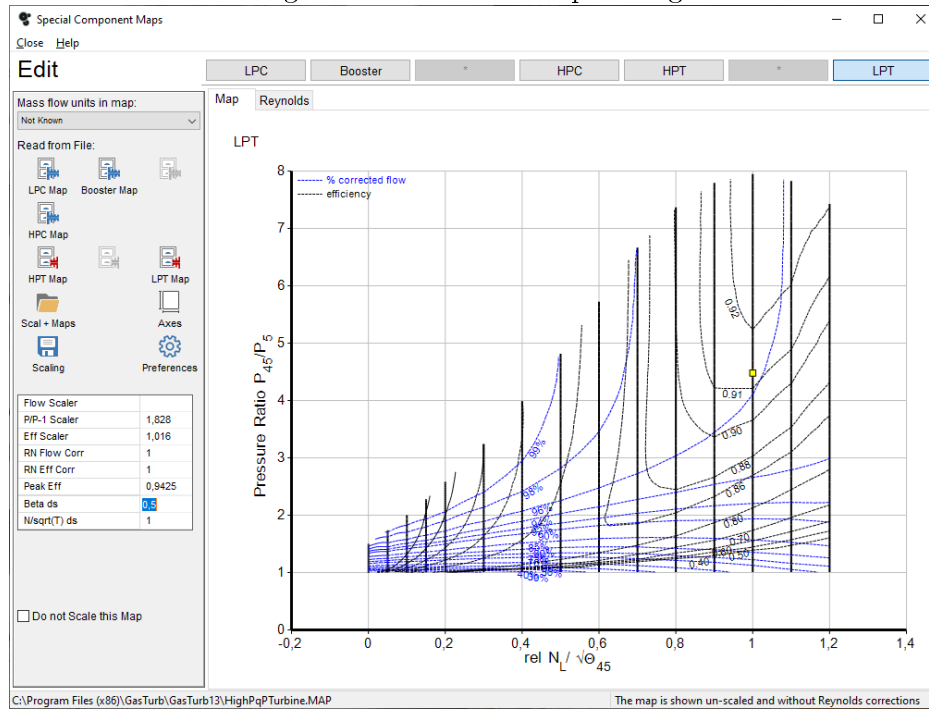


Fig. 7.6: GE9X LPT map settings



Operating lines

The operating lines are created by points which have been calculated by decreasing the High-Pressure spool speed by equal steps of 0.025 as explained in section 5.3.2 .

Speed lines are re-labeled as explained in subsection 5.3.3 since the booster map presented a nearly horizontal operating line which intersected the surge line at high mass flows. It was not possible to set this procedure using real measured data since it is not available. The procedure is then done step-by-step in order to assure a reasonable surge margin. All the slider settings used to set a Delta speed for each point are not summarized below since at each step, the map is overwritten and the Delta speed is reset to zero for each point.

Surge margin remains adequate in all maps except for the booster map at lowest spool speeds during cruise at 36000 [ft] at $M=0.8$. Since the airplane during this flight configuration will not encounter such low spool speed configuration, the map and the resultant operating line are equally acceptable. However, a bleed schedule in this case has been implemented in order to reduce the surge margin.

Fig. 7.7: GE9X LPC operating line at Cycle Design Point (Take-Off)

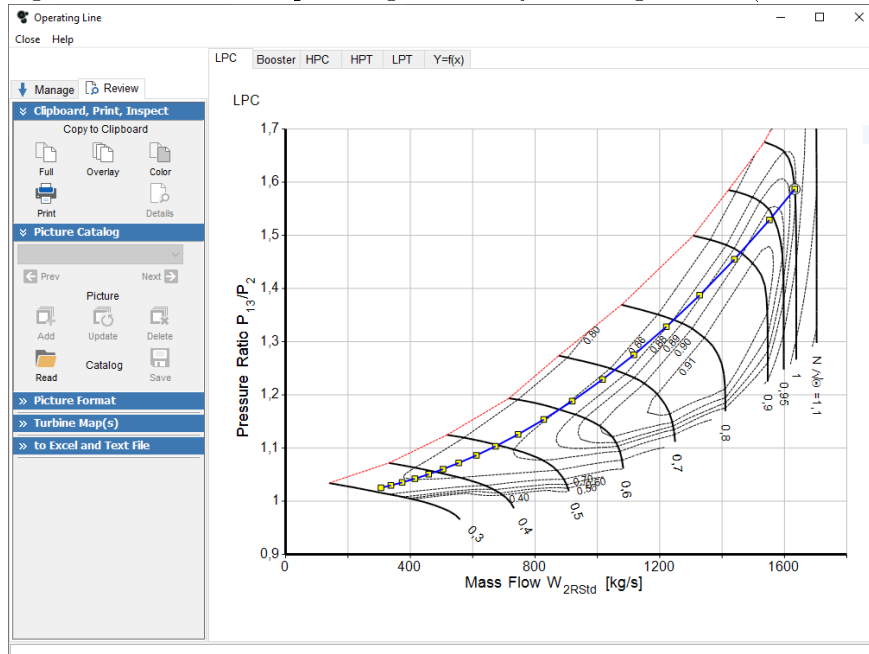


Fig. 7.8: GE9X IPC operating line at Cycle Design Point (Take-Off)

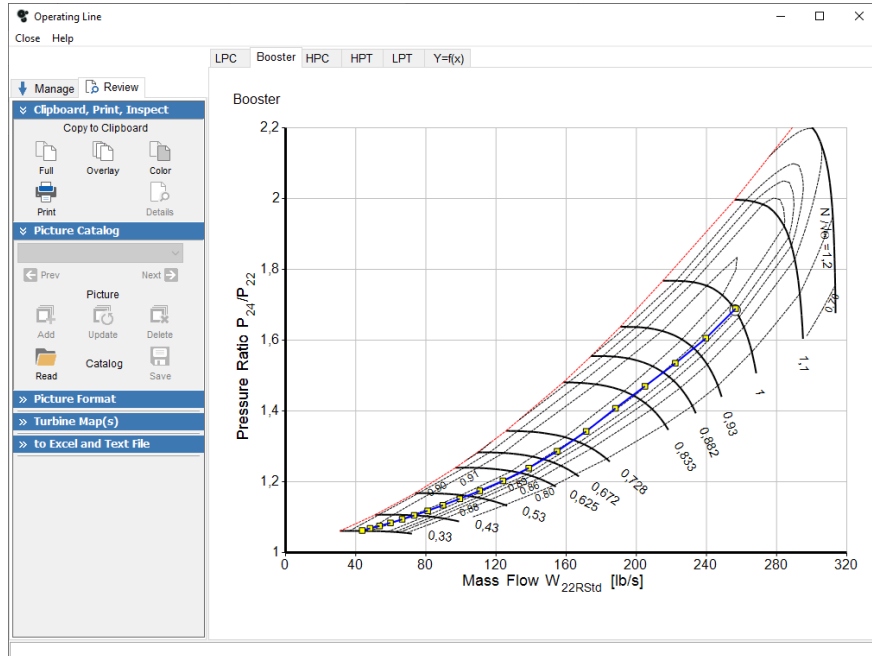


Fig. 7.9: GE9X HPC operating line at Cycle Design Point (Take-Off)

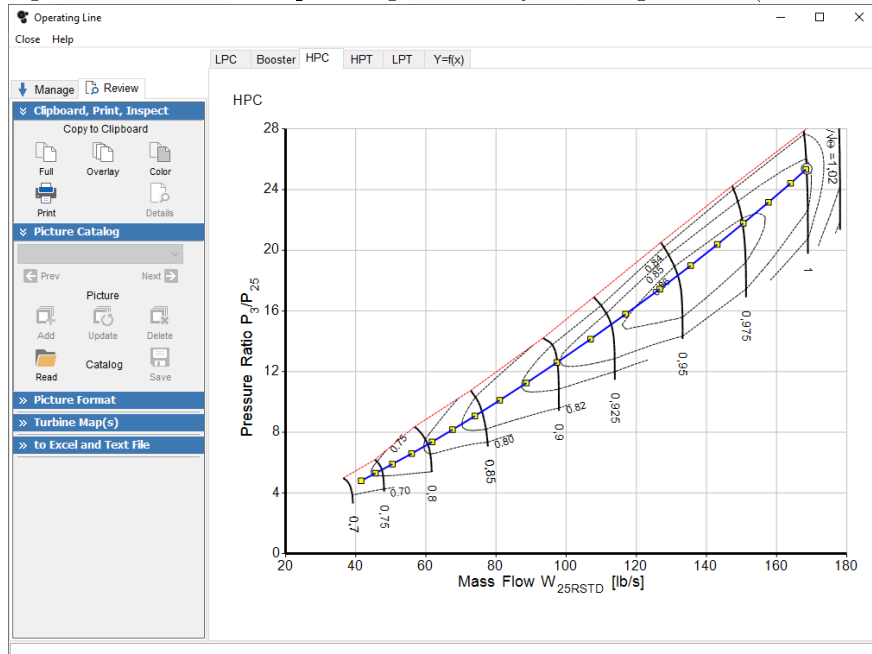


Fig. 7.10: GE9X HPT operating line at Cycle Design Point (Take-Off)

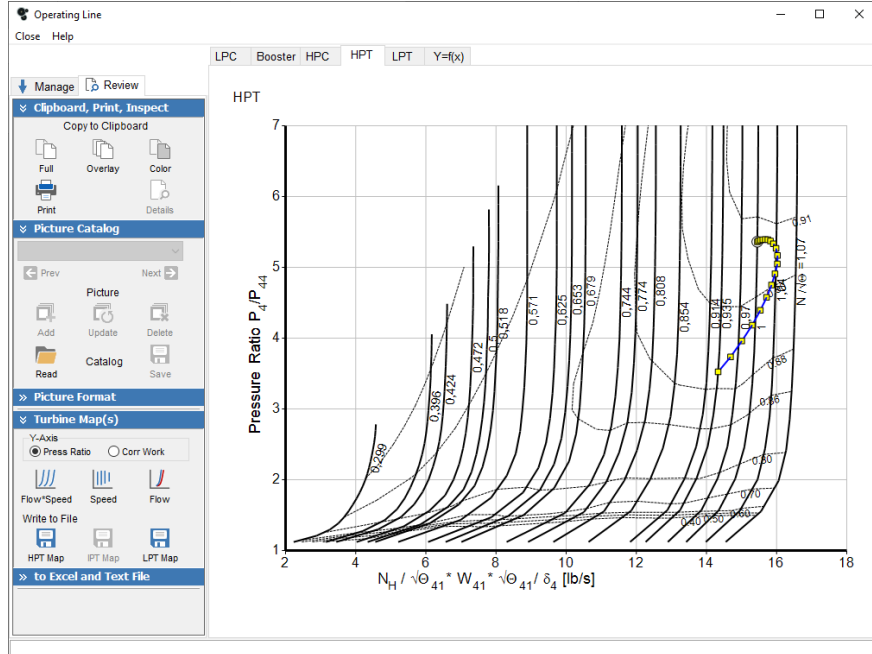


Fig. 7.11: GE9X LPT operating line at Cycle Design Point (Take-Off)

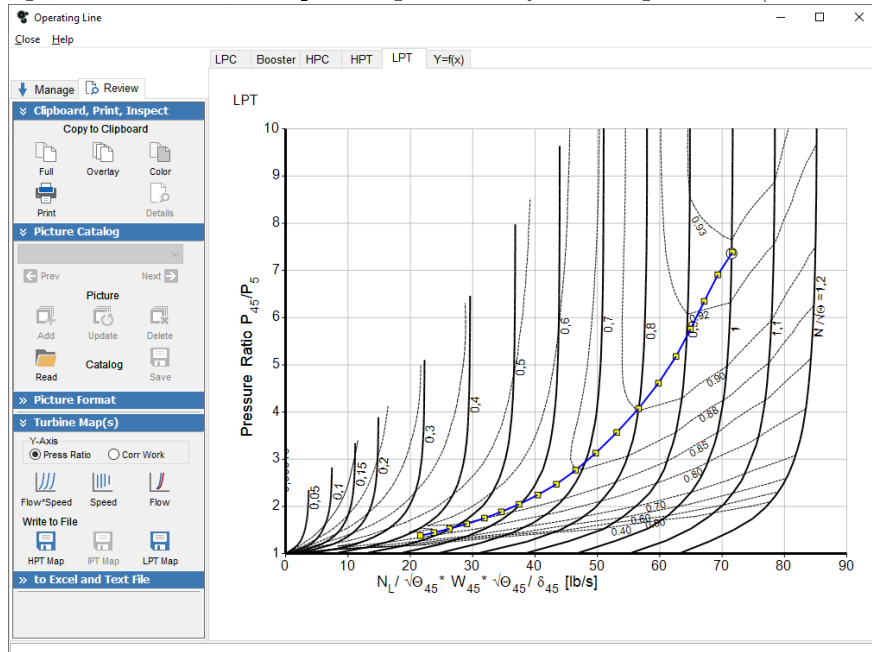


Fig. 7.12: GE9X LPC operating line at Off-Design Point (Cruise)

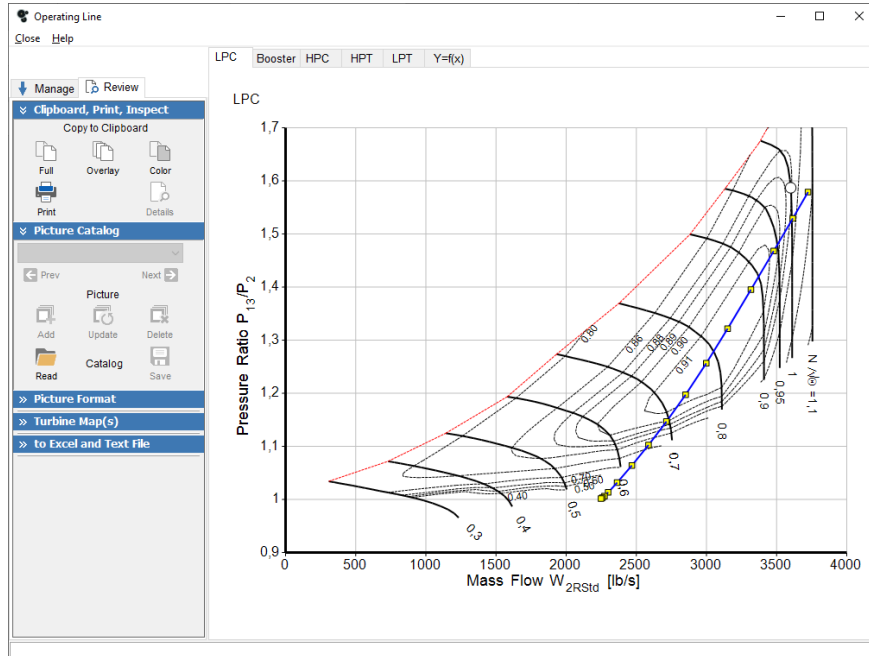


Fig. 7.13: GE9X IPC operating line at Off-Design Point (Cruise)

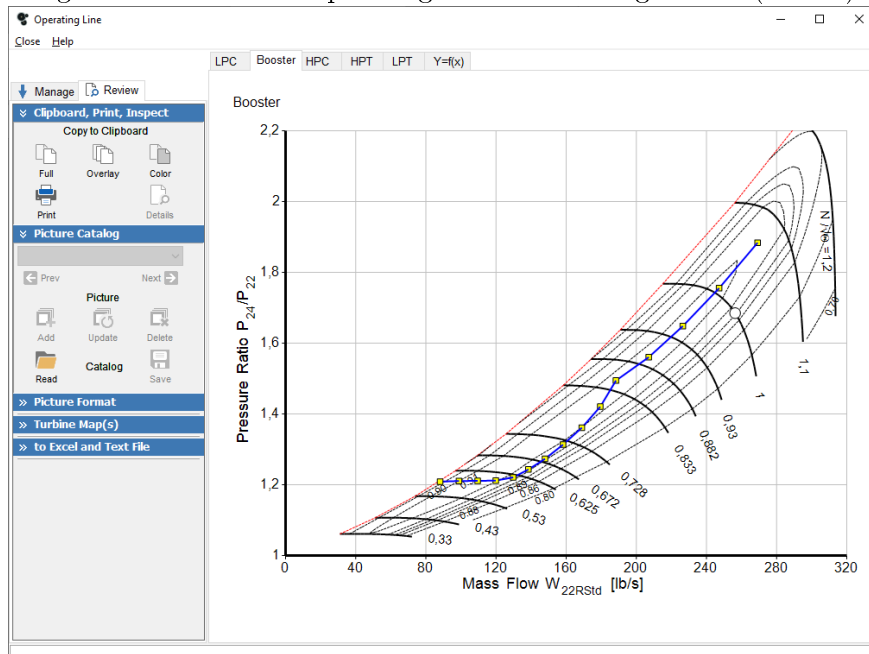


Fig. 7.14: GE9X HPC operating line at Off-Design Point (Cruise)

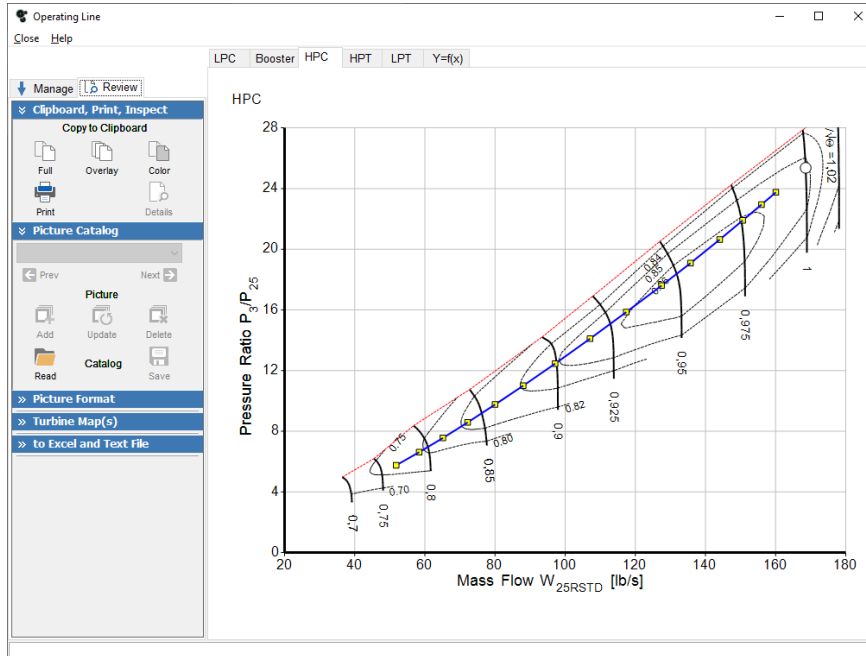


Fig. 7.15: GE9X HPT operating line at Off-Design Point (Cruise)

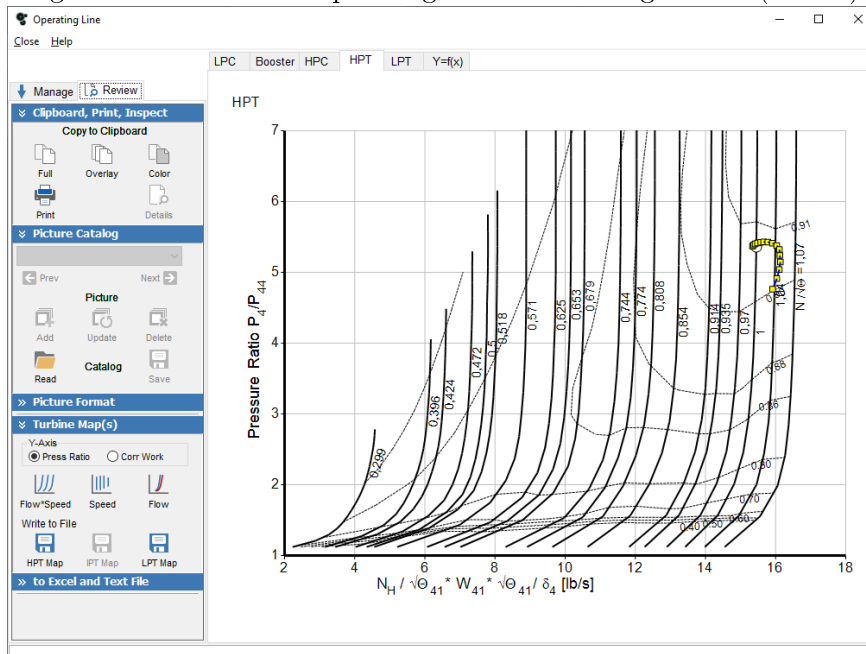
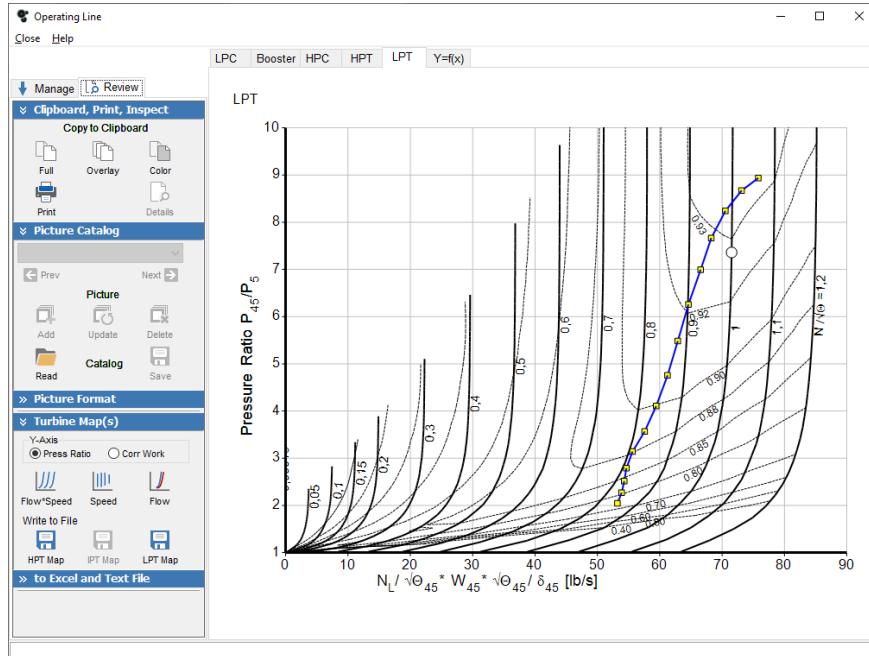


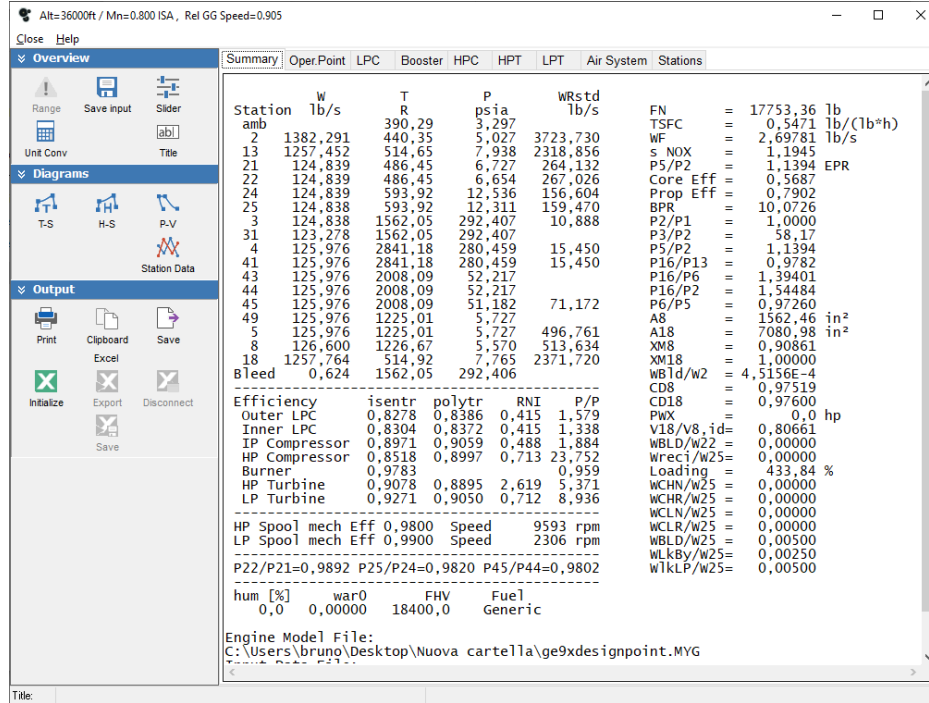
Fig. 7.16: GE9X LPT operating line at Off-Design Point (Cruise)



Results

Finally the engine Off-Design cycle summary page from GasTurb is shown below:

Fig. 7.17: GE9X Off-Design Cycle: Cruise h=36000 [ft], M=0.8



7.2 PW1124G-JM

7.2.1 Off-design point: Take-Off

All measured input data obtained from the TCDS are summarized in the table below:

<i>Condition</i>	<i>Quantity</i>	<i>Unit</i>	<i>Value</i>
SL, static	Flat rated temp.	[°C]	ISA+15
All conditions	Fuel lower heating value	[KJ/kg]	42798
SL, static	Take-Off Thrust	[KN]	132.38
SL, static	Maximum ITT temperature	[°C]	1083
Maximum	Low-Pressure spool velocity	[rpm]	10047
Maximum	High-Pressure spool velocity	[rpm]	22300
Maximum	Nacelle anti-ice		1.2% W25

Tab. 7.2: PW1124G-JM TCDS information

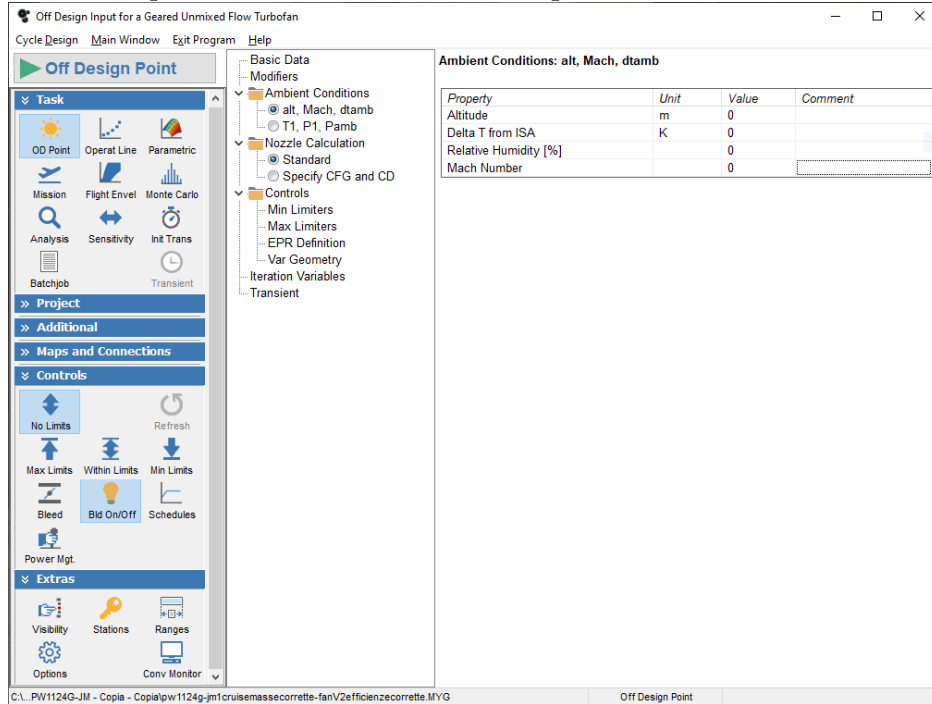
TCDS thrust certification provide the maximum amount of thrust measured in real condition during Take-Off operations. The maximum thrust in particular is obtained while the engine is running at fixed point.

TCDS also provides the maximum Indicated Turbine Temperatures (ITT) that are used as constraints for the cycle design. In Pratt & Whitney engines the ITT temperature is usually measured in the interstage between the High-Pressure Turbine and the Low-Pressure Turbine. This particular thermodynamic station inside the engine model in GasTurb is the number 45: then the constrained value for T_{45}° is set.

The resulting Off-Design cycle have to guarantee a reasonable operating margin from the constraints reported above.

GasTurb: Ambient Conditions

Fig. 7.18: PW1124G-JM Off-Design ambient conditions

*GasTurb: Components maps*

It is now possible to obtain components maps by selecting the Off-Design program scope. Special maps provided with GasTurb are used instead of standard maps in order to simulate more accurately the engine operation. I selected the following maps for the components running at cycle design point which is by default set at High-Pressure spool speed of 1 (which is 22300 [rpm] for the PW1124G-JM set at TCDS maximum speed):

<i>Component</i>	<i>Map type</i>	<i>Map description</i>
LPC	GasTurb Special Map	Single-stage fan
IPC	GasTurb Special Map	Transonic compressor
HPC	GasTurb Special Map	Medium-pressure ratio compressor
HPT	GasTurb Special Map	Two-stage turbine
LPT	GasTurb Special Map	High-pressure ratio turbine

Tab. 7.3: PW1124G-JM selected GasTurb maps

All maps are shown below with their scaling on the left side of the window.

Fig. 7.19: PW1124G-JM LPC map settings

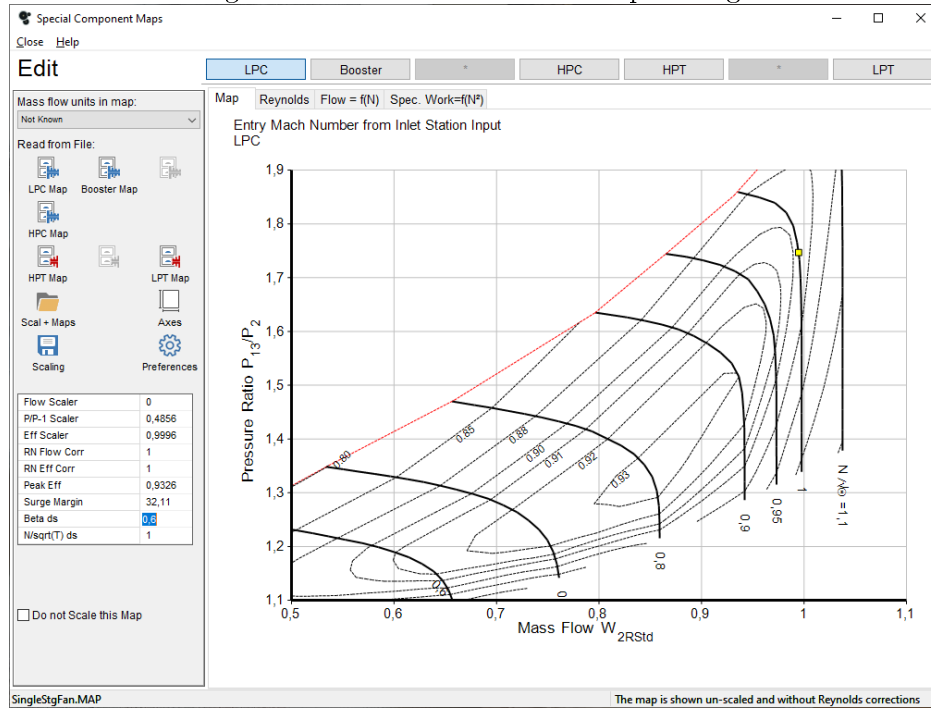


Fig. 7.20: PW1124G-JM IPC map settings

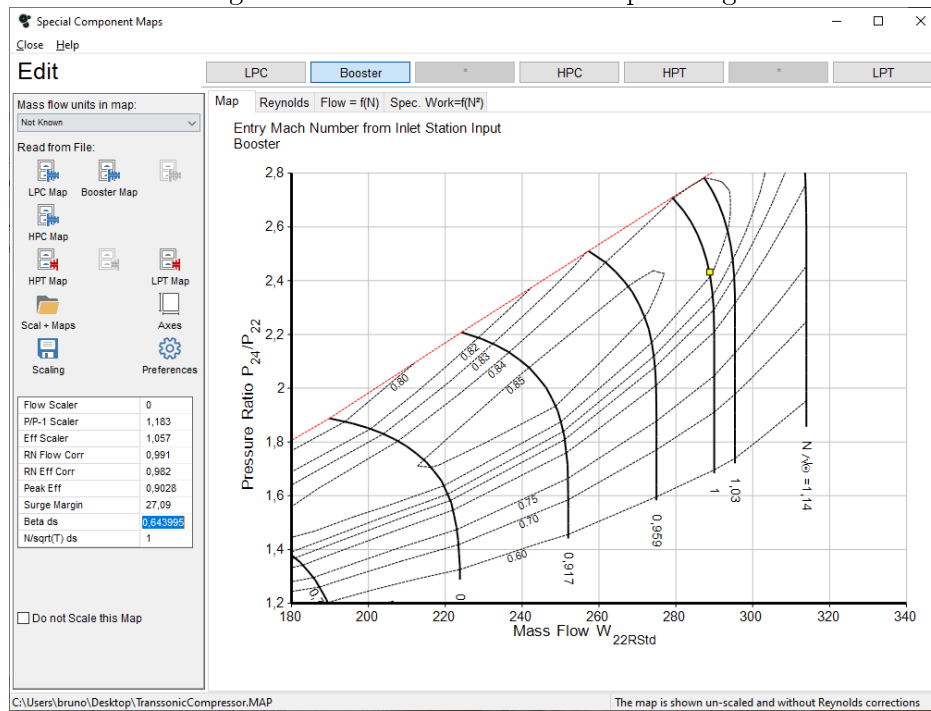


Fig. 7.21: PW1124G-JM HPC map settings

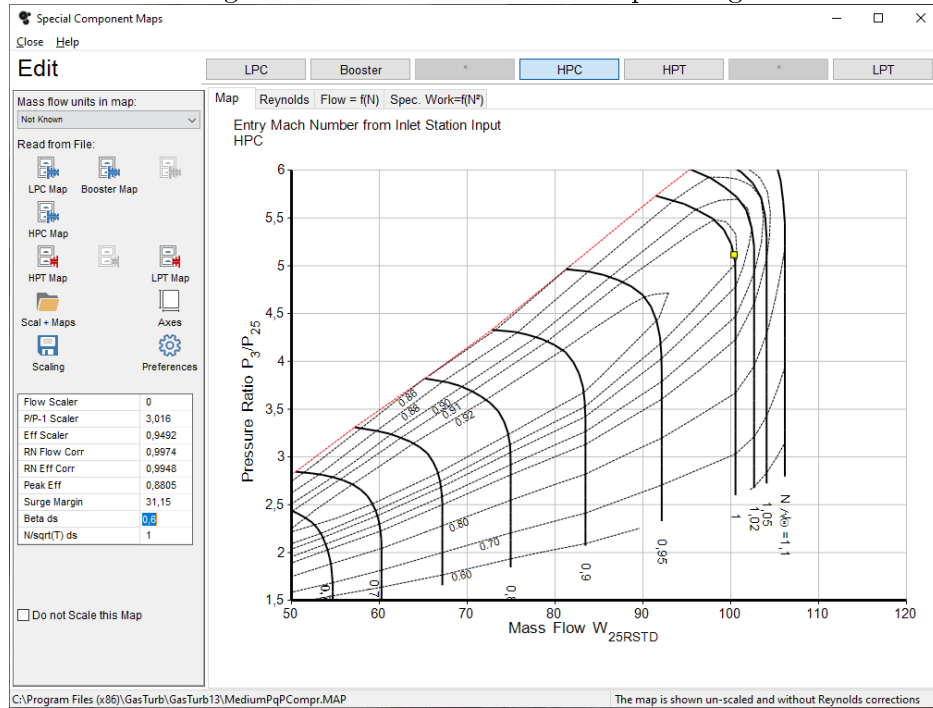


Fig. 7.22: PW1124G-JM HPT map settings

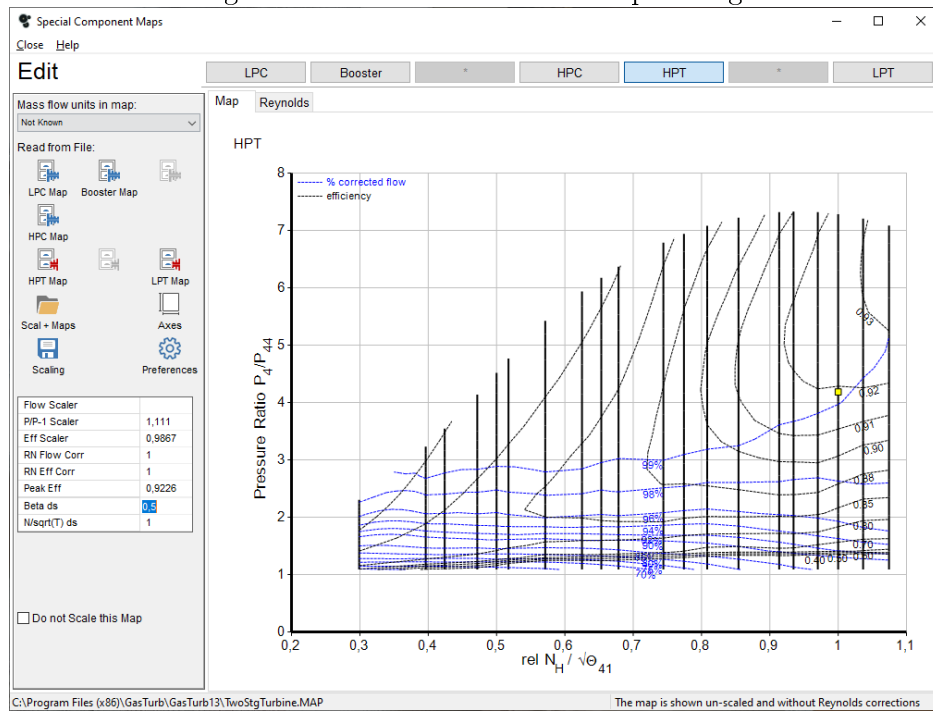
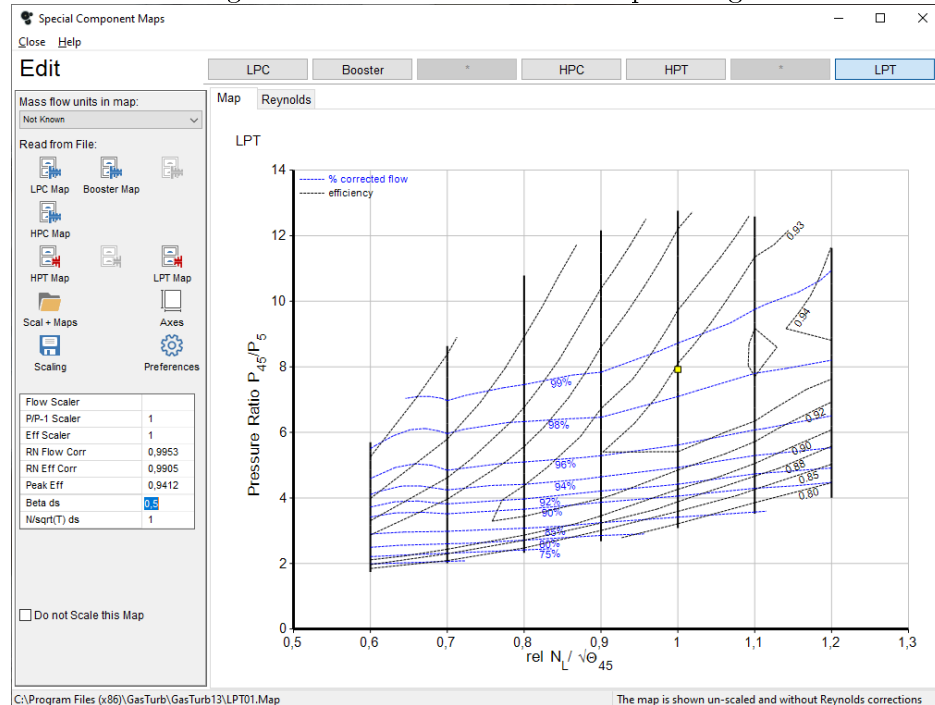


Fig. 7.23: PW1124G-JM LPT map settings



Operating lines

As done for the GE9X, The operating lines are created by points which have been calculated by decreasing the High-Pressure spool speed by equal steps of 0.025 as explained in section 5.3.2 .

Speed lines are re-labeled also in this case, as explained in subsection 5.3.3, since the booster map presented an horizontal operating line which intersected the surge line. Real measured data was unavailable so the procedure was done step-by-step in order to assure a reasonable surge margin. All the slider settings used to set a Delta speed for each point are not summarized below since at each step, the map is overwritten and the Delta speed is reset to zero for each point.

Surge margin remains adequate in all maps except for the booster map at lowest spool speeds during cruise at 36000 [ft] at $M=0.85$. The same assumption made for the GE9X is done: since the airplane during this flight configuration will not encounter such low spool speed configuration, the map and the resultant operating line are equally acceptable. A bleed schedule in this case has been implemented in order to reduce the surge margin.

Fig. 7.24: PW1124G-JM LPC operating line at Cycle Design Point (Cruise)

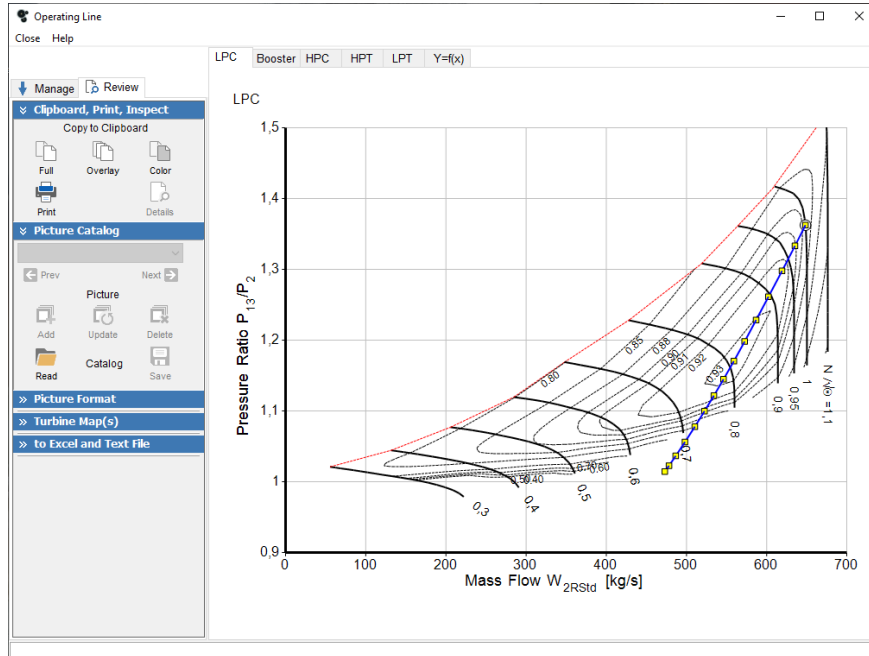


Fig. 7.25: PW1124G-JM IPC operating line at Cycle Design Point (Cruise)

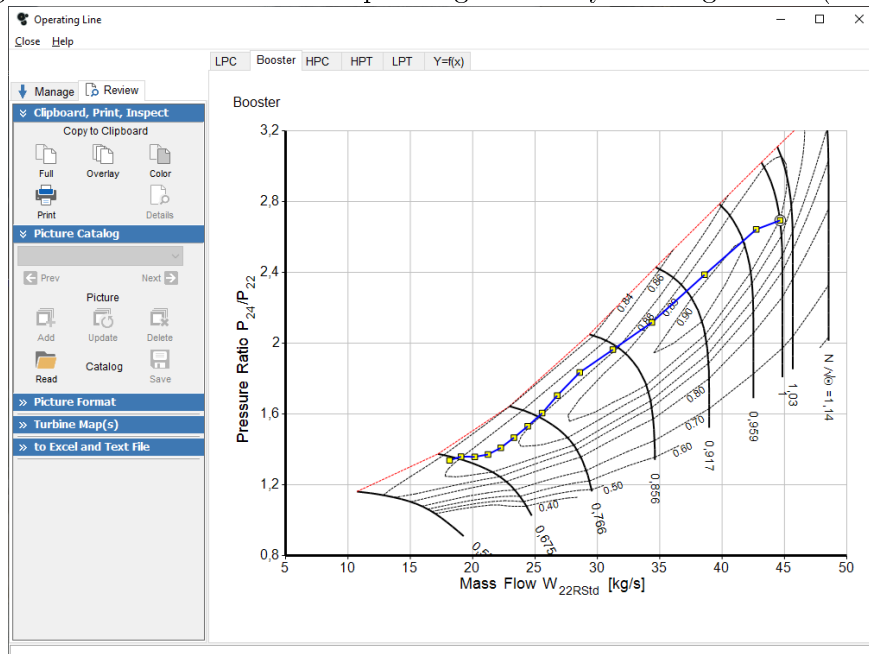


Fig. 7.26: PW1124G-JM HPC operating line at Cycle Design Point (Cruise)

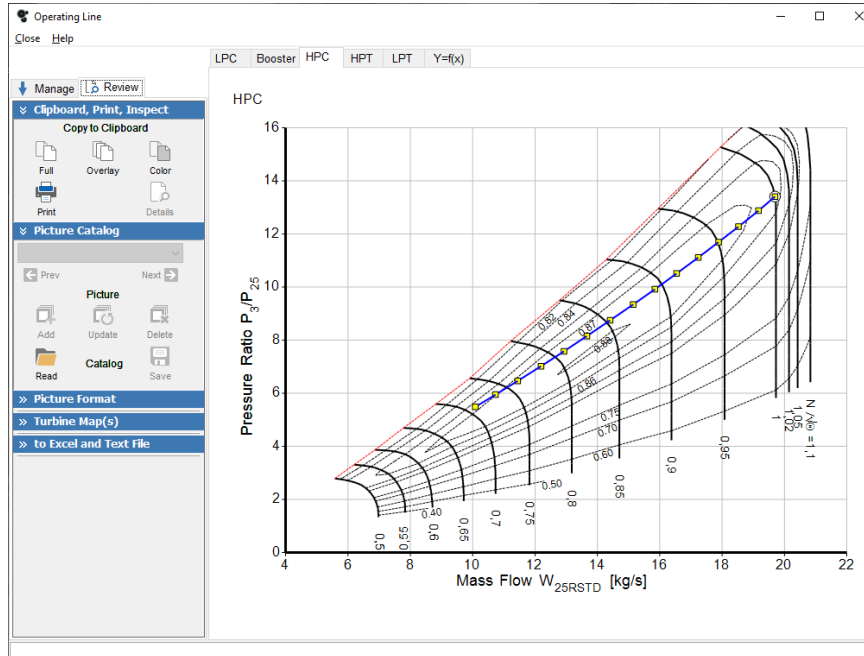


Fig. 7.27: PW1124G-JM HPT operating line at Cycle Design Point (Cruise)

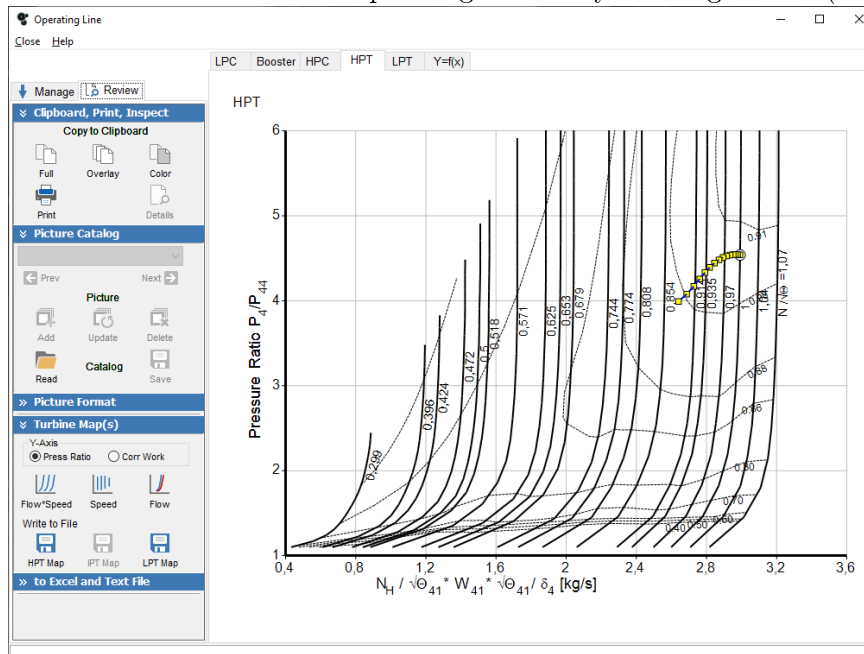


Fig. 7.28: PW1124G-JM LPT operating line at Cycle Design Point (Cruise)

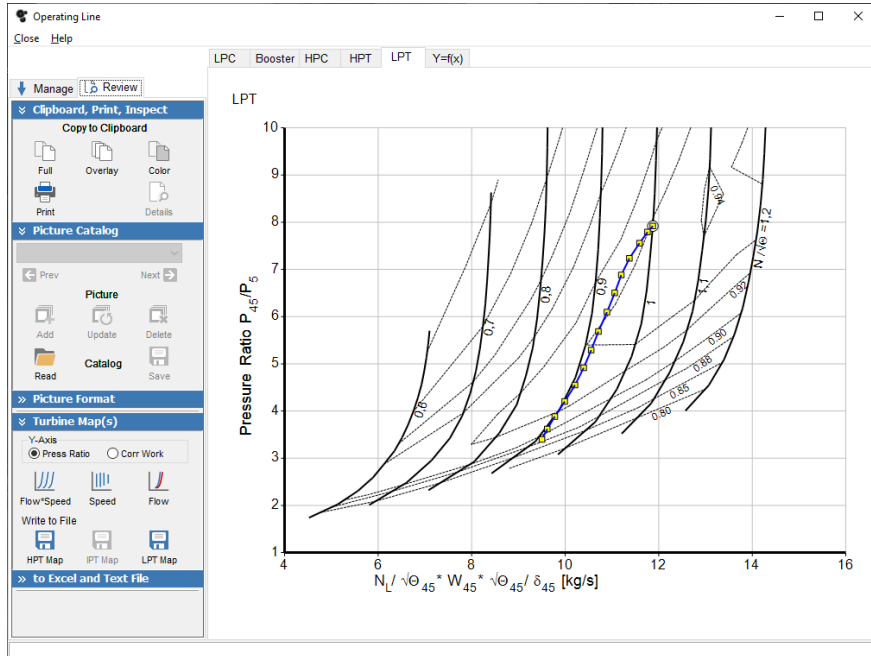


Fig. 7.29: PW1124G-JM LPC operating line at Off-Design Point (Take-Off)

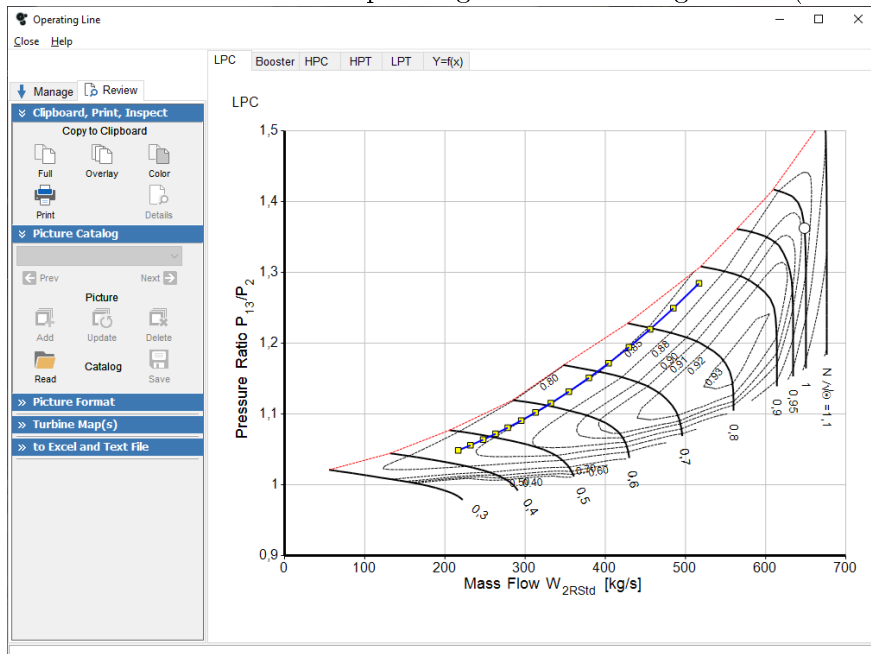


Fig. 7.30: PW1124G-JM IPC operating line at Off-Design Point (Take-Off)

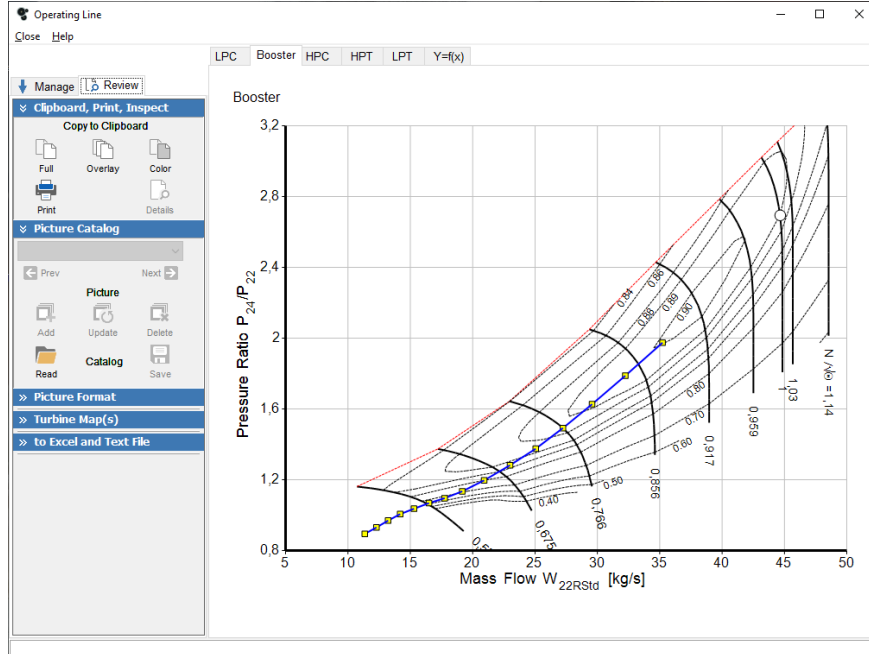


Fig. 7.31: PW1124G-JM HPC operating line at Off-Design Point (Take-Off)

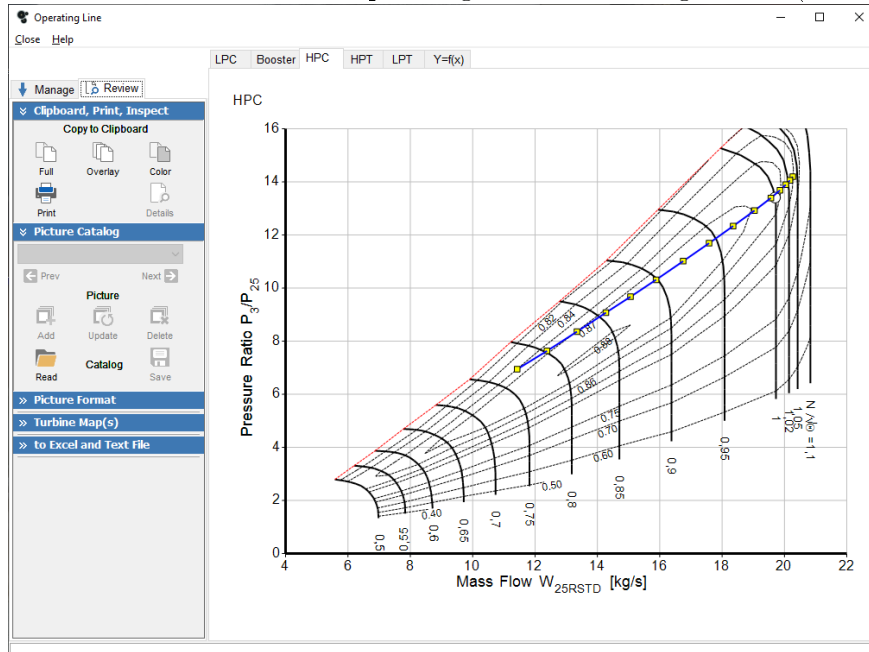


Fig. 7.32: PW1124G-JM HPT operating line at Off-Design Point (Take-Off)

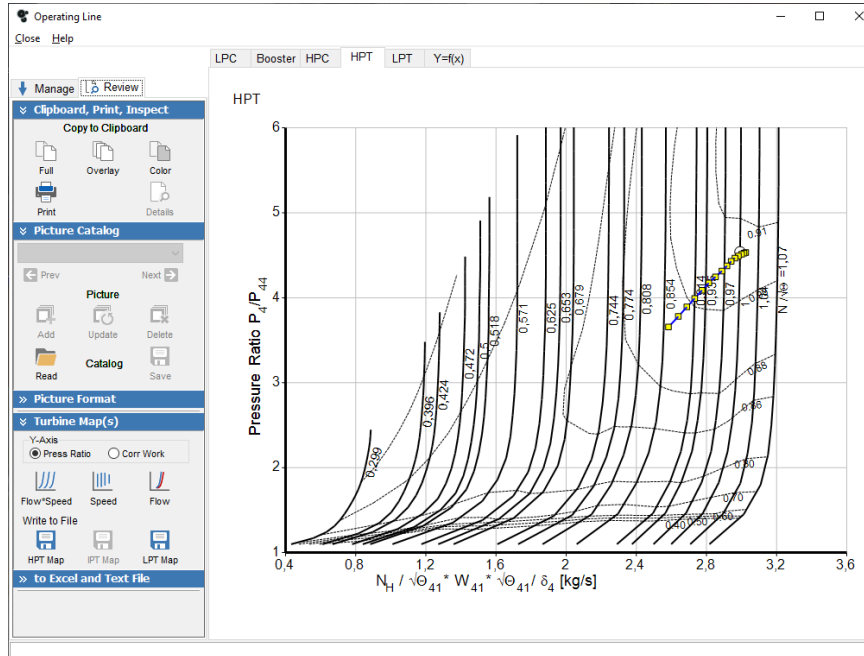
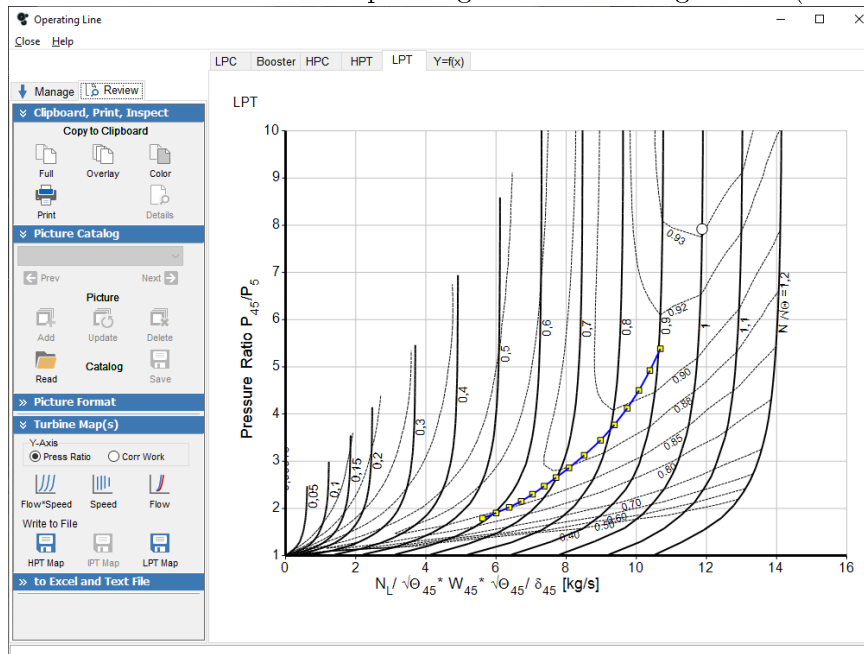


Fig. 7.33: PW1124G-JM LPT operating line at Off-Design Point (Take-Off)

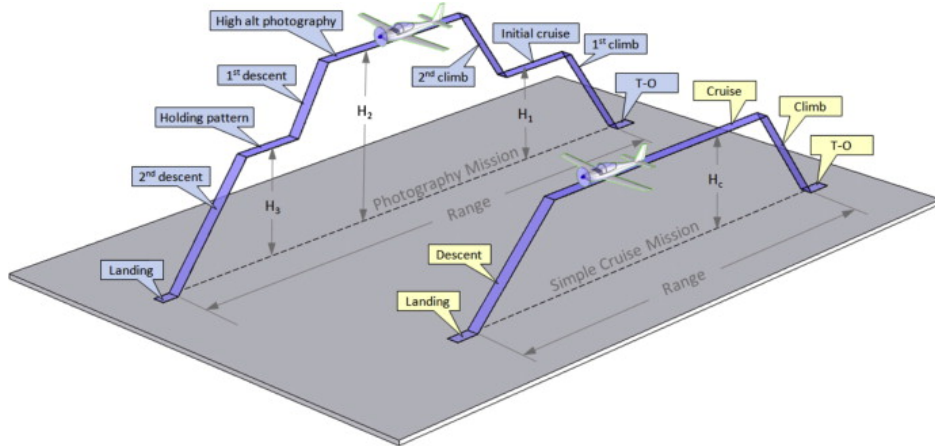


8. SIMULATED MISSION

At this point the engine model is set up and fixed: starting from the Design Point all the possible off-design points are taken into account by using the scaled operating maps of the engine components.

Now it is requested to simulate the engine behaviour during an hypothetical flight in order to compare benefits and disadvantages of the two engine peculiarities, the high-bypass unmixed turbofan engine with or without a gearbox.

Fig. 8.1: Aircraft missions (Gudmundsson, see [13])



The flight simulation in GasTurb software corresponds to a multi point mission analysis which permits to evaluate different operating points simultaneously. However, it does not evaluate a complete single flight envelope. Flight starts with take-off conditions at sea level altitude. The engine is set to the design point corresponding to Take-Off, which can be a Design point in case of the GE9X engine or an Off-Design point in case of the PW1124G-JM engine. I considered a Take-Off duration of 2 minutes.

Then there is the cruise segment set to an altitude of 36000 [ft] at $M=0.85$. The aircraft will spend most of the time in cruise which is the most efficient flight condition, and it is considered a 2-hour cruise flight time.

Finally the landing segment at sea level altitude which is set at an average

altitude of 500 [m] at $M=0.25$ for 3 minutes .

I also considered a 20 minutes holding at an altitude of 4000 [m] at $M=0.44$ which corresponds to a True Air Speed (TAS) of about 227 [kts] and a Calibrated Air Speed (CAS) of about 229 [kts], since the ICAO imposes a maximum Indicated Air Speed (IAS) of 230 [kts]. Usually the IAS is slightly higher than the corresponding CAS value.

Thrust requirements for each flight segment are necessary in order to set up the Mission Calculation in GasTurb, and are now estimated below with a method reported in literature [21].

During Take-Off and cruise flight the thrust requirements are given by the engine design point, but for the holding phase the required thrust are an unknown parameter. However, it is possible to evaluate the lift coefficient in cruise flight for flight with minimum drag, at maximum efficiency E_{max} as

$$C_{L,md} = \frac{\pi \cdot AR \cdot e}{2 \cdot E_{max}} \quad (8.1)$$

The aspect ratio AR can be evaluated from the aircraft technical specification, the Oswald factor e can be assumed in a range from 0.7 to 0.85 and the maximum efficiency E_{max} of the aircraft can be retrieved in literature. The actual lift coefficient could be evaluated as

$$C_L = \frac{C_{L,md}}{(V/V_{md})^2} \quad (8.2)$$

The actual lift-to-drag ratio in cruise flight is equal to

$$E = \frac{2 \cdot E_{max}}{\frac{1}{\left(\frac{C_L}{C_{L,md}}\right)} + \left(\frac{C_L}{C_{L,md}}\right)} \quad (8.3)$$

A flight that produces the biggest range for a jet aircraft requires $V/V_{md} = 1.316$ but usually for many aircraft $V/V_{md} = 1 \div 1.316$ is valid. Choosing an acceptable value for V/V_{md} , for example by assuming that during the holding flight segment the value permits to obtain nearly the best flight range, it is possible to evaluate the efficiency during the holding flight. Finally the holding required thrust can be evaluated as

$$F_{hold} = \frac{MTOW \cdot g}{E_{hold}} \quad (8.4)$$

In the table below there are summarized all the data necessary to calculate the required holding thrust for both the engine. More assumptions are made

for the GE9X engine since the aircraft powered by the engine is under development and technical specifications are still unknown.

<i>Quantity</i>	<i>Unit</i>	<i>PW1124G-JM</i>	<i>GE9X</i>
AR		10.3	11.04
E_{max}		18	21
Oswald factor e		0.8	0.8
Calculated $C_{L,md}$		0.719	0.661
V/V_{md}		1.316	1.316
Calculated C_L		0.415	0.382
Calculated E_{hold}		15.59	18.195
MTOW	[kg]	75500	351534
Required F_{hold}	[kN]	47.492	189.468

Tab. 8.1: Mission: holding phase required thrust

During the landing phase the engine are assumed to produce a net thrust equal to 33% of the Take-Off thrust.

8.1 GasTurb mission setup

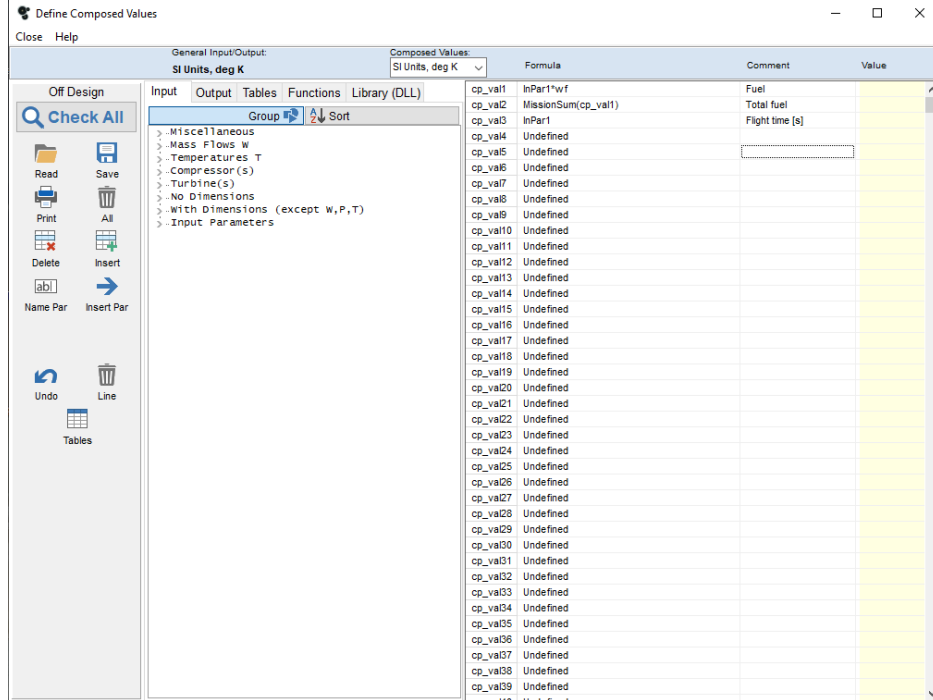
In order to initialize the mission calculation the user has to create two composed values using the GasTurb formula editor. As introduced in subsection 5.3.6 composed values are used to take into account the effective flight time spent in each mission phase, the fuel consumed in each phase and the total fuel burnt.

The input parameter *InPar1* indicates the time spent in each flight phase and is measured in [s].

The parameter *SementFuel* is used to evaluate the total fuel mass burnt in each flight phase and is measured in [kg] or [lb] depending on the unit of measure used during the cycle design.

The parameter *MissionSum* is used to sum all the single phase fuel consumptions and it calculates the total fuel burnt during the entire mission (flight), and it is expressed in [kg] or [lb].

Fig. 8.2: Formula editor and mission composed values



8.2 Engine comparison and results

Results obtained for both the engines are now summarized below:

<i>Quantity</i>	<i>Unit</i>	<i>Take-Off</i>	<i>Cruise</i>	<i>Holding</i>	<i>Landing</i>
Net thrust	[kN]	466.947	76.718	190.101	152.394
Flight time	[s]	120	7200	1200	180
Fuel flow	[kg/s]	3.898590	1.213582	2.352022	1.679190
Fuel	[kg]	467.8308	8737.7904	2822.4264	302.2542
TSFC	[g/(kN*s)]	8.34911	15.81874	12.37249	11.01874
Total fuel	[kg]		12330.30		

Tab. 8.2: GE9X Mission summary

<i>Quantity</i>	<i>Unit</i>	<i>Take-Off</i>	<i>Cruise</i>	<i>Holding</i>	<i>Landing</i>
Net thrust	[kN]	106.706	21.027	47.253	34.403
Flight time	[s]	120	7200	1200	180
Fuel flow	[kg/s]	0.736869	0.328398	0.551898	0.383027
Fuel	[kg]	88.4243	2364.46	662.277	68.9449
TSFC	[g/(kN*s)]	6.90561	15.6183	11.6841	11.1336
Total fuel	[kg]		3184.11		

Tab. 8.3: PW1124G-JM Mission summary

In order to compare two different turbofan engines I think it is useful to consider the Thrust-Specific Fuel Consumption (TSFC) which is the best parameter to describe the efficiency in terms of fuel consumption.

As can be seen from the simulated mission data, both the engines are characterized by similar TSFCs in all the flight segments except for the Take-Off phase. In this case the GE9X's TSFC is 20.9% higher than the PW1124G-JM's TSFC. It is important to consider that GE9X engine Cycle Design point is set at Take-Off while the PW1124G-JM Cycle Design point is set at Cruise.

Taking into consideration core efficiencies: the GE9X's core efficiency is 0.5128 while the PW1124G-JM core efficiency is 0.4545 .

The major difference is the combustor total temperature rise which is higher in the GE9X engine and could explain why the fuel consumption is higher in this phase.

During Cruise the PW1124G-JM engine has a TSFC which is 1.28% lower than the GE9X TSFC while during the holding phase the PW1124G-JM is 5.89% lower than the one of the GE9X.

At landing the GE9X engine has a TSFC which is 1.04% lower than the PW1124G-JM TSFC.

It is so difficult to compare such similar results since the engine model simulated in GasTurb are made by making several assumptions that could alter the TSFC result. The engines were simulated without precise technical data, and a comparison of fuel consumptions require the information contained in the engine workshop manual to be precise, accurate and reliable.

GasTurb mission analysis is therefore a useful and easy tool to compare both the efficiencies of different engines running at the same flight conditions or the efficiency of a single engine running at different conditions.

Below it is reported the GasTurb window containing the mission calculation results for both the engines separately.

Fig. 8.3: GE9X mission results window

Description		Point 1 Take-Off	Point 2 Cruise	Point 3 Landing	Point 4 Holding
Number of Iteration Loops		1.1	38.1	65.1	32.1
Altitude	ft	0	36000	1640	13123,4
Delta T from ISA	R	27	0	0	0
Relative Humidity [%]		0	0	0	0
Mach Number		0	0,85	0,3	0,44
Overboard Bleed	lb/s	0	0	0	0
Power Offtake	hp	0	0	0	0
Bypass/Core Press Ratio P18/P6		1,1959	1,44149	1,21642	1,28172
Ideal Jet Velocity Ratio V18/V8		0,808731	0,825094	1,1201	0,858159
Core Inlet Duct Press Loss [%]		0,999878	1,02813	0,553596	0,978825
Comp Interduct Press Loss [%]		2,00051	1,76534	1,57848	1,86156
Burner Pressure Loss [%]		4,00069	4,09911	4,25641	4,07636
Non-Chargeable HPT Wcl/W25		0	0	0	0
Chargeable HPT Wcl/W25		0	0	0	0
Turb Interduct Press Loss [%]		2,00003	1,98369	1,99222	1,99846
Non-Chargeable LPT Wcl/W25		0	0	0	0
Chargeable LPT Wcl/W25		0	0	0	0
Turbine Exit Press Loss [%]		1,99931	2,74576	1,01252	2,1637
Bypass Press Loss [%]		1,99986	2,17888	1,64598	2,13241
Core-Byp Heat Transfer dT13	R	0	0	0	0
Core-Byt Heat Transfer dT3	R	0	0	0	0
Cooling Air Cooling dT13	R	0	0	0	0
Cooling Air dT	R	0	0	0	0
Bleed Air Cooling dT13	R	0	0	0	0
Bleed Air dT	R	0	0	0	0
Propulsive Efficiency		0	0,809527	0,620746	0,637716
Core Efficiency		0,512796	0,569817	0,452184	0,529882
Interduct Pressure Ratio		0,98	0,980183	0,980078	0,980015
Engine Pressure Ratio P5/P2		1,32707	1,09286	1,05659	1,2062
Equivalent Airspeed (knots)		0	268,059	193,824	228,457
#1:InPart		120	7200	180	1200
#2:InPart*wf		1031,39	19263,5	666,356	6222,28
#3:MissionSum(cp_val2)		1031,39	20294,9	20961,3	27183,6
HP Spool Speed (RPM)		10600	9593	9434	9964

Fig. 8.4: PW1124G-JM mission results window

Description		Point 1 Cruise	Point 2 Take-Off	Point 3 Holding	Point 4 Landing
Number of Iteration Loops		1.1	31.1	19.1	85.1
Altitude	m	10973	0	4000	500
Delta T from ISA	K	8,88889	0	0	15
Relative Humidity [%]		0	0	0	0
Mach Number		0,85	0	0,44	0,25
Overboard Bleed	kg/s	0	0	0	0
Power Offtake	kW	0	0	0	0
Ideal Jet Velocity Ratio V18/V8		0,807167	0,831606	0,872199	1,15224
Core Inlet Duct Press Loss [%]		2	1,28533	1,56484	0,693402
Comp Interduct Press Loss [%]		2	2,12304	2,09056	3,12604
Burner Pressure Loss [%]		4	3,90481	3,95823	3,82352
Non-Chargeable HPT Wcl/W25		0	0	0	0
Chargeable HPT Wcl/W25		0	0	0	0
Turb Interduct Press Loss [%]		2,00001	1,99891	2,01322	1,8954
Non-Chargeable LPT Wcl/W25		0	0	0	0
Chargeable LPT Wcl/W25		0	0	0	0
Turbine Exit Press Loss [%]		2,00002	1,01745	1,37034	0,437838
Bypass Press Loss [%]		1,78131	1,2568	1,61239	0,986958
Core-Byp Heat Transfer dT13	K	0	0	0	0
Core-Byt Heat Transfer dT3	K	0	0	0	0
Cooling Air Cooling dT13	K	0	0	0	0
Cooling Air dT	K	0	0	0	0
Bleed Air Cooling dT13	K	0	0	0	0
Bleed Air dT	K	0	0	0	0
Propulsive Efficiency		0,857462	0	0,720838	0,666683
Core Efficiency		0,542277	0,451498	0,485974	0,36715
Interduct Pressure Ratio		0,98	0,980011	0,979868	0,981046
Engine Pressure Ratio P5/P2		1,03567	1,16132	1,09738	1,01229
Equivalent Airspeed (knots)		268,043	0	228,457	161,507
#1:InPart*wf		2364,46	88,4243	662,277	68,9449
#2:MissionSum(cp_val1)		2364,46	2452,89	3115,17	3184,11
#3:InPart		7200	120	1200	180
HP Spool Speed (RPM)		18680	19333,8	18960,2	18381,1
Rel. HP Spool Speed		1	1,035	1,015	0,984

9. FAN DESIGN

In this section the objective is to evaluate how the engine model simulated using the GasTurb software can approximate real engine model in terms of fan design. The design is focused on the PW1124G-JM turbofan since it is the engine with more detailed and measured data.

Assuming all the considerations and all assumptions which brought to the cycle design of the engine, now it is time to focus in the geometrical properties of the fan.

9.1 *The fan*

As introduced at the beginning of the thesis, the development of turbofan engines allowed to increase efficiency, thus reducing fuel consumption compared to traditional jet engines.

The fan rotor is made up by a row of large fan blades. In modern high-bypass turbofan engines the fan includes about 20 blades which are designed to maximize the aerodynamic loading. This parameter, defined as the ratio of specific enthalpy rise across the blade over the square of velocity at blade tip at the design point, is limited by stall and flutter phenomena due to the compression of the airflow across the fan.

It is important that the fan design ensures acceptable stall margin while achieving aerodynamic loading values as high as 0.29, in order to get fan pressure ratios of about 1.5.

Modern high-bypass turbofans employ large fans rotating at high rotational speeds which could achieve supersonic speeds at blade tips, bringing to the generation of shock waves.

The blades are designed to work with a subsonic airflow near the blade root and a supersonic flow near the blade tip.

Fig. 9.1: Isometric view of a turbofan (US7374403B2 patent, see [26])

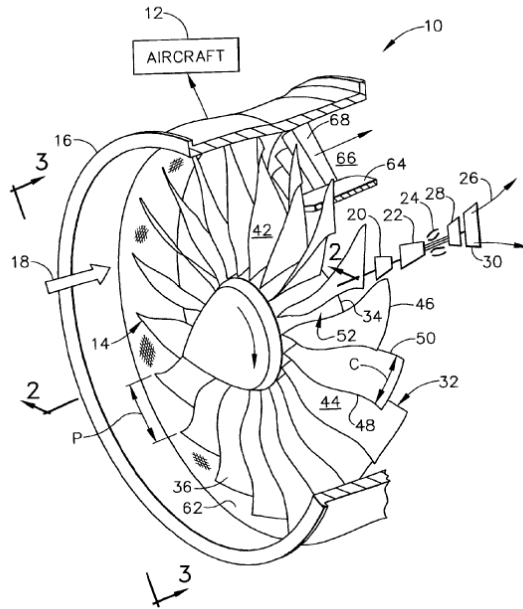


Fig. 9.2: Axial sectional view through the turbofan portion of the engine (US7374403B2 patent, see [26])

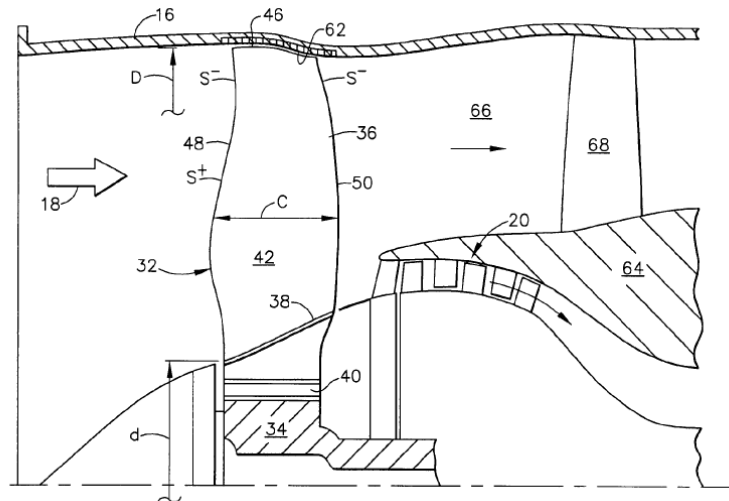
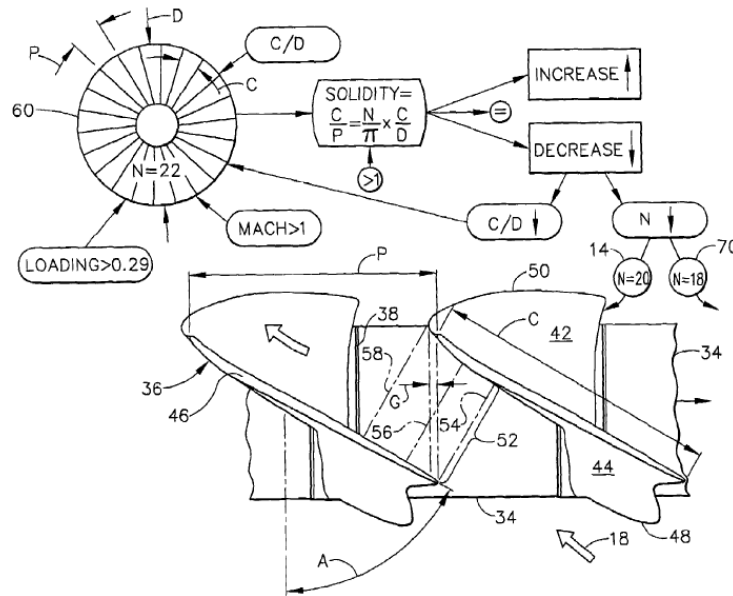


Fig. 9.3: Top planiform view of two adjacent fan blades (US7374403B2 patent, see [26])



As shown in Figure 9.1, the air is directed through the fan in channels that are defined from the pressure side of one blade and the suction side of another blade. Usually fan blades are twisted with different stagger angles that vary from root to tip.

Important design parameters are aerodynamic loading, blade row solidity and blade aspect ratio.

The blade row solidity is defined as the ratio between the blade chord and the circumferential spacing of the blades at a given radius. Modern turbofans are characterized by high values of blade solidity at blade tips, which is as high as 1.29 in a common turbofan with bypass ratio of 7 as reported in literature [26]. Common fan designs suggest that the blade row solidity at blade tip equals the blade tip relative Mach number.

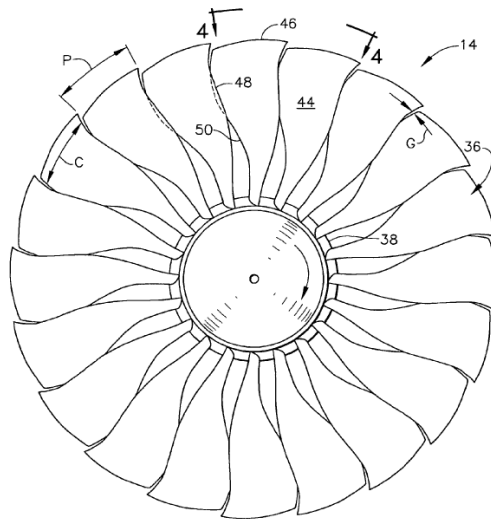
In Figure 9.1 it is possible to see that the high blade stagger angle cause the trailing edge of one blade to be circumferentially adjacent to pressure side of the adjacent blade in the outer part of the fan, while being axially spaced in the tip region in order to create a discharge channel for the airflow. As the solidity increases, one blade overlaps the adjacent one.

The stagger angle varies from root to tip and the chord length increases from root to tip.

Blades are designed to create a converging airflow passage between the inlet

and the throat , and a diverging airflow passage between the throat and the outlet. This is done in order to maximize the efficiency at blade tip where the relative flow is supersonic. Shock waves are generated and the airflow speed is reduced. Sonic conditions are reached at the passage throat and the subsonic flow diffues from the throat to the outlet section.

Fig. 9.4: Forward-facing-aft elevational view of the turbofan (US7374403B2 patent, see [26])



9.2 Real data

Real geometrical properties of the engine could be derived from the cutaway figure of the engine reported in fig... and from technical reports.

The diameter of the fan ($D_{FAN}=81$ [in]) and the number of fan blades which is 20 are known. From the cutaway image it is possible to evaluate hub and tip radii and the distribution of axial chords along the fan blade.

The fan is a single-stage unit, without IGVs.

Considering the cutaway figure of the engine it is possible to define the geometrical ratio between the hub diameter D_h and the tip diameter D_t (or in terms of hub and tip radii) of the fan as

$$\nu = \frac{D_h}{D_t} = \frac{r_h}{r_t} \quad (9.1)$$

From literature it is possible to obtain characteristics of the real engine running at average cruise and take-off, which are listed in the table below:

Measured information			
Quantity	Unit	Average Cruise	Max Take-Off
Thrust	[lbf]	4729	25678
Fan face corr. Flow	[lbm/s]	1429.4	1438.8
Fan OD corr. Flow	[lbm/s]	1322.6	1330.2
Fan face physical flow	[lbm/s]	543.4	1452.2
Fan OD physical flow	[lbm/s]	502.7	1342.4
Second speed (fan)	[rpm]	2748	3117
First speed (power turbine)	[rpm]	8416	9546
Engine Unit Thrust Parameter		0.05	0.09

Tab. 9.1: PW1124G-JM avg. cruise and max take-off measured data

I assume that the average cruise occurs at a flight altitude of 10000 [m] at flight Mach number of 0.85 while the take-off Mach number is considered to be 0.25 . Calculations will be performed taking into account the standard ISA atmosphere. These assumption are reported in the table below along with ISA ambient conditions during cruise and take-off.

Assumptions			
Quantity	Unit	Average Cruise	Max Take-Off
Altitude	[m]	10000	0
Mach number		0.85	0.25
Temperature	[K]	223.2	288.2
Density	[kg/m ³]	0.414	1.225

Tab. 9.2: PW1124G-JM flight condition assumptions

It is possible to verify if the fan is a subsonic or a transonic unit using the information above. The blade linear velocity at the fan's tip can be calculated from the Low-Pressure spool speed and the fan diameter which are both known parameters. It results

$$u_{tip} = \omega_{LP} \cdot \frac{D_{lpc}}{2} \quad (9.2)$$

while the axial flow velocity at fan's inlet section can be derived from the fan face physical flow \dot{m} , the airflow density ρ and the fan face area A as

$$c_{axial} = \frac{\dot{m}}{\rho \cdot A} \quad (9.3)$$

The relative velocity of the air stream at the fan's rotor inlet results

$$w = \sqrt{c_{axial}^2 + u_{tip}^2} \quad (9.4)$$

and, assuming for the air $k = 1.4$ and $R = 286.9 \frac{\text{m}^2}{\text{s}^2\text{K}}$, the relative Mach number at rotor's inlet is therefore

$$M = \frac{w}{\sqrt{k \cdot R \cdot T}} \quad (9.5)$$

Results obtained for both cruise and maximum take-off conditions are summarized in the table below

Results			
Quantity	Unit	Average Cruise	Max Take-Off
u_{tip}	[m/s]	296	336
c_{axial}	[m/s]	179	162
w	[m/s]	346	373
M		1.156	1.095

Tab. 9.3: Cruise and Maximum Take-Off fan results

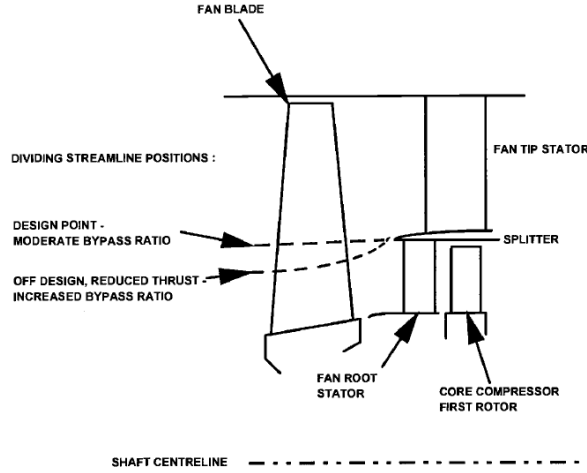
which confirm that the outer part of the fan is transonic.

9.3 GasTurb simulated data

GasTurb calculations provide mass flows and thermodynamic properties of airstream across the fan for each station reported in figure Figure 5.21 It also provides cycle design pressure ratios separately for both the inner and the outer part of the fan.

In the inner part of the fan flows the airflow that will be elaborated by the engine core while in the outer part of the fan flows the bypass airflow as summarized in Figure 9.5 below from literature [15].

Fig. 9.5: Typical single-stage fan configuration (Walsh Fletcher, see [15])



9.4 Preliminary fan design

The objective now is to estimate the differences between real geometrical data and theoretical geometrical data calculated for the simulated engine model.

By considering literature [9] it is possible to set a preliminary fan design.

It is possible to consider a generic fan stage composed of a rotor and a stator and to indicate the rotor's intake with the subscript 1, the rotor's outlet (or stator's inlet) with the subscript 2 and the stator's outlet with the subscript 3.

I considered cruise at 10973 [m] with ISA+9 [°C] conditions at flight Mach Number $M_a=0.85$ as the fan design point.

Airstream's properties at the fan face downstream the diffuser are calculated using GasTurb software and listed below

$$T_1^0 = 258.40 [K]$$

$$p_1^0 = 36.464 [kPa]$$

$$M_1^0 = 0.6708$$

$$k = 1.4$$

$$c_p = 1004 \left[\frac{J}{kg \cdot K} \right]$$

$$R = 287.05 \left[\frac{J}{kg \cdot K} \right]$$

It is possible to derive static conditions at fan's intake as

$$T_1 = \frac{T_1^0}{1 + \frac{k-1}{2} Ma_a^2} \cong 237.1 \text{ [K]} \quad (9.6)$$

$$p_1 = \frac{p_1^0}{\left[1 + \frac{k-1}{2} Ma_a^2\right]^{\frac{k}{k-1}}} \cong 26.97 \text{ [kPa]} \quad (9.7)$$

$$\rho_1 = \frac{p_1}{R \cdot T_1} = 0.396 \left[\frac{\text{kg}}{\text{m}^3} \right] \quad (9.8)$$

so the axial flow velocity results

$$c_{axial} = Ma_1 \sqrt{k \cdot R \cdot T_1} \cong 207 \text{ [m/s]}$$

and considering the assumption of constant axial flow velocity across the rotor

$$c_{axial,1} = c_{axial,2} \quad (9.9)$$

The continuity equation for steady and uniform flow could be used in order to calculate the flow area at fan's face as

$$A_1 = \frac{\dot{m}_a}{\rho_1 \cdot c_{m,1}} \quad (9.10)$$

Now it is time to focus on fan's discharge conditions. It is now important to consider that GasTurb results are obtained for both the inner and the outer part of the fan's outlet section. The problem can be solved considering both the inner and the outer part of the fan's exit section as two different compressors arranged in parallel sharing the same inlet conditions. Obviously outlet conditions will therefore be different since it is an unmixed turbofan engine.

The subscript *in* will refer to the inner part of the fan while the subscript *out* will refer to the outer part of the fan.

Since the fan is a single stage unit, its exit section will be described with the subscript 3.

The total pressure and total temperature at fan's outlet, given by pressure ratios calculated using GasTurb software and polytropic efficiencies of both inner and outer part of the fan, are equal to

$$p_{3,in}^0 = \pi_{fan,in} \cdot p_{1,in}^0 = 1.219 \cdot p_1^0 \cong 44.45 \text{ [kPa]} \quad (9.11)$$

$$p_{3,out}^0 = \pi_{fan,in} \cdot p_{1,in}^0 = 1.365 \cdot p_1^0 \cong 49.77 \text{ [kPa]} \quad (9.12)$$

$$T_{3,in}^0 = (\pi_{fan,in})^{\frac{k-1}{k\eta_{p,in}}} \cdot T_1^0 \cong 275.2 [K] \quad (9.13)$$

$$T_{3,out}^0 = (\pi_{fan,out})^{\frac{k-1}{k\eta_{p,out}}} \cdot T_1^0 \cong 285.6 [K] \quad (9.14)$$

The above total temperatures at fan's exit section will be used as temperature targets of the iterative method at rotor exit sections of the inner and outer part of the fan, precisely in equations (9.59) and (9.96), in order to obtain the right design for this single-stage fan.

It is possible to assume that the fan discharge is swirl free, and together with the assumption that implies a constant axial velocity along the fan, results

$$c_3 = c_{axial,1} = c_{axial,2} \quad (9.15)$$

The static temperature of the gas at fan's outlet section is calculated for both the inner and the outer part of the fan as

$$T_{3,in} = T_3^0 - \frac{c_3^0}{2 \cdot c_{p,3}} \cong 253.8 [K] \quad (9.16)$$

$$T_{3,out} = T_3^0 - \frac{c_3^0}{2 \cdot c_{p,3}} \cong 264.2 [K] \quad (9.17)$$

It is now possible to evaluate the speed of sound at fan's exit section as

$$a_{3,in} = \sqrt{(k-1) c_{p,3} \cdot T_{3,in}} \cong 319 [m/s] \quad (9.18)$$

$$a_{3,out} = \sqrt{(k-1) c_{p,3} \cdot T_{3,out}} \cong 326 [m/s] \quad (9.19)$$

which makes possible to calculate the fan's exit axial Mach number

$$M_{3,in} = \frac{c_3}{a_3} \cong 0.65 \quad (9.20)$$

$$M_{3,out} = \frac{c_3}{a_3} \cong 0.64 \quad (9.21)$$

The static pressure at fan's exit section results

$$p_{3,in} = \frac{p_3^0}{\left[1 + \frac{k-1}{2} M_3^2\right]^{\frac{k}{k-1}}} \cong 33.51 [kPa] \quad (9.22)$$

$$p_{3,out} = \frac{p_3^0}{\left[1 + \frac{k-1}{2} M_3^2\right]^{\frac{k}{k-1}}} \cong 37.93 [kPa] \quad (9.23)$$

The density of the gas at fan's exit section results

$$\rho_{3,in} = \frac{p_{3,in}}{R \cdot T_{3,in}} = 0.460 \left[\frac{kg}{m^3} \right] \quad (9.24)$$

$$\rho_{3,out} = \frac{p_{3,out}}{R \cdot T_{3,out}} = 0.500 \left[\frac{kg}{m^3} \right] \quad (9.25)$$

Now it is important to consider the conceptual idea about two ideal compressors (fans) arranged in parallel which was introduced above.

It is possible to calculate the radius that separates the inner part of the fan from the outer one by taking into account GasTurb data about fan face mass flows and summarized below

$$\begin{aligned} \dot{m}_{tot} &= 246.39 \text{ [kg/s] fan face mass flow} \\ \dot{m}_a &= 18.41 \text{ [kg/s] core mass flow} \\ \dot{m}_{af} &= 227.98 \text{ [kg/s] bypass mass flow} \end{aligned}$$

The total area A_{tot} at fan's face is calculated by taking into account fan's hub and tip radii derived from the cutaway image of the engine. It results

$$A_{tot} = \pi (r_{tip}^2 - r_{hub}^2) \quad (9.26)$$

It is now possible to evaluate the core flow area A_a and the bypass flow area A_{af} as

$$A_a = \frac{\dot{m}_a}{\dot{m}_{tot}} \cdot A_{tot} = 0.224 \text{ [m}^2\text{]} \quad (9.27)$$

$$A_{af} = \frac{\dot{m}_{af}}{\dot{m}_{tot}} \cdot A_{tot} = 2.778 \text{ [m}^2\text{]} \quad (9.28)$$

The radius R which separates the two ideal compressors (fans) is now calculated as

$$R = \sqrt{\frac{A_a}{\pi} + (r_{hub})^2} = 0.417 \text{ [m]} \quad (9.29)$$

$$R = \sqrt{\frac{-A_{af}}{\pi} + (r_{tip})^2} = 0.417 \text{ [m]} \quad (9.30)$$

considering now that $R = r_{tip}$ for the inner part of the fan and $R = r_{hub}$ for the outer part of the fan.

9.4.1 Fan inner part (subsonic)

Pitchline calculations

The procedure starts with the definition of the pitchline radius as

$$r_m = \frac{r_{hub} + r_{tip}}{2} = \frac{r_{hub} + R}{2} = \frac{0.320 + 0.417}{2} = 0.369 \text{ [m]} \quad (9.31)$$

where the tip radius coincides with the separation radius R .

The Low-Pressure spool speed is 2748 [rpm] and it was derived from measured data of the engine.

The blade linear velocity at tip radius is

$$u_{tip} = \omega_{LP} \cdot r_{tip} = 2748 \cdot \frac{2\pi}{60} \cdot 0.417 \cong 120 \text{ [m/s]} \quad (9.32)$$

The rotor speed at pitchline is therefore

$$u_m = u_{tip} \cdot \frac{r_m}{r_{tip}} = 120 \cdot \frac{0.369}{0.417} \cong 106 \text{ [m/s]} \quad (9.33)$$

Taking into consideration the assumption of no IGVs, the flow angles at the inlet section of the rotor are

$$\alpha_{1,m} = 0 \text{ [}^\circ\text{]} \quad (9.34)$$

$$\beta_{1,m} = \arctan\left(\frac{u_m}{c_{axial}}\right) = \arctan\left(\frac{106}{207}\right) \cong 27.1 \text{ [}^\circ\text{]} \quad (9.35)$$

The relative velocity at pitchline is

$$w_{1,m} = \sqrt{u_m^2 + c_{axial}^2} \cong 232 \text{ [m/s]} \quad (9.36)$$

and the relative inlet Mach number results

$$M_{1,m} = \frac{w_{1,m}}{a_1} \cong 0.75 \quad (9.37)$$

which confirms that the pitchline is subsonic and suitable for NACA 65-series airfoils.

Taking into consideration the De Haller criterion implies that

$$\frac{w_2}{w_1} \geq 0.72 \quad (9.38)$$

in order to limit the amount of diffusion in the blade. D-Factors above 0.55 are not allowed because in that case the boundary layer separation occurs

bringing to stall.

Employing the De Haller criterion, and choosing a value of 0.89 for the ratio between the relative velocities in order to obtain the maximum available total temperature raise at rotor exit section, the exit relative velocity at pitchline results

$$w_{2,m} = 0.8901 \cdot w_{1,m} \cong 207 \text{ [m/s]} \quad (9.39)$$

and therefore

$$\beta_{2,m} = \arccos\left(\frac{c_{axial}}{w_{2,m}}\right) = 0 \text{ [}^\circ\text{]} \quad (9.40)$$

The relative swirl at the rotor exit results

$$w_{\theta 2,m} = c_{axial} \cdot (\tan \beta_{2,m}) = 0 \text{ [m/s]} \quad (9.41)$$

The absolute swirl is

$$c_{\theta 2,m} \approx u_m - w_{\theta 2,m} \cong 106 \text{ [m/s]} \quad (9.42)$$

The loading parameter at the pitchline is

$$\psi_m = \frac{c_{\theta 2,m}}{c_{axial}} = 1 \quad (9.43)$$

The absolute flow angle at the rotor exit at pitchline is

$$\alpha_2 = \arctan\left(\frac{c_{\theta 2,m}}{c_{axial}}\right) \cong 27.1 \text{ [}^\circ\text{]} \quad (9.44)$$

The absolute velocity at the rotor exit is

$$c_{2,m} = \sqrt{c_{axial}^2 + c_{\theta 2,m}^2} \cong 233 \text{ [m/s]} \quad (9.45)$$

and the obtained degree of reaction at pitchline is equal to

$${}^\circ R_m = 1 - \frac{c_{\theta 1,m} + c_{\theta 2,m}}{2u_m} = 0.5 \quad (9.46)$$

as was evident from flow angles and flow velocities.

Rotor blade design at pitchline

In the subsonic part of the fan a NACA 65-series cascade blade is chosen for rotor blade airfoils.

First of all, it is important to determine the minimum chord length that is

required for the turbulent boundary layer formation on the blade. Usually the criterion $Re_c \geq 300000$ is used, and it must be satisfied at all altitudes. The required chord length is therefore calculated at high altitude flight conditions where the air density is lower.

At 16000 [m] the air density is $\rho_1 = 0.167 [kg/m^3]$ and the kinematic viscosity of the air is $\nu_1 = 8.54 \cdot 10^{-5} [m^2/s]$ so the criterion gives the minimum chord length c_m

$$Re_c = \frac{w_{1,m} \cdot c_m}{\nu_1} \geq 300000 \quad (9.47)$$

$$c_m \geq 0.09 [m] \quad (9.48)$$

The minimum chord length could be increased for structural purposes but also to achieve better stall margin and to control blade vibrational modes. The blade spacing at the pitchline $s_{r,m}$ results

$$s_{r,m} = \frac{2 \cdot \pi \cdot r_{m1}}{N_{blades}} = 0.116 [m] \quad (9.49)$$

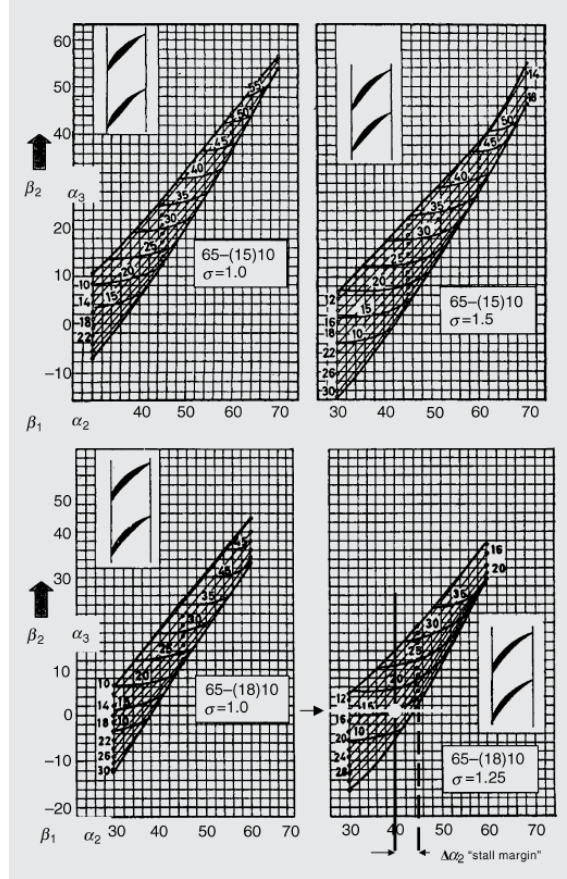
where N_{blades} is the number of rotor blades which is set to be 20 from technical data of the engine. In the iterative solution it will be found a suitable blade chord length $l_{r,m}$ in order to obtain an axial blade chord equal to the one measured from the cutaway image of the engine.

Considering equation (9.53) it is possible to estimate the minimum value for blade row solidity at pitchline since the maximum diffusion factor is assumed to be 0.45 as suggested by Lieblein. The minimum blade row solidity is therefore equal to

$$\sigma_{r,m} \geq \frac{c_{\theta 2,m} - c_{\theta 1,m}}{2 \cdot w_{1,m} \left[0.45 - \left(1 - \frac{w_{2,m}}{w_{1,m}} \right) \right]} = 0.67 \quad (9.50)$$

The flow at inner fan part is subsonic as confirmed by Equation 9.37 so I assumed that for subsonic purposes NACA 65-series cascade airfoils are used for the inner fan blades and thus measured data from Mellor is used to choose an appropriate configuration. In his study Mellor described various NACA 65 series cascade profiles by plotting curves of constant camber angle and constant incidence angle for different values of blade row solidity. These curves are shown in the following Figure 9.6 from literature [9].

Fig. 9.6: NACA 65-series Mellor data (Farokhi, see [9])



The axial blade chord evaluated from the cutaway is 0.28 [m] long. Choosing a blade chord length equal to

$$l_{r,m} = 0.297 [m] \quad (9.51)$$

and considering equation (9.49), the actual blade row solidity is then equal to

$$\sigma_{r,m} = 2.57 \quad (9.52)$$

It is important to check if the amount of turning of the net flow is acceptable. If it is excessive it causes the boundary layer to separate. The check is performed using the D-Factor calculation method. D-Factor is defined as

$$D_{r,m} = 1 - \frac{w_{2,m}}{w_{1,m}} + \frac{|\Delta c_\theta|}{2 \cdot \sigma_{r,m} \cdot w_{1,m}} \quad (9.53)$$

where σ_m is the blade row solidity at pitchline.

It is possible to calculate the D-Factor for the rotor, and it is equal to

$$D_{r,m} = 1 - \frac{w_{2,m}}{w_{1,m}} + \frac{|\Delta c_\theta|}{2 \cdot \sigma_{r,m} \cdot w_{1,m}} = 0.20 < 0.55 \quad (9.54)$$

Since there are no Mellor charts that provide information for such high blade row solidity values, it is then generated a Matlab script in order to extrapolate the stagger angle for the calculated value of blade row solidity.

It is then chosen the NACA 65(15)-10 cascade profile, and the estrapolated stagger angle results

$$\gamma_{r,m}^\circ \cong 20.4 [^\circ] \quad (9.55)$$

and the angle of attack

$$\alpha_2 - \gamma_{s,m}^\circ \cong 6.7 [^\circ] \quad (9.56)$$

It is possible to calculate the axial blade chord lenght which is equal to

$$l_{axial} = 0.278 [m] \quad (9.57)$$

which is equal to the one measured in the cutway image of the engine, thus the geometrical design is finally set.

Stator blade design at pitchline

The design of the stator blade at pitchline is set from the flow angles and Mach numbers in the absolute frame.

From the rotor calculations it results

$$\begin{aligned} \alpha_{2,m} &\cong 27.1 [^\circ] \\ \alpha_{3,m} &= 0 [^\circ] \end{aligned}$$

since it was made the axial flow assumption at the fan outlet section. In order to evaluate the Mach number at the stator's inlet it is necessary to know the static temperature and the speed of sound at the pitchline radius downstream the rotor.

Considering the Euler equation

$$T_{2,m}^0 = T_{1,m}^0 + \frac{u_m (c_{\theta 2,m} - c_{\theta 1,m})}{c_p} \quad (9.58)$$

Taking into consideration previous assumptions of no radial shift across the rotor and calorically perfect gas, and considering the following properties

$$\begin{aligned}
T_{1m}^0 &= 258.4 [K] \\
u_m &\cong 106 [m/s] \\
c_{\theta 1,m} &= 0 [m/s] \\
c_{\theta 2,m} &\cong 106 [m/s] \\
c_p &= 1004 [\frac{J}{kg \cdot K}]
\end{aligned}$$

so the total temperature at rotor's exit results

$$T_{2,m}^0 \cong 269.6 [K] \quad (9.59)$$

which is lower than the one calculated from equation (9.13).

The maximum total temperature raise along the rotor is lower than the one imposed by GasTurb model simulation because of a inner fan compression ratio of 1.219 .

The maximum total temperature raise given by flow conditions in the rotor actually gives the following maximum inner fan compression ratio as

$$\pi = \left(\frac{T_2^0}{T_1^0} \right)^{\frac{\eta_{p,lpc} \cdot k}{k-1}} = 1.143 \quad (9.60)$$

which is lower than the required pressure ratio set by the GasTurb simulation. The inner fan pressure ratio obtained from equation (9.60) is therefore used in GasTurb to modify the engine cycle design in order to verify if it represents anyway a suitable value. The new design cycle is obtained using GasTurb optimization tool and positively checked. It is now possible to continue the inner fan preliminary design.

The static temperature at rotor's outlet section therefore is

$$T_{2,m} = T_{2,m}^0 - \frac{c_{2,m}^2}{2c_p} \cong 248.3 [K] \quad (9.61)$$

It is possible to calculate then the speed of sound and the Mach number of the absolute flow at stator's inlet as

$$M_{2,m} = \frac{c_{2,m}}{a_{2,m}} \cong 0.74 \quad (9.62)$$

so the stator blade at the pitchline is subsonic.

It is now possible to choose a NACA-65 series cascade profile for the stator blade section from the data provided by Mellor, in order to best match inlet and outlet flow angles and to guarantee a sufficient stall margin.

I chose a 65-(18)10 cascade airfoil with a blade row solidity of $\sigma_{s,m}=1.23$.

It is important to check if the amount of turning of the net flow is acceptable

using the D-Factor calculation method. The stator D-Factor is in fact equal to

$$D_{s,m} = 1 - \frac{c_{3,m}}{c_{2,m}} + \frac{|\Delta c_\theta|}{2 \cdot \sigma_{s,m} \cdot c_{2,m}} = 0.27 < 0.55 \quad (9.63)$$

Using extrapolation from the graph reported in Figure 9.6, the intersection of the stator's inlet flow angle α_2 and the stator's outlet flow angle α_3 gives the stagger angle

$$\gamma_{s,m}^\circ \cong 14.9 [^\circ] \quad (9.64)$$

and the angle of attack

$$\alpha_{2,m} - \gamma_{s,m}^\circ \cong 12.1 [^\circ] \quad (9.65)$$

Considering a stator mean radius $r_{s,m} = 0.181 [m]$ derived from the cutaway image, the blade spacing at the pitchline $s_{s,m}$ results

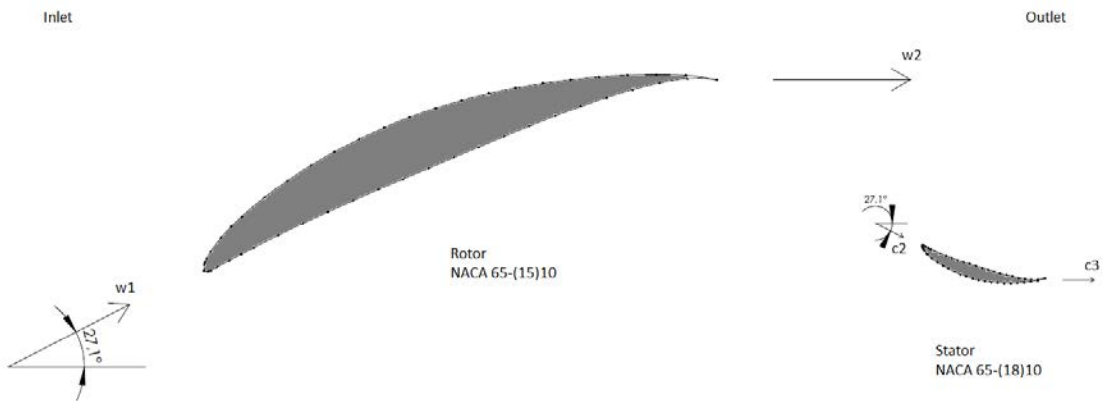
$$s_{s,m} = \frac{2 \cdot \pi \cdot r_{s,m}}{N_{blades}} = 0.057 [m] \quad (9.66)$$

The axial blade chord evaluated from the cutaway is 0.068 [m] long while the resulting axial blade chord is equal to

$$l_{axial} = \sigma_{s,m} \cdot s_{s,m} \cdot \cos(\gamma_{s,m}^\circ) = 0.068 [m]$$

so the iteration is complete and the final geometrical design of the subsonic (inner) part of the fan is obtained and reported in the Figure 9.7 below.

Fig. 9.7: LPC rotor and stator configuration for the inner subsonic part



9.4.2 Fan outer part (transonic)

Pitchline calculations

The design procedure is similar to the previous one adopted for the fan's inner part. The only difference is that now DCA (Double-Circular Arc) profiles are employed for the blades instead of the NACA-65 Series which are usually adopted for subsonic sections.

Similarly, it is possible to define the pitchline radius as

$$r_m = \frac{r_{hub} + r_{tip}}{2} = \frac{R + r_{tip}}{2} = \frac{0.417 + 1.029}{2} = 0.723 \text{ [m]} \quad (9.67)$$

where the hub radius coincides with the separation radius R which separates the subsonic inner part from the transonic outer part of the fan.

The Low-Pressure spool speed is 2748 [rpm] and it was derived from measured data of the engine.

The blade linear velocity at tip radius is

$$u_{tip} = \omega_{LP} \cdot r_{tip} = 2748 \cdot \frac{2\pi}{60} \cdot 1.029 \cong 296 \text{ [m/s]} \quad (9.68)$$

The rotor speed at pitchline is therefore

$$u_m = u_{tip} \cdot \frac{r_m}{r_{tip}} = 296 \cdot \frac{0.723}{1.029} \cong 208 \text{ [m/s]} \quad (9.69)$$

Taking into consideration the assumption of no IGVs, the flow angles at the inlet section of the rotor are

$$\alpha_{1,m} = 0 \text{ [}^\circ\text{]} \quad (9.70)$$

$$\beta_{1,m} = \arctan\left(\frac{u_m}{c_{axial}}\right) = \arctan\left(\frac{208.0062}{206.9625}\right) \cong 45.1 \text{ [}^\circ\text{]} \quad (9.71)$$

The relative velocity at pitchline is

$$w_{1,m} = \sqrt{u_m^2 + c_{axial}^2} \cong 293 \text{ [m/s]} \quad (9.72)$$

and the relative inlet Mach number results

$$M_{1,m} = \frac{w_{m1}}{a_1} \cong 0.95 \quad (9.73)$$

which confirms that the pitchline is transonic and suitable for DCA airfoils. It is necessary that

$$\frac{w_2}{w_1} \geq 0.72 \quad (9.74)$$

in order to limit the amount of diffusion in the blade. D-Factors above 0.55 are not allowed because in that case the boundary layer separation occurs bringing to stall.

Employing the De Haller criterion, and choosing a value of 0.753 for the ratio between the relative velocities in order to obtain the desired iterated total temperature at rotor exit section, the exit relative velocity at pitchline results

$$w_{2,m} = 0.753 \cdot w_{1,m} \cong 221 \text{ [m/s]} \quad (9.75)$$

and therefore

$$\beta_{2,m} = \arccos\left(\frac{c_{axial}}{w_{2,m}}\right) \cong 20.4 \text{ [}^\circ\text{]} \quad (9.76)$$

The relative swirl at the rotor exit results

$$w_{\theta 2,m} = c_{axial} \cdot \tan(\beta_{2,m}) \cong 77 \text{ [m/s]} \quad (9.77)$$

The absolute swirl is

$$c_{\theta 2,m} \approx u_m - w_{\theta 2,m} \cong 131 \text{ [m/s]} \quad (9.78)$$

The loading parameter at the pitchline is

$$\psi_m = \frac{c_{\theta 2,m}}{c_{axial}} \cong 0.59 \quad (9.79)$$

The absolute flow angle at the rotor exit at pitchline is

$$\alpha_{2,m} = \arctan\left(\frac{c_{\theta 2,m}}{c_{axial}}\right) \cong 32.3 \text{ [}^\circ\text{]} \quad (9.80)$$

The absolute velocity at the rotor exit is

$$c_{2,m} = \sqrt{c_{axial}^2 + c_{\theta 2,m}^2} \cong 245 \text{ [m/s]} \quad (9.81)$$

Now let us verify if the De Haller criterion is satisfied for the stator

$$\frac{c_{3,m}}{c_{2,m}} = \frac{c_{axial}}{c_{2,m}} = 0.845 \geq 0.72 \quad (9.82)$$

Finally the obtained degree of reaction at pitchline is equal to

$${}^\circ R_m = 1 - \frac{c_{\theta 1,m} + c_{\theta 2,m}}{2 \cdot u_m} \cong 0.69 \quad (9.83)$$

Rotor blade design at pitchline

In the transonic part of the fan a double-circular arc (DCA) blade is chosen. In these type of profiles the relative flow is tangent to the upper surface.

It is important in this case to choose a blade thickness-to-chord ratio at pitchline. The minimum t/c ratio is at the tip and it is limited to 3% for structural purposes. The hub t/c ratio could be set to 10%. Normally it is imposed a linear variation of the t/c ratio along the fan radius.

First of all, it is important to determine the minimum chord length that is required for the turbulent boundary layer formation on the blade. Usually the criterion $Re_c \geq 300000$ is used, and it must be satisfied at all altitudes. The required chord length is therefore calculated at high altitude flight conditions where the air density is lower.

At 16000 [m] the air density is $\rho_1 = 0.167 [kg/m^3]$ and the kinematic viscosity of the air is $\nu_1 = 8.54 \cdot 10^{-5} [m^2/s]$ so the criterion gives the minimum chord length c_m

$$Re_c = \frac{w_{1m} \cdot c_m}{\nu_1} \geq 300000 \quad (9.84)$$

$$c_m \geq 0.09 [m] \quad (9.85)$$

The minimum chord length could be increased for structural purposes but also to achieve better stall margin and to control blade vibrational modes.

In the iterative solution it is chosen a blade chord $c_{r1,m}$ of 0.366 [m] in order to obtain at the end of the iterative process an axial blade chord equal to the one measured from the cutaway image of the engine.

It is possible now to estimate the blade row solidity of the first attempt since the number of fan blades is known (20 blades from technical data) and the blade spacing which is calculated using geometrical information of the fan.

The blade spacing at the pitchline $s_{r1,m}$ results

$$s_{r,m} = \frac{2 \cdot \pi \cdot r_m}{N_{blades}} = 0.227 [m] \quad (9.86)$$

where N_{blades} is the number of rotor blades which is set to be 20 from technical data of the engine.

The relative inlet flow is aligned with the upper surface as mentioned above, and therefore the incidence angle could be defined as

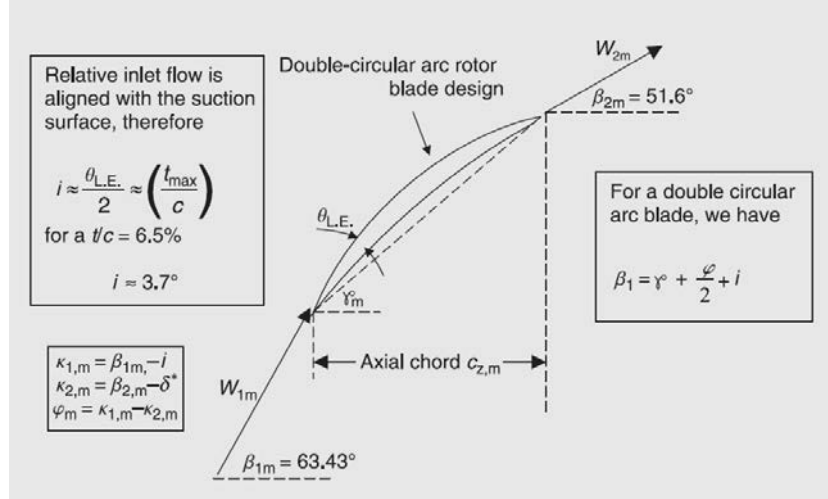
$$i \approx \frac{\theta_{L.E.}}{2} \approx \frac{t_{max}}{c} \cong 3.7 [^\circ] \quad (9.87)$$

The deviation angle could be derived from the Carter's basic rule and supplemented by 2° because of the shock boundary layer interaction on the suction

surface which causes an higher deviation angle

$$\delta^* \approx \frac{\Delta\beta}{4\sqrt{\sigma}} + 2^\circ \cong 6.9 [^\circ] \quad (9.88)$$

Fig. 9.8: DCA rotor blade design angles (Farokhi, see [9])



The blade leading edge angle $\kappa_{1,m}$ is

$$\kappa_{1,m} = \beta_{1,m} - i \cong 41.4 [^\circ] \quad (9.89)$$

The blade trailing edge angle $\kappa_{2,m}$ is

$$\kappa_{2,m} = \beta_{2,m} - \delta^* \cong 13.5 [^\circ] \quad (9.90)$$

and the camber angle φ_m results

$$\varphi_m = \kappa_{1,m} - \kappa_{2,m} \cong 27.9 [^\circ] \quad (9.91)$$

The stagger angle of a double-circular arc blade γ° is therefore

$$\gamma^\circ = \beta_1 - \frac{\varphi_m}{2} - i \cong 27.5 [^\circ] \quad (9.92)$$

It is possible to estimate the rotor blade row solidity at the pitchline obtained from the iterative method using the iterated stagger angle, the blade spacing from cutaway image and the measured axial blade chord from cutaway, and it is therefore equal to

$$\sigma_{r,m} = \frac{l_{axial,m}}{s_{r,m}} \cong 1.61 \quad (9.93)$$

which determines the end of the iterative process ends since the axial chord (or the blade row solidity) calculated from previous iterative quantities is equal to the axial blade chord (or blade row solidity) measured from the cutaway image of the engine.

It is possible to calculate the D-Factor of the rotor which is equal to

$$D_{r,m} = 1 - \frac{w_{2,m}}{w_{1,m}} + \frac{|\Delta c_\theta|}{2 \cdot \sigma_{r,m} \cdot w_{1,m}} = 0.386 < 0.55 \quad (9.94)$$

Stator blade design at pitchline

The design of the stator blade at pitchline is set from the flow angles and Mach numbers in the absolute frame.

From the rotor calculations it results

$$\begin{aligned} \alpha_{2,m} &\cong 32.3 [^\circ] \\ \alpha_{3,m} &= 0 [^\circ] \end{aligned}$$

since it was made the axial flow assumption at the fan outlet section.

In order to evaluate the Mach number at the stator's inlet it is necessary to know the static temperature and the speed of sound at the pitchline radius downstream the rotor.

Considering the Euler equation

$$T_{2,m}^0 = T_{1,m}^0 + \frac{u_m (c_{\theta 2,m} - c_{\theta 1,m})}{c_p} \quad (9.95)$$

Taking into consideration previous assumptions of no radial shift across the rotor and calorically perfect gas, and considering the following properties

$$\begin{aligned} T_{1m}^0 &= 258.4 [K] \\ u_m &\cong 208 [m/s] \\ c_{\theta 1,m} &= 0 [m/s] \\ c_{\theta 2,m} &\cong 131 [m/s] \\ c_p &= 1004 [\frac{J}{kg \cdot K}] \end{aligned}$$

so the total temperature at rotor's exit results

$$T_{2,m}^0 \cong 285.6 [K] \quad (9.96)$$

which is equal to the one calculated from equation (9.14).

The static temperature at rotor's outlet section therefore is

$$T_{2,m} = T_{2,m}^0 - \frac{c_{2,m}^2}{2c_p} \cong 255.6 [K] \quad (9.97)$$

It is possible to calculate then the speed of sound and the absolute Mach number at stator's inlet as

$$M_{2,m} = \frac{c_{2,m}}{a_{2,m}} \cong 0.76 \quad (9.98)$$

so the stator blade at the pitchline is a subsonic section.

It is now possible to choose a NACA-65 series cascade profile for the stator blade section from the data provided by Mellor, in order to best match inlet and outlet flow angles and to guarantee a sufficient stall margin.

It is chosen a 65-(18)10 cascade airfoil.

Considering a stator mean radius $r_{s,m} = 0.770$ [m] derived from the cutaway image, the blade spacing at the pitchline $s_{s1,m}$ results

$$s_{s,m} = \frac{2 \cdot \pi \cdot r_{s,m}}{N_{blades}} = 0.242 \text{ [m]} \quad (9.99)$$

Selecting a blade row solidity equal to

$$\sigma_{s,m} = 0.69 \quad (9.100)$$

makes possible to calculate the D-Factor of the stator which is equal to

$$D_{s,m} = 1 - \frac{c_{3,m}}{c_{2,m}} + \frac{|\Delta c_\theta|}{2 \cdot \sigma_{s,m} \cdot c_{2,m}} = 0.369 < 0.55 \quad (9.101)$$

and the stagger angle obtained by extrapolation from Mellor charts using a Matlab script results

$$\gamma_{s,m}^\circ \cong 12.8 \text{ [}^\circ\text{]} \quad (9.102)$$

This produces an angle of attack equal to

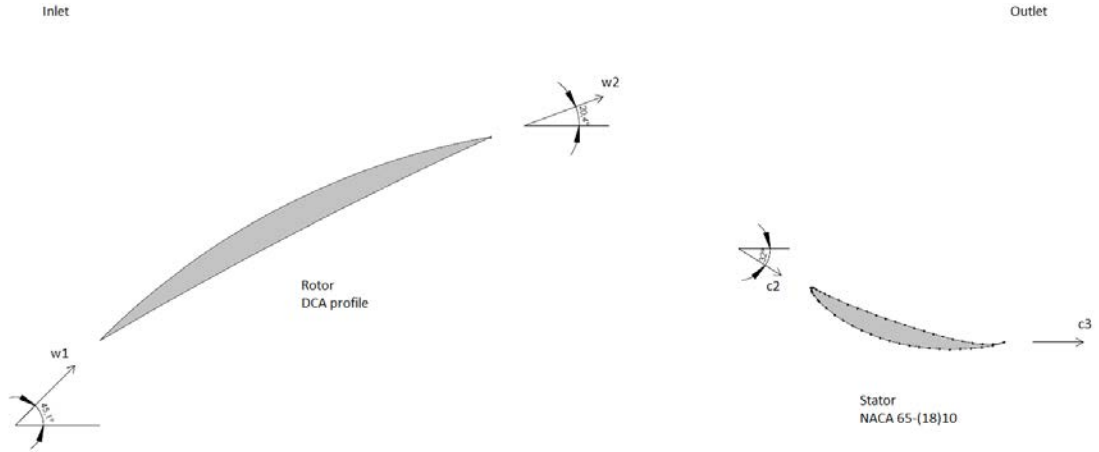
$$\alpha_{2,m} - \gamma_{s,m}^\circ \cong 19.6 \text{ [}^\circ\text{]} \quad (9.103)$$

The axial blade chord evaluated from the cutaway is 0.163 [m] long while the resulting axial blade chord is equal to

$$l_{axial} = \sigma_{s,m} \cdot s_{s,m} \cdot \cos(\gamma_{s,m}^\circ) = 0.163 \text{ [m]}$$

which allows to define finally the geometrical design of the transonic (outer) part of the fan, reported in the Figure 9.9 below.

Fig. 9.9: LPC rotor and stator configuration for the outer transonic part



The resultant fan preliminary design is therefore compatible with the fan illustrated in the cutaway image reported in Figure 3.7 from literature [2].

Tip radius calculations

For completeness I also wanted to estimate a third profile configuration corresponding to the fan rotor design at the tip radius.

In order to design the blade at tip radius the procedure is the same as the previous one adopted for the fan's outer part at pitchline radius.

From cutaway image the tip radius results

$$r_{tip} = 1.0287 [m] \quad (9.104)$$

The Low-Pressure spool speed is 2748 [rpm] and it was derived from measured data of the engine.

The blade linear velocity at tip radius is

$$u_{tip} = \omega_{LP} \cdot r_{tip} = 2748 \cdot \frac{2\pi}{60} \cdot 1.029 \cong 296 [m/s] \quad (9.105)$$

Taking into consideration the assumption of no IGVs, the flow angles at the inlet section of the rotor are

$$\alpha_{1,tip} = 0 [^\circ] \quad (9.106)$$

$$\beta_{1,tip} = \arctan\left(\frac{u_{tip}}{c_{axial}}\right) \cong 55.0 [^\circ] \quad (9.107)$$

The relative velocity at tip radius is

$$w_{1,tip} = \sqrt{u_{tip}^2 + c_{axial}^2} \cong 361 [m/s] \quad (9.108)$$

and the relative inlet Mach number results

$$M_{1,tip} = \frac{w_{1,tip}}{a_1} \cong 1.17 \quad (9.109)$$

which confirms that the flow at tip radius is transonic and suitable for DCA airfoils. It is necessary that

$$\frac{w_2}{w_1} \geq 0.72 \quad (9.110)$$

in order to limit the amount of diffusion in the blade.

I took into consideration the free vortex condition in order to evaluate flow velocities at tip radius which are necessary for the De Haller criterion. The equation below describes this assumption as

$$L_m = u_m \cdot (c_{\theta 2,m} - c_{\theta 1,m}) = L_{tip} = u_{tip} \cdot (c_{\theta 2,tip} - c_{\theta 1,tip}) \quad (9.111)$$

The De Haller criterion, once chosen a value of 0.8045 for the ratio between the relative velocities gives the exit relative velocity at tip radius which results

$$w_{2,tip} = 0.753 \cdot w_{1,tip} \cong 291 [m/s] \quad (9.112)$$

and therefore

$$\beta_{2,tip} = \arccos\left(\frac{c_{axial}}{w_{2,tip}}\right) \cong 44.6 [^\circ] \quad (9.113)$$

The relative swirl at the rotor exit results

$$w_{\theta 2,tip} = c_{axial} \cdot \tan(\beta_{2,tip}) \cong 204 [m/s] \quad (9.114)$$

The absolute swirl is

$$c_{\theta 2,tip} \approx u_{tip} - w_{\theta 2,tip} \cong 92 [m/s] \quad (9.115)$$

The loading parameter at tip radius is

$$\psi_{tip} = \frac{c_{\theta 2,tip}}{c_{axial}} \cong 0.32 \quad (9.116)$$

The absolute flow angle at the rotor exit at tip radius is

$$\alpha_{2,tip} = \arctan\left(\frac{c_{\theta 2,tip}}{c_{axial}}\right) \cong 24.0 [^\circ] \quad (9.117)$$

The absolute velocity at the rotor exit is

$$c_{2,tip} = \sqrt{c_{axial}^2 + c_{\theta 2,tip}^2} \cong 227 [m/s] \quad (9.118)$$

Finally the obtained degree of reaction at tip radius is equal to

$$^\circ R_{tip} = 1 - \frac{c_{\theta 1,tip} + c_{\theta 2,tip}}{2 \cdot u_{tip}} \cong 0.85 \quad (9.119)$$

Rotor blade design at tip radius

At tip radius a double-circular arc (DCA) blade is chosen. In these type of profiles the relative flow is tangent to the upper surface.

It is important in this case to choose a blade thickness-to-chord ratio at tip radius. In this case the minimum t/c ratio is set at the tip and it is limited to 3% for structural purposes.

First of all, it is important to determine the minimum chord length that is required for the turbulent boundary layer formation on the blade. Usually the criterion $Re_c \geq 300000$ is used, and it must be satisfied at all altitudes. The required chord length is therefore calculated at high altitude flight conditions where the air density is lower.

At 16000 [m] the air density is $\rho_1 = 0.167 [kg/m^3]$ and the kinematic viscosity of the air is $\nu_1 = 8.54 \cdot 10^{-5} [m^2/s]$ so the criterion gives the minimum chord length c_{tip}

$$Re_c = \frac{w_{1,tip} \cdot c_{tip}}{\nu_1} \geq 300000 \quad (9.120)$$

$$c_{tip} \geq 0.09 [m] \quad (9.121)$$

The minimum chord length could be increased for structural purposes but also to achieve better stall margin and to control blade vibrational modes.

In the iterative solution it is chosen a blade chord $c_{r1,tip}$ of 0.350 [m] in order to obtain at the end of the iterative process an axial blade chord equal to the one measured from the cutaway image of the engine.

It is possible now to estimate the blade row solidity of the first attempt since the number of fan blades is known (20 blades from technical data) and the

blade spacing which is calculated using geometrical information of the fan. The blade spacing at the tip radius $s_{r1,tip}$ results

$$s_{r1,tip} = \frac{2 \cdot \pi \cdot r_m}{N_{blades}} = 0.323 \text{ [m]} \quad (9.122)$$

where N_{blades} is the number of rotor blades which is set to be 20 from technical data of the engine.

The relative inlet flow is aligned with the upper surface as mentioned above, and therefore the incidence angle could be defined as

$$i \approx \frac{\theta_{L.E.}}{2} \approx \frac{t_{max}}{c} \cong 1.7 \text{ [}^\circ\text{]} \quad (9.123)$$

The deviation angle could be derived from the Carter's basic rule and supplemented by 2° because of the shock boundary layer interaction on the suction surface which causes an higher deviation angle

$$\delta^* \approx \frac{\Delta\beta}{4\sqrt{\sigma}} + 2^\circ \cong 4.5 \text{ [}^\circ\text{]} \quad (9.124)$$

The blade leading edge angle $\kappa_{1,tip}$ is

$$\kappa_{1,tip} = \beta_{1,tip} - i \cong 53.3 \text{ [}^\circ\text{]} \quad (9.125)$$

The blade trailing edge angle $\kappa_{2,tip}$ is

$$\kappa_{2,tip} = \beta_{2,tip} - \delta^* \cong 40.1 \text{ [}^\circ\text{]} \quad (9.126)$$

and the camber angle φ_{tip} results

$$\varphi_{tip} = \kappa_{1,tip} - \kappa_{2,tip} \cong 13.3 \text{ [}^\circ\text{]} \quad (9.127)$$

The stagger angle of a double-circular arc blade γ° is therefore

$$\gamma^\circ = \beta_1 - \frac{\varphi_{tip}}{2} - i \cong 46.7 \text{ [}^\circ\text{]} \quad (9.128)$$

It is possible to estimate the rotor blade row solidity at the tip radius obtained from the iterative method using the iterated stagger angle, the blade spacing from cutaway image and the measured axial blade chord from cutaway, and it is therefore equal to

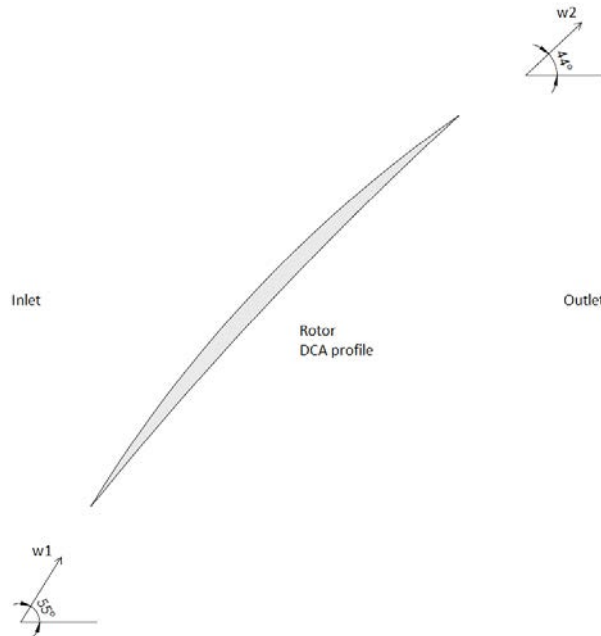
$$\sigma_{r,tip} = \frac{l_{axial,tip}}{s_{r1,tip}} \cong 1.08 \quad (9.129)$$

which determines the end of the iterative process ends since the axial chord (or the blade row solidity) calculated from previous iterative quantities is equal to the axial blade chord (or blade row solidity) measured from the cutaway image of the engine.

It is possible to calculate the D-Factor of the rotor which is equal to

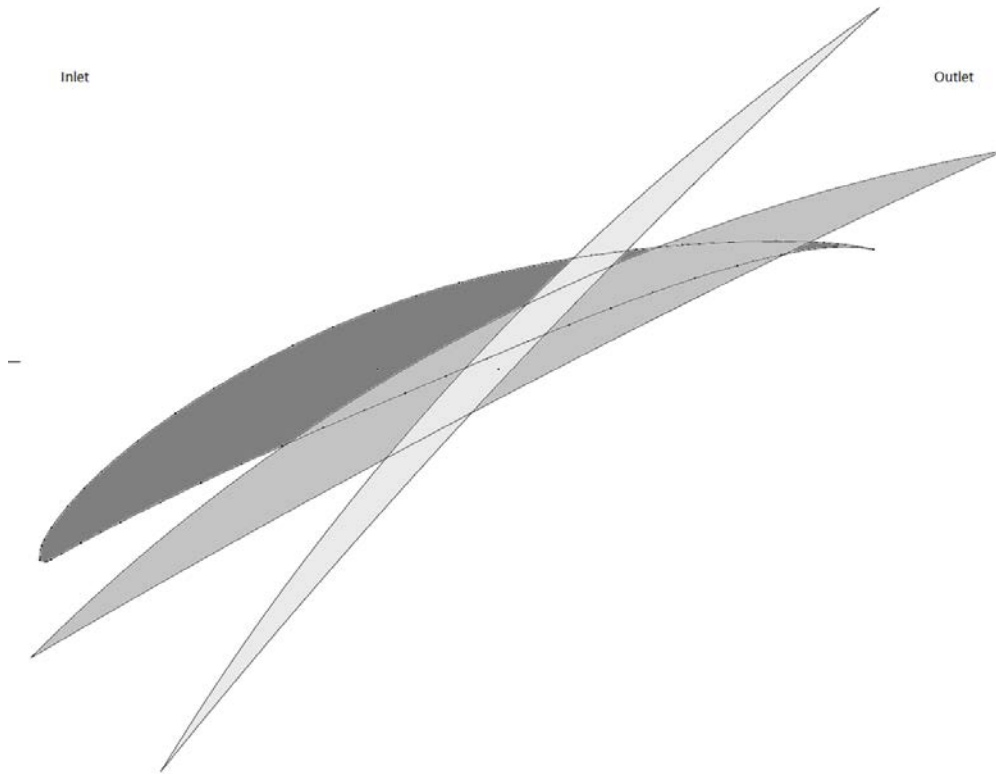
$$D_{r,tip} = 1 - \frac{w_{2,tip}}{w_{1,tip}} + \frac{|\Delta c_\theta|}{2 \cdot \sigma_{r,tip} \cdot w_{1,tip}} = 0.313 < 0.55 \quad (9.130)$$

Fig. 9.10: LPC rotor profile configuration at tip radius for the outer transonic part



Finally below in Figure 9.11 there are reported the three profiles of both the inner and the outer part rotor blades previously designed, in a single view with the same scale. The reciprocal axial position of the blades is derived from the cutaway image of the engine reported in Figure 3.7.

Fig. 9.11: LPC rotor profiles of both the inner and the outer part of the fan



10. CONCLUSIONS AND FURTHER IMPROVEMENTS

This thesis was written with the intention of providing a preliminary guide to users that for the first time are going to make use of the GasTurb software in order to analyse and optimise gas turbine cycles.

All the basic functions are described and introduced, and a preliminary design of modern unmixed turbofan engines is analysed. It is shown the importance of retrieving experimental and measured real data in the definition of the engine design cycle and moreover in its off-design operating line. The use of a component-level engine model implies that user set component maps that must be as real as possible in order to obtain simulation results that are precise and that are an accurate estimate of the simulated engine. A lot of assumptions are necessary to be made in the definition of each component efficiency and behaviour. The GasTurb software offers a wide variety of simulation tools that are capable of analysing different aspects of the engine operation with ease using iterative methods, optimization processes and user-friendly plot functions. It is possible to analyse simple cycle design points, engine off-design operating lines, flight envelopes or flight missions. A further simulation step is to set up a transient simulation of the engine operation

Another possible study could consist of performing a geometrical engine design using the implemented GasTurb tools. In this case it would be necessary to take into consideration an engine with provided engine workshop manual.

REFERENCES

- [1] E. Benini, "Propulsione aerea", CLEUP (2014)
- [2] Joachim Kurzke, Ian Halliwell, "Propulsion and Power: An Exploration of Gas Turbine Performance Modeling", Springer International Publishing (2018)
- [3] Jack D. Mattingly, William H. Heiser, David T. Pratt, "Aircraft Engine Design", American Institute of Aeronautics and Astronautics Education Series (2002)
- [4] "Gasturb 13: Design and Off-Design Performance of Gas Turbines", GasTurb GmbH (2018)
- [5] Nicholas Cumpsty, "Jet Propulsion: A simple guide to the aerodynamic and thermodynamic design and performance of jet engines", Cambridge University Press (2012)
- [6] Daniel P. Raymer, "Aircraft Design: A Conceptual Approach (Sixth Edition)", American Institute of Aeronautics and Astronautics Education Series (2018)
- [7] L. R. Jenkinson, P. Simpkin, D. Rhodes, "Civil jet aircraft design", Arnold (1999)
- [8] "General operating instructions: axial compressor nonafterburning turbojet and turbofan engines", Pratt & Whitney Aircraft Group (1976)
- [9] Saeed Farokhi, "Aircraft Propulsion", Wiley (2014)
- [10] Ahmed F. El-Sayed, "Fundamentals of Aircraft and Rocket Propulsion", Springer International Publishing (2016)
- [11] David G. Wilson, Theodosios Korakianitis, "The Design of High-Efficiency Turbomachinery and Gas Turbines", MIT Press (2014)
- [12] Rolls-Royce, "The Jet Engine", Wiley (2015)

- [13] S. Gudmundsson, "General Aviation Aircraft Design: Applied Methods and Procedures", Butterworth-Heinemann (2014)
- [14] Philip G. Hill, Carl R. Peterson, "Mechanics and thermodynamics of propulsion", Addison-Wesley Publishing Company (1992)
- [15] Philip P. Walsh, S. Fletcher, "Gas Turbine Performance", Blackwell Science (2004)
- [16] EASA Type Certificate Data Sheets (TCDS)
<https://www.easa.europa.eu/document-library/type-certificates>
- [17] ICAO Aircraft Engine Emissions Databank
<https://www.easa.europa.eu/easa-and-you/environment/icao-aircraft-engine-emissions-databank>
- [18] General Electric GE9X website
<https://www.geaviation.com/commercial/engines/ge9x-commercial-aircraft-engine>
- [19] GE9X - Technologies for the Next Engine Generation
https://www.icas.org/ICAS_ARCHIVE/ICAS2014/data/papers/2014_1024_paper.pdf
- [20] Pratt & Whitney PW1000G website
<https://pwgtf.com/>
- [21] Dieter Scholz, "Aircraft Design", Hamburg Open Online University (2015)
- [22] GSP Development Team Members, "GSP 11 User Manual", National Aerospace Laboratory NLR Amsterdam (2017)
- [23] Joachim Kurzke, "How to Create a Performance Model of a Gas Turbine From a Limited Amount of Information", ASME Turbo Expo (2005)
- [24] MTU Aero Engines website on PW1100G-JM
<https://www.mtu.de/maintenance/commercial-aircraft-engine-services/engine-portfolio-mro/narrowbody-and-regional-jets/pw1100g-jm/>
- [25] NASA, "The Promise and Challenges of Ultra High Bypass Ratio Engine Technology and Integration"
<https://ntrs.nasa.gov/archive/nasa/casi.ntrs.nasa.gov/20110011737.pdf>

-
- [26] J. J. Decker, P. N. Szucs, W. J. Solomon, V. L. Wilson, General Electric Company, "United States Patent No. US7374403B2" (May 20, 2008)
<https://patents.google.com/patent/US7374403>
- [27] Wikipedia, "Airbus A320neo family"
https://en.wikipedia.org/wiki/Airbus_A320neo_family
- [28] Modern Airlines, "Boeing 777X"
<http://www.modernairliners.com/boeing-777/boeing-777x/>
- [29] Wikipedia, "Thrust-specific fuel consumption"
https://en.wikipedia.org/wiki/Thrust-specific_fuel_consumption
- [30] Wikipedia, "Lift-to-drag ratio"
https://en.wikipedia.org/wiki/Lift-to-drag_ratio
- [31] C. Svoboda, "Turbofan engine database as a preliminary design tool", Elsevier Aircraft Design vol. 3 (2000)